DEPARTMENT OF THE INTERIOR

U.S. GEOLOGICAL SURVEY

Seismicity Associated with Volcanism in Hawaii: Application to the 1984 Eruption of Mauna Loa Volcano

by

Robert Y. Koyanagi

U.S. Geological Survey
Hawaiian Volcano Observatory
Hawaii National Park, HI 96718

Open-File Report 87-277

TABLE OF CONTENTS

ABSTRACT

Multi-disciplined study of the extensive collection of seismic and deformation data at Kilauea over its recent decades of intense volcanism provide the conceptual basis to understand the mechanisms that underlie neighboring Mauna Loa Volcano. A test of this understanding was provided by temporal and spatial patterns of seismicity that climaxed with the major eruption of Mauna Loa in 1984. Study of this eruption is part of a continuing program of seismic data collection aimed at understanding volcanic processes in Hawaii.

Earthquake hypocenters trace a major transport system extending from a central magma source 30-60 km beneath south Hawaii to shallow storage systems beneath three surrounding volcanoes Kilauea, Mauna Loa, and newly-forming Loihi. The northernmost component ascends subvertically to supply magma to Mauna Loa's summit-rift storage complex centered on a reservoir system 3-9 km beneath the summit-caldera Mokuaweoweo. As at Kilauea the shallow reservoir is defined as a zone of greatly reduced seismicity ("seismic shadow") as well as by modeling of ground deformation accompanying inflation and deflation of Mauna Loa. The eruption cycle leading to the 1984 eruption was seismically documented by the gradually increasing number of earthquakes along the subvertical magma-transport system accompanying nine years of inflation following the brief summit eruption in 1975. The activity culminates into an intrusive swarm hours or days before the outbreak of lava. Shallow earthquakes and high-frequency harmonic tremor characterize the intrusive swarms. Upon eruption and development of an "open-conduit" system earthquakes decrease and harmonic tremor prevail. The eruption tremor varies in amplitude according to the eruptive intensity, and its amplitude and dominant frequency attenuates as a function of distance from the active vent. Seismicity concludes during post-eruption with small earthquakes and tremor bursts associated with micro-structural and thermal adjustments at the vent and summit-deformation center, and degassing acoustics.

Deeper crustal-earthquakes continue over a wider range of space-time-magnitude in response to far-field stresses induced by the summit-rift intrusion. These events document the tectonic growth of the volcanic island from intrusion-induced rift-spreading and flank-displacements along the subhorizontal zone of weakness between the oceanic floor and overlying volcanic rocks.

As observed at Kilauea, sustained high-rate of volcanic activity promotes an increasingly continuous and efficiently balanced pressure system in the conduit-complex. The lava output in a rift-eruption is matched with a relative deflation pattern at the summit. Eruption tremor becomes increasingly constant and earthquake-free as constrictions minimize along the conduit system. High-volume eruptions and major tectonic events that tend to relieve shallow stresses effectively translate the pressure reduction deeper along the magma transport system and increase the

supply rate from the mantle that, in turn, would sustain prolonged or frequent eruptions and high lava production rates.

INTRODUCTION

The progressive development of a modern seismograph network on the island of Hawaii since about 1954 made it possible for the Hawaiian Volcano Observatory (HVO) to systematically document the seismic activity related to renewed eruptive activities at Mauna Loa starting in 1974. Further advances including island-wide signal telemetry and computer-based data processing generated a seismic data-set that was sufficiently accurate and chronologically complete to provide a coherent model of the internal structure of Mauna Loa and to follow the sequence of magma movement and the response of the Mauna Loa edifice to the volcanic process before, during and following the eruption of 1984.

This report outlines the sequence of instrumental development that led to increasingly accurate hypocenter determinations. Critical to this was the orderly placement of seismic sensors based on geologic data and an improved knowledge of seismic-velocity structure from seismic-refraction experiments and related geophysical data. The geological and geophysical background-data are described sequentially to put into perspective the approach used in the data compilation and summarization of the seismic data.

Continuous monitoring provided the means to prepare a detailed chronological accounting of the events surrounding the Mauna Loa eruption of 1984. The dominant earthquake sequences described the internal condition of stress and set the stage for eruption. Harmonic tremor and deflation-related earthquakes were observed during the eruption. Post-eruption stage included the decaying pattern of seismicity associated with gradually decreasing degassing and crustal adjustments at the eruptive vent and new lava flows, and structural adjustments at the summit and flank induced by magmatic withdrawal and emplacement.

The summarization of the seismic data updated to 1985 incorporates and expands on the concepts of volcanic structure and magma-transport process conceived in earlier years by the author and other geo-scientists with their varied applications of the HVO data. The general similarities of summit-rift eruptive features and pattern of seismicity between Hawaii's two most active volcanoes Mauna Loa and Kilauea provide a comparative base in understanding their behavior. Because of the continuously high activity at Kilauea over the past 3 decades, the concepts on structure and process have been substantially refined for this volcano. The data summarized in this report show that many of these concepts are equally applicable to Mauna Loa.

GEOLOGIC SETTING AND PATTERN OF HISTORIC ERUPTIONS

Mauna Loa, the great shield volcano, is considered the largest in the world (Macdonald and Abbott, 1970). It measures 4,170 m above sea level and nearly 9 km above the oceanic floor. Mauna Loa's eruptive features are outlined by the 6x2.4-km summit caldera Mokuaweoweo, and elongated along the connecting two principal rift zones (figure 1). These major rift zones that extend northeast and southwest from Mokuaweoweo mark the gently-sloping topography with a series of fissures, cones and craters. The northeast rift zone extends 22 km in length, with an initial northeast direction that gradually bends and fades to the southeast. The more pronounced southwest rift zone extends 26 km southwestwards from Mokuaweoweo, changing to a southward trend for 35 km more toward the southern tip of the island.

There have been 37 historically documented eruptions between 1832 and the end of the major southwest rift eruption in 1950, averaging one eruption each 3.6 years. The eruptive rates along the southwest rift zone of Mauna Loa are described in detail by Lipman (1980). Mauna Loa eruptions have usually started with a fissure outbreak at the summit. Frequently, summit activity is followed by migration of the active fissures into one of the rift zones. Eruptions of Mauna Loa have lasted from less than a day to several months. During a sustained eruption lava fountaining that is initially emitted from a series of linear fissures later converges to a more isolated system of vents, and eventually to a single vent. The final stages of sustained lava fountaining from a single vent is generally followed by many months of degassing at a gradually decreasing rate. An estimated 80 to 600 million cubic meters of basaltic lava has been produced by each of the major eruptions since 1832. Fountain heights varied from a few to several hundred meters.

The last major southwest rift eruption in 1950 was followed in 1951 by a significant 6.9-magnitude earthquake beneath the adjacent west flank of the volcano. A 25-year eruptive repose prevailed before the next outbreak at the summit of Mauna Loa in 1975. This short summit-outbreak in July of 1975 was followed 9 years later by the most recent and sustained summit-flank eruption in March-April 1984 (Lockwood et. al. 1985). Geophysical monitoring advanced substantially during the years encompassing these two eruptions, and the seismic evaluation of the volcanic processes at Mauna Loa presented in this report is based essentially on the data collected for this period.

HISTORY OF INSTRUMENTATION AND DATA PROCESSING

Operation of seismographs was started early in the history of the Hawaiian Volcano Observatory in order to monitor seismic activity associated with volcanism in Hawaii. A chronology of

the instrumental development at HVO is documented by Klein and Koyanagi (1980). The instrumental evolution was highlighted by marked improvements from about 1954 when replacement of mechanical seismographs with higher sensitivity electro-magnetic systems was initiated. Network expansion and cable-telemetry for critical stations provided timing improvements and more rapid assessment of the state of seismicity. Timing relays were incorporated with the clock system to allow WWVH radio-time signals in seconds to be instrumentally written onto the standard drum-records once each day to provide time corrections. The improved timing and instrumental sensitivity enabled construction of a reasonable seismic-velocity structure for earthquake-locating routines based on relative timing of P- and S- waves from strong earthquakes recorded on a network of local stations (Eaton, 1962). To improve the velocity model for the crust beneath the island of Hawaii, precisely timed detonation of explosives were used to conduct seismic-refraction experiments (Ryall and Bennett, 1968; Hill, 1969). Additional refraction work was done later to refine the structural model beneath specifically active regions across the east rift zone of Kilauea and the summit-flank of Mauna Loa (Zucca and Hill, 1980b; Zucca, et. al., 1982).

In 1967, the standard recording format using optical or smoke rotating-drums at 60 mm per minute for daily records was supplemented with the Develocorder system. The Develocorder provided continuous strip-film recording of 20 channels which included 18 seismic traces, and 2 time traces on opposite sides of the film. The system assured relative timing of events to be made more rapidly with a higher resolution of at least 0.1-second. The installation of the Develocorder was accompanied by the development of radio-telemetry seismic systems, the combination of which paved the way for an extensive islandwide seismic network.

Manual calculations of earthquake locations using equal-time charts (isochrons) for overlays on gridded maps became increasingly impractical and biased as the network of stations grew. In 1970, earthquake processing shift from manual to a computer-based procedure using a location program called HYPOLAYR (Eaton, 1969). Seismic-wave times and amplitudes were read at HVO and sent to the USGS western center at Menlo Park, California to be key-punched on cards and processed for locations (Endo et. al., 1972).

In 1975 a Bell and Howell 3700B instrumentation tape recorder was installed to record the network signals, and in 1978 HVO acquired an Eclipse minicomputer and digitizer,providing the Observatory with full capability to computer-process all of the recorded earthquakes in Hawaii. Data was processed on a daily routine using the location program HYPOINVERSE (Klein, 1978).

At Mauna Loa, following the eruption of 1975, the seismographic coverage at the summit was expanded. Three stations (MOK, WIL, SWR) on edge of the summit-caldera Mokuaweoweo form a 3-km wide tripartite. Station WIL on the southeast edge of the caldera was modified from a

single-component vertical to a 3-component system. Additional stations were added along the flanks of the volcano to improve the geometry of the network and thus increase the precision of earthquake determination.

At the end of 1985, 50 stations with 70 vertical-and-horizontal components continuously transmitted their signals by radio-telemetry to HVO where they were recorded and processed (figure 2). The seismic network furnishes a dense coverage in the southern parts of the island where seismicity is highest beneath the active volcanoes Kilauea and Mauna Loa, and a skeletal coverage over the remaining northern side of Hawaii. A single independently-recording seismograph station is operated on each of the islands of Maui and Oahu for added coverage of events that may occur in the outlying regions of the Hawaiian Archipelago. Detailed description of the seismic network operation and the seismic and volcanic data collected at HVO in 1984 is summarized in Nakata et. al. (1986). The HVO short-period network includes 1-Hz vertical- and horizontal-component geophones. Most stations were single-component vertical units designed with high-sensitivity to capture the sharp onset times and directions of P-waves. Three-component stations each comprised of one vertical and two horizontal sensors were selectively deployed (1) along the peripheral edge of the island network to improve identification of S-wave arrival-times that constrain hypocentral distances in focal determinations of deep earthquakes or those outside the network and, (2) in the summit regions of the active volcanoes where anomolous attenuation of S-wave velocities and amplitudes due to structural variations and magmatic activity will most expectedly be reflected in the earthquake signals. The frequency response for the systems is graphically described in figure 3.

In the routine processing of seismic records at HVO, microfilm and drum seismograms are scanned and seismic events are categorized according to locality based on arrival-time differences at key stations, and type based on coda waveforms (Koyanagi, 1982). Accordingly earthquakes as small as about 0.1-magnitude are normally detected and classified according to the following volcanically significant structural regions on Mauna Loa: shallow summit, Mauna Loa deep, northeast rift zone, and Kaoiki (southeast flank) (see also figure 1). Short-period earthquakes are separated from long-period ones according to their coda waveforms. Short-period events are the common type with sharp P and S wave onset and frequencies that temporally decrease from about 15 to 1 Hz throughout the coda. Alternatively, the long-period varieties are characterized by generally elongated signals with temporally uniform frequencies within a limited band that usually peaks at about 1-5 Hz throughout the coda.

Harmonic tremor, a seismic signal proven to be associated with magma movement in Hawaii, is logged according to time, duration, location, and relative strength. Harmonic tremor is a sustained signal with relatively uniform frequencies within a limited band that peaks from about 1 to 10 Hz throughout its occurrence. It is routinely classified according to epicentral location and relative depth based on amplitude-attenuation

pattern across the seismic network and locatable long-period earthquakes that sometimes accompany the tremor episode.

In the daily scanning process, earthquakes that are clearly recorded on about ten or more stations and possess signal-duration magnitudes larger than 1.0 are selected for quantitative processing of hypocenter and magnitude. P- and S-wave arrival-times are picked to the nearest .01-second for location-processing, and directions of first motion are documented for optional determination of focal mechanism. The station readings for these well-recorded earthquakes are archived, and their focal parameters along with daily-count tabulations of smaller events are routinely catalogued in annual seismic-summaries of the Hawaiian Volcano Observatory. Processed earthquakes are chronologically filed according to their calculated origin time in year-month-day-hour-minute-second sequence. The standard derivation of earthquake parameters include degrees and minutes of latitude and longitude for epicenter, focal depth in km below the epicenter, and magnitude based on the Richter Scale.

GEOPHYSICAL BACKGROUND

A. Corroborative Data

Our interpretation of volcanic structure and magmatic process at Mauna Loa draws heavily on the concepts developed by the intense research conducted at Kilauea during recent decades. The similarities between Kilauea and Mauna Loa in their volcanic behavior and seismic pattern allow a logical basis for comparison. From the analyses of seismicity and ground deformation at Kilauea, concepts of the internal structure and processes that generate eruptions along the summit-rift complex were developed (Eaton, 1962). Seismic network expansion and improvements in earthquake-hypocenter determination set the foundation to quantify volumetric constraints of the summit reservoir and the temporal pattern of summit-to-rift transfer of magma (Koyanagi, et. al, 1976). Patterns observed from detailed monitoring of the frequent volcanic events at Kilauea led Fiske and Jackson (1972) to prepare gelatin models of the volcano for controlled experimentation on the effects of pressure introduced in the summit-rift magma system.

The spatial and temporal distribution of earthquakes also outlined the deep magma transport system beneath Kilauea. The principal plumbing system connected to the shallow-summit reservoir centered at 4-km below the summit-caldera was determined to extend subvertically to a depth of about 60 km. Magma is fed to the shallow reservoir from the deep mantle source. Over-pressurization of the summit-reservoir, monitored by increased seismicity and inflationary ground-tilt, is accommodated by either a summit-eruption or intrusion of magma into one of two rift zones that radiate laterally from the summit reservoir and plumbing system. The rift zones are seismically defined to be several km wide and no deeper than about 10 km from the

ground surface. The region within 5 km of the surface is shown to be active during magmatic intrusion or eruption. Rift intrusions cause stresses to generate normal to the direction of magma-pressure propagation. Accumulated strain is relieved on the unbuttressed seaward slopes of the volcano. The flanks are persistently displaced southward along its interface with the oceanic floor onto which the volcanic rocks rest at a depth of 10-15 km. This process cause the seaward expansion of the rift zone, and combined with extrusive activity provide the mechanism of growth for the Hawaiian Islands.

The stresses, influenced by the existence of buttress on the northern flanks of many Hawaiian volcanic edifices defined by previous volcanic growth along the progressively older systems, form an asymmetric pattern of lateral strain. The growth of the summit-rift system is seaward along the unbuttressed south flank of the volcano, as the buttressed north flank remain relatively stable and immobile. The asymmetrical distribution of earthquakes across the dynamic east-rift zone of Kilauea described by the temporal sequence of shallow-rift to deeper south-flank earthquakes that infer the seaward growth of the east-rift zone was reported by Koyanagi, et. al. (1972). Extensive collection and detailed analyses of deformation data emphasized and further quantified the pattern of seaward growth (Swanson, et. al., 1976).

The recognition of these fundamental concepts prompted multi-disciplinary interest in treatment of data from the continuing seismic program at HVO. Focal mechanism analyses from first motions, precursory patterns for earthquake and eruption prediction, volcano-structure studies and seismic-engineering applications are among the numerous research topics being conducted with the Hawaii seismic data by an international collaboration of seismologists and volcanologists.

The broad circum-Pacific zone of active seismicity that provide a wide azimuthal seismic-source for the dense telemetry network on the island of Hawaii has prompted seismologists to evaluate teleseismic data recovered on the Hawaii network. Johnston and others (Johnston, 1978; Johnston, et al, 1982) examined station-to-station variations in local P-wave velocities prior to a major earthquake. P-wave differences for critical stations located in the epicental area of the major 7.2-magnitude crustal earthquake in the south flank of Kilauea on 29 November 1975 indicated a sequence of seismic-velocity decrease and increase consistent with changes expected in earthquake-precursory dilatancy models. Teleseismic signals that furnish uniform seismic-ray patterns were used to examine spatial distribution of P-velocity anomalies beneath central Kilauea for applications in outlining the magma-plumbing system (Ellsworth and Koyanagi, 1977). Anomalously low velocity-zones defining the magma conduit system surrounded by high velocities concurred with the model of a steeply-dipping primary conduit beneath the summit of Kilauea tapping magma from a source 60-km below, as was initially inferred by the confining distribution of local earthquake-hypocenters.

The normally-constant generation of magma from the mantle through subvertical conduits, reservoirs and eruptive vent-systems

at the volcanic surface are episodically disrupted by major eruptive and tectonic events. Such persistent or catastrophic events at Kilauea as the 1969-74 Mauna Ulu and 1983-86 Puu Oo eruptions, and the 7.2-magnitude Kalapana earthquake in November 1975 would effectively reduce pressure in the magma-conduit system. The pressure reduction in the shallow region is expected to translate deeper along the conduit system to intermittently accelerate the flow-rate of magma to Kilauea (Dzurisin, et al, 1984; Koyanagi, et. al., 1986).

Data on deep tremor and long-period events delineate the region of the deep magma source in the mantle, and the process which feeds the separate volcanoes. The locations of long-period events that correlate with deep harmonic tremor define a common source region for mantle magma central to the active volcanoes (Koyanagi and others, 1986; Aki and Koyanagi, 1981). A comprehensive collection of hypocenter determinations for long-period events outline a 30-km wide central complex 30 to 60 km beneath south Hawaii, and 5-km-wide conduit systems connecting to Mauna Loa, Kilauea, and a newly-forming submarine volcano Loihi (Klein, 1982).

The pattern of re-distribution of magma accumulated in a shallow summit-reservoir and laterally extensive rift-zones radiating from the summit complex were further documented by seismic and ground deformation data expanded for 1980 to 1985 (Dzurisin, et al, 1984; Koyanagi and others (in press).

Post-eruption seismicity for significant flank events may include episodes of seismic swarms reflecting gradual adjustments of residual magma in secondary storage zones that form at major discontinuities along the linear rift-conduit system (Koyanagi, et. al., 1981). Following the last lower east rift eruption of Kilauea in 1960 swarms of earthquakes that frequently continued for several weeks recurred at decreasing intervals over a period of at least a decade. Many thousands of 0.1- to 2.0- magnitude earthquakes confined within a few-km wide zone at less than 5-km in depth comprised a several-week-long swarm along the rift anomaly. Larger earthquakes registering up to about 4.0-magnitude spread deeper and farther along the adjacent south flank. These seismic responses to localized adjustments do not strongly influence the summit-rift magma-pressure system. Deflationary tilt at the summit that characterize normal rift-intrusions does not accompany these post-eruption events.

B. Mauna Loa Events

After a 24-year period of volcanic rest at Mauna Loa, small-summit earthquakes noticeably increased in late April 1974. The activity increased in rate and magnitude of earthquakes and provided HVO with a database of 171 locatable earthquakes ranging in magnitude between 1.5 and 4.6, and many thousands of smaller earthquakes detected on a limited number of stations. An eruption forecast based on the evaluation of the pattern of seismicity from 1962 to the increased activity in 1974 was published by Koyanagi and others (1975). Earthquake frequency followed a long-term pattern of progressively stronger bursts that recurred episodically

at intervals of several years. Increasingly noticeable highs in activity were centered in 1962, 1967, 1970 and 1974. Earthquakes that closely accompanied summit inflation occurred in swarms at about 2 to 5 km beneath the caldera region. Aftershock-sequences and swarms of deeper earthquakes at about 5 to 15 km flanked the summit activity in clusters located normal to the major summit-rift axis; these followed the long-term inflationary process of the volcano. Following a short summit-eruption on July 5-6, 1975, and a subsequent intrusive swarm the volcano remained in a seismically dormant state for the next five years.

In 1978 a seismic-refraction experiment designed to study the crustal structure beneath Mauna Loa was conducted by the U.S. Geological Survey. The west to east profile was established with pre-determined explosion-shotpoints off the west coast of Hawaii and land-based seismic receivers using the HVO seismic network reinforced with additional portable seismographs deployed in critical areas. Using the seismic data derived from this experiment, and available gravity data, Zucca, et. al. (1982) modeled seismic velocity and density structures beneath Mauna Loa. They defined a landward-dipping Moho-crust interphase at depths below sea-level ranging from about 14 km near the coast of the island to about 18.5 km near the summit of Mauna Loa.

Resurgence of activity from about 1980 led Decker and others (1983) to forecast another eruption at Mauna Loa. The increasing pattern of shallow earthquakes less than 5 km in depth along the summit-rift axis and intermediate-depth events 5 to 10 km in depth along the northwest flank were examined relative to the inflationary pattern of the ground-deformation data. In addition to indicating the increased probability for eruption, they presented a magma-reservoir model based on the summit-flank distribution of earthquakes, the inflation pattern, and pressure center derived from the ground-deformation pattern. The active magma-reservoir system about 5-km in diameter placed at about 3 to 7 km beneath the summit-caldera was fed from a connecting conduit-system below.

On November 16, 1983, during the continuing inflation of Mauna Loa, a damaging earthquake of 6.6-magnitude occurred in the Kaoiki region on the southeast flank of the volcano about 14 km from Mokuaweoweo. The distribution of aftershocks defined a stress zone 20 km in areal extent and centered at about 5 to 10 km below the ground surface (Koyanagi and others, 1984). P-wave first-motions for principal shocks recorded in the Kaoiki region indicate a strike-slip pattern with northeast-southwest and northwest-southeast trending nodal planes (Koyanagi and others, 1966). Complex linear-patterns in hypocentral distribution of aftershocks, ground-cracks and deformation patterns favor right-lateral strike-slip faulting along the northeast-southwest component (Koyanagi et. al., 1984; Endo, 1985). The inferred pattern of faulting is interpreted to be due to compressional stresses induced by opposing inflationary growth of Mauna Loa and Kilauea in the mid-sectional region between the two centers.

Analyses of P-wave first-motions for swarm-earthquakes northwest of Mokuaweoweo that occurred previously in September

1983 also indicated strike-slip faulting (Endo et. al., in preparation). The pattern is consistent with outward displacement of the north flank caused by lateral stresses from the inflating volcano, complementing the southeasterly movement towards the Kaoiki on the opposite side.

The anticipated eruption in March-April 1984 was extensively monitored geologically, geochemically and geophysically (Lockwood et. al., 1985). The eruption that initiated in the summit and migrated into the northeast rift developed into a major eruption producing an estimated 220 million cubic meters of lava after 3 weeks of activity. A dramatic inflationary episode and seismic swarm accompanied the initial intrusion and eruptive outbreak at the summit. Sustained summit deflation and harmonic tremor accommodated the prolonged flank eruption that followed. The seismic events that furnished the base for many of the interpretations mentioned in the above paragraphs are chronologically quantified with respect to their size and spatial distribution in the subsequent sections.

SEISMIC PERSPECTIVE FOR MAUNA LOA ERUPTIONS

Earthquakes outlined the pattern of increased stress since the resurgence of magmatic activity at Mauna Loa in 1974, which led to a short eruption in July 1975 and ultimately to the major outbreak in March-April 1984. The seismicity developed and accelerated episodically in a temporal and spatial configuration that accommodated the strain generated by the inflating volcano.

A. Earthquake Frequency

The increasing rate of seismicity was first recognized on the daily count of earthquakes from the stations at Mauna Loa summit. The increase of small earthquakes in the lower magnitude range were detected since the ending of April 1974 (figure 4a). The activity increased episodically with bursts numbering several to many hundreds of shocks per day that occurred above a generally increasing background level until the eruption on July 5, 1975.

Following the short summit-eruption, the frequency of microearthquakes gradually decreased to nearly the pre-eruption level until about 1980. The seismicity returned gradually from 1980, and developed into another episodically increasing pattern from mid-1982 (figure 4b). The activity increased progressively from bursts of earthquakes numbering several tens per day that lasted several days to those with many hundreds per day sustained for several weeks culminating with an eruption on March 25, 1984.

These episodic swarms that systematically increased before the 1975 and 1984 eruptions recurred at intervals of 3 to 6 months. A few days of relative decrease in microearthquake frequency also is indicated in the short-term fluctuations immediately before the final intrusive-swarm and onset of eruption. This feature is noticeable before the outbreak in 1975, and the one in 1984.

B. Hypocentral Distribution of Earthquakes

The spatial configuration of seismic zones that developed and advanced sequentially through the stages of inflation, eruption, intrusion, and re-inflation from 1974 until the major eruption on March 25, 1984 is outlined by hypocenter maps in three chronological increments (figure 5). Figure 5a from 1 January 1974 to 31 July 1975 covers the development of shallow (0-5 km) inflation-related summit earthquakes and the increases in deeper flank-earthquakes at 5-13 km depth normal to the major summit-rift axis. The persistently active Kaoiki zone on the southeast flank of the volcano was emphasized by aftershocks in late 1974 generated by a 5.5-magnitude earthquake on November 30 and a 4.8-magnitude earthquake on December 15. Their northeast-southwest hypocentral alignment is consistent with P-wave first-motion patterns and the preferred northeast-southwest trending fault plane that complements right-lateral strike-slip faulting for principal shocks as described earlier (Koyanagi et. al., 1984; Endo, 1985). The northeast-southwest alignment of seismic concentration on the extreme southeast portion of the map relates to a Kilauea southwest rift intrusion and eruption that started on December 31, 1974 and continued in January 1975 (Koyanagi, et. al., 1978a; Koyanagi et. al., 1978b). The short summit-eruption on 5-6 July 1975 was followed by about a week of intrusion-related swarm outlined by earthquakes along the northeast rift zone about 7 to 17 km from the summit caldera and extending in depth from near surface to about 10 km. The high seismicity that lasted for about a week (Decker et. al., 1983) was accompanied by summit deflation and dilation of the northeast rift zone (Koyanagi et. al., 1978b).

Figure 5b covers the period of volcanic rest between 1 August 1975 to 31 December 1979. Crustal earthquakes in the summit-rift zone produced by magma-intrusions were few. Mantle earthquakes at depth greater than 20 km persisted moderately beneath the southeast summit region. The major 7.2-magnitude earthquake that struck the southeast flank of Kilauea on 29 November 1975 (Koyanagi et. al., 1978b) did not show any appreciable effect on the pattern of shallow seismicity along the intrusive and eruptive zones of Mauna Loa, as it did for Kilauea (Tilling et. al, 1976; Ando, 1979; Crosson and Endo, 1981). The consequent increase for part of the seismicity along Kilauea's southwest rift zone is apparent along the southeastern boundary of the hypocenter map. Seismic activity persisted in the Kaoiki region reflecting continued interaction of stresses generated by Kilauea and Mauna Loa.

The third time-increment of earthquake hypocenters mapped for 1 January 1980 to 30 April, 1984 (figure 5c) describes the pattern of seismicity associated with renewed magma-activity and eruption at Mauna Loa. Shallow earthquakes (0-5 km depth) beneath the summit and upper southwest rift accelerated noticeably from late 1980, and the accompanying increase of intermediate-depth (5-10 km depth) earthquakes on the northwest flank climaxed with a significant swarm in September 1983 (Endo et. al., in preparation; also described in a later section). On 16 November 1983, a strong 6.6-magnitude earthquake centered in the Kaoiki region (Koyanagi, et. al., 1984). The right-lateral strike-slip faulting resolved for the Kaoiki earthquake was attributed to compressional stresses induced by magma pressure from Mauna Loa and Kilauea.

The northern extent of the stress drop outlined by the aftershock region approaches the southern boundary of the northeast rift zone near the place of intrusion in 1975. The sequence triggered a flurry of shallow earthquakes in the leading edge of the northeast-rift intrusion zone signifying dilation of the rift zone. These events ultimately set the stage for the eruption which commenced on 25 March 1984. The initial outbreak at the summit migrated nearly aseismically into the northeast rift zone culminating in the locality intruded by magma in 1975, and where the emplaced dikes were subsequently weakened by the November 1983 Kaoiki earthquake.

The compilation of hypocenters for the entire period of increased Mauna Loa activity from 1 January 1974 to 30 April 1984 outlines the spatial distribution of seismicity to constrain the structural configuration of the magma system within the volcano (figure 6a). Inflation-related shallow earthquakes (0-5 km) were concentrated in the summit region and upper southwest-rift zone. Intrusion-related crustal-earthquakes were clustered along the elongation of the northeast rift zone. Deep earthquakes occurred at 20 km or more in depth beneath the southeast summit region. Crustal earthquakes mostly at 5-10 km in depth flank the volcanic center normal to the summit-rift axis. A major seismic zone persisted in the southeast flank due to stresses from Mauna Loa and Kilauea.

A cross-sectional portrayal of hypocenters in a 5-km wide zone centered on the northwest-southeast line A-B keyed onto figure 6a details the depth-distribution normal to the summit-rift axis (figure 6b). The shallow-summit earthquakes were relatively confined within a depth of 4 km of the surface. Flank earthquakes that presumably accommodate lateral stresses clustered at depths of 5-10 km on the northwest and were offset at 6 to 12 km on the southeast flank; this bias may be partly due to seismic-network geometry. Sub-crustal earthquakes migrate along a variably-steep subvertical column shown to extend to a depth of about 50 km.

Alternatively, a cross-section centered on the southwest-northeast trending line C-D in figure 6a shows the hypocentral distribution along the summit-rift axis (figure 6c). The distribution of inflation-deflation related cluster of shallow-summit earthquakes concentrated at depths within 4 km of the surface shown earlier in section A-B is relatively elongated along the summit-rift axis consistent with the map-view zonation in figure 6a. The shallow concentration linked to a wider separation of earthquakes below to about 10 km in depth. The summit-rift alignment of earthquakes extended into the northeast rift zone in an array of sequential clusters. The summit-rift seismic concentration was interrupted along a 7-km length of the mid-section. The northeast rift earthquakes peaked along a 9-km-long zone 7 to 16 km from the summit seismic-zone. A small concentration of near-surface earthquakes about 15 km from the summit outlined the eruption-related stresses at the distal edge of the 1984 northeast-rift intrusion and eruption. The shallow concentration expanded into the broadly-intense 9-km-long seismic zone below to a depth of about 10 km.

The combined map and depth-section describe a columnar distribution of earthquakes beneath the summit region that extended into the mantle to a depth of about 50 km.

C. Temporal Distribution of Earthquakes in Depth and Magnitude

The temporal pattern of earthquakes at magnitude 1.5 or greater were oriented by depth and magnitude at Mauna Loa in figure 7. The increasing number of earthquakes in the dynamic regions beneath Mauna Loa responding to crustal adjustments from magmatic stresses were primarily confined to depths of about 10 km or less, comparable to depth patterns of volcanically induced earthquakes beneath Kilauea. Migration from deep to shallow source regions is notable during the gradually increasing rate of seismicity from about 1977 to 1981. The subsequent increase in both deep and shallow crustal-earthquakes indicated the accelerated interaction of deep and shallow source regions before the 1984 eruption. The increasingly rapid change in focal-depth with advancing seismicity described the progressively effective translation of stresses from the magmatic-pressure source at the summit-rift complex to the adjacent flanks.

Earthquake magnitude increased episodically during the increasing rate of earthquakes leading to eruptions. Flank earthquakes at about 5 to 10 km in depth pronouncely higher in magnitude before the 1984 outbreak climaxed with a 6.6-magnitude Kaoiki earthquake on November 16, 1983, whereas, shallower summit earthquakes were equally significant in magnitude increase prior to the 1975 eruption.

D. Seismic Rate

The seismic rate in terms of earthquake number and moment may then be plotted cumulatively to quantify its temporal relationship to volcanic events and impending tectonic earthquakes (figure 8). The temporal and spatial distribution of earthquakes examined earlier provides a means to categorize seismic effects of the volcanic process. The pattern of seismicity in the summit region governed by magmatic pressure around a shallow reservoir and along a connecting subvertical conduit-system accessing magma from the mantle may be examined incrementally at significant depth intervals (figure 8 a-c). These "volcanic events" are characterized by swarms of low-magnitude short- and long-period earthquakes occasionally accompanied by sustained signals of harmonic tremor. Tectonic events that affect the central magma-system are generated in the outer stress-zone as indicated by the intensively active Kaoiki region on the eastern flank of Mauna Loa (figure 8d). Such a region is marked by earthquakes widely distributed in time, space and magnitude; aftershock patterns prevail over swarms and harmonic tremor.

Numerical reductions of seismic rate for sequential time increments separated by significant changes in the linear pattern of earthquake frequency are tabulated in table 1. The earthquake rate for the 4 regional categories in the cumulative plots in figure 6 were calculated in number of earthquakes per month.

Seismic moment rate was projected from a cumulative compilation of seismic moment. Seismic moment was derived by magnitude of earthquakes using the formulation:

Seismic Moment = $10^{(A + B \times \text{magnitude})} \times 10^{21}$ dyne-cm; where the constants for A and B are -6 and 1.4, respectively.

Accordingly, a magnitude 5.0 earthquake would be equivalent to 10^{22} dyne-cm of seismic moment and the 6.6-magnitude Kaoiki earthquake in November 1983 would equal 1.7×10^{24} dyne-cm. Where seismic moment rate is exaggerated by high-magnitude tectonic earthquakes that occur episodically, earthquake rate emphasizes swarms with individual earthquakes that may be low in magnitude but occur more frequently in the volcanic domain. The ratio of seismic moment and earthquake rates is listed in table 1 to provide an index of the average size of the earthquake, a parameter that describes the stress condition and regime relating seismicity to the volcanic processes. Erratic changes in linear trends introduced by short swarms and large earthquakes were generally not considered in our calculation of seismic rate.

The inflationary process at Mauna Loa from about 1980 and during the years preceding the 1984 eruption correlated with a pronounced increase in shallow earthquakes (0-5 km depth) in the summit region (Decker, et. al., 1983). The increase in earthquake rate during the year preceding the 1975 eruption is dramatically higher. The relatively minor changes in seismic rate extrapolated back to 1962 follow an episodic pattern with increases in 1964 and 1967-71 alternating with relative quiescence in 1965-66 and 1971-74. The low earthquake rate during 1971-74 interval consisted of isolated moderate-magnitude earthquakes as indicated by the relatively high seismic-moment for the average earthquake (Mo/N ratio). The accelerated earthquake rate from April to December in 1974 consisted of increased numbers of small earthquakes as indicated by the relatively low seismic-moment rate and Mo/N ratio. In the subsequent period from January 1975 until the eruption in early July 1975 the seismic rate in earthquake number and seismic moment dramatically increased by more than an order of magnitude above the previously accelerated rate. Increase in the average magnitude of the earthquakes is apparent by the higher Mo/N ratio. The summit-flank swarms accompanying the short eruption subsided within a few weeks, and a seismic-low prevailed until the end of 1979. From January 1980 until the end of 1982 seismicity increased to a persistently linear earthquake rate of 1.43 earthquake per month accompanied by a seismic moment rate of $.014 \times 10^{21}$ dyne-cm per month. Average earthquake size remained relatively unchanged. From early 1983 until the eruption in March 1984, the earthquake and seismic moment rate accelerated for the second time as it did before the previous eruption in 1975. The increase this time, however, was only by about half an order of magnitude in comparison to the dramatic tenfold increase of earthquake rate in 1975. The Mo/N ratio increased by about 5x similar to the change in 1975. The seismic swarm accompanying magma-intrusion and summit-deflation during the eruption was followed by a period of quiescence that persisted from mid-1984 to the end of 1985. The continuing

low-seismicity describes the relieved state of stress in the summit-reservoir region.

Intermediate depth earthquakes at 5-13 km beneath the summit region result from lateral stresses that accommodate magma movement to the summit-reservoir and rift-zones. Long- and short-period earthquakes and occasional short bursts of harmonic tremor occurred episodically in response to pressure-buildup in the deep crustal region beneath the summit interacting with the inflationary process of the shallow-reservoir system. The generally increasing patterns of shallow and intermediate-depth seismicity varied temporally in rate indicating that the loci of strain release episodically shifted or alternated along the pressured column of magma. The earthquake rate for intermediate-depth events remained relatively constant from 1963 to early 1970 and then assumed a 3x higher rate until July 1974. The earthquake rate progressively increased before the 1975 eruption. The rate of advance during the August 1974 to March 1975 interval by 2x over the previous rate, subsequently increased to nearly 8x more during the final increment before the July eruption. The relatively low Mo/N ratio inferred generally small earthquakes during the accelerating intervals from August 1974 to June 1975. Seismic moment rate generally episodic from 1963 to the end of 1973 and, during the rapidly accelerating earthquake rate from early 1974, assumed a persistently increasing rate until the 1975 eruption. The short-lived eruption in July 1975 was immediately followed by more than a week of intense intrusion-related seismic swarm in the northeast rift zone about 6-15 km northeast of Mokuaweoweo (Koyanagi et. al., 1978b, figure 8a). Accompanying summit-deflation and rift-extension from ground deformation data verified the intrusive process. The low seismic rate from mid-July 1974 until early 1978 described the relieved state of stress following the eruptive activity. From March to June 1978 the earthquake rate increased by nearly 3x. From July 1978 the earthquake rate maintained a decreased rate of .40 earthquake per month until August 1982. From then until August 1983, the seismicity both in earthquake and seismic moment rates increased by nearly half an order of magnitude. September 1983 experienced a swarm of moderate-sized earthquakes about 5 to 10 km northwest of Mokuaweoweo. Focal mechanism solutions from P-wave first motions indicated compressional stresses oriented normal to the northeast-southwest trending summit-rift axis (Endo, et. al., in preparation). This pattern of first motion that commonly infer right-lateral strike-faulting and low-angle-dip faulting dominating at 5-10 km depth is consistent with the pattern that produces seaward displacement of the south flank of Kilauea. The September swarm was followed by a relatively high average earthquake rate of 4.33 events per month which persisted from October 1983 until the eruption in March 1984. Seismic moment rate was relatively high also, and average earthquake size was moderate. Post-eruption seismic quiescence resumed and continued throughout 1985.

Deep seismicity at 13 to 60 km beneath the summit region was low and constant relative to the intermediate and shallow categories. These events link with a common and persistent source of harmonic tremor and long-period events in a region of

expected magma generation in the mantle nearly 60 km beneath south Hawaii (Aki and Koyanagi, 1981). Swarms of earthquakes and harmonic tremor from a depth of 55 km beneath Kilauea were reported months before the major Kilauea Iki eruption in November, 1959 (Eaton, 1962), although these events were uniquely centered north of the summit region.The relatively constant rate of tremor generated from the deep-central source since then accelerated after major volcanic eruptions or crustal earthquakes to infer deep-magma excitation induced by pressure reduction translated downward along the vertical column beneath Kilauea (Koyanagi and others (in press). Figure 8c shows the subtle changes in seismic rate of deep Mauna Loa earthquakes before and after the eruptions in 1975 and 1984. The interval from mid-1965 to early 1971 registered the highest earthquake and seismic moment rate. An interval of relative quiescence prevailed for about two years from early 1971 to 1973. A second increase in seismic rate comparable to the 1965-71 rate occurred from early 1973 to late 1974. The deep seismic rate decreased to a lower level for nearly three-quarters of a year prior to the 1975 eruption, and continued for 2.6 years. The years of relaxed seismicity was interrupted in early 1978 by a burst in seismic rate followed by about 6 years of accelerated rate until the eruption in March 1984.

The pattern of strain release in the Kaoiki region describes the mechanism by which stresses along the magma-conduit system are translated and relieved in the flanks. Lateral stresses from summit-inflation and rift-intrusions induce earthquakes in the Kaoiki region, and major earthquake activity in turn, tend to relieve stresses along the deep-mantle region of the plumbing system. The temporal and focal-mechanism patterns of Kaoiki earthquakes that indicate outward stresses from the summit-rift axes of both Mauna Loa and Kilauea generate compressional stresses that are relieved within the volcanic pile mid-section between the two volcanoes (Koyanagi, et. al., 1966; Koyanagi, et. al., 1984; Endo, 1985). The volcanoes grow as the flanks are displaced from the summit-rift axes in the directions of least buttress laterally along the sub-horizontal zone of weakness separating the broad oceanic floor and volcanic rocks that locally accumulate above to form the Hawaiian ridge. Following a 6.1-magnitude earthquake on June 27, 1962, the earthquake rate continued at a gradually increasing rate until multiple aftershock sequences in September and October 1963. The earthquakes then assumed a relatively constant rate of 4.06 per month until mid-1966. The seismic-moment rate represented in figure 8d is influenced strongly by at least 3 earthquakes that exceeded 5.5 in magnitude, and the scale does not accommodate the relatively gradual changes caused by large numbers of small earthquakes. Following half year of erratic increase, a better than two-fold increase in recurrence rate was sustained until mid-1974. An acceleration in rate for several months thereafter climaxed into a higher rate and magnitude of earthquakes in November-December 1974. Following this period of intense activity, the earthquake rate assumed a pattern of a minor increase followed by successive decreases before the 6.6-magnitude earthquake consistent with the concept of precursory seismic quiescence (Koyanagi, et. al., 1984; Wyss, 1986). The dilatancy model requires increasing stress reflected

by the decreased earthquake rate in the epicentral region that persist for a variable length of time proportional to the magnitude of the subsequent major-earthquake. The tectonic effects of the 6.6-magnitude earthquake that struck the Kaoiki on November 16, 1983 was inferred to strongly influence the time and place of the 1984 eruption (Koyanagi, et. al., 1984). Seismicity at the lower-crustal and mantle regions along the magma-plumbing system decreased relatively following the apparent dilation-induced relaxation of stresses. Deformation measurements indicated extensions across the northeast rift zone (unpublished HVO data). These events were inferred to reduce flow restrictions along the subvertical plumbing system and the connections to the northeast rift zone, thus encouraging increased supply rate of magma to the summit reservoir and increasing the possibility of eruption along the northeast rift zone. Following the March-April eruption logrithmic-decay pattern of the 1983 aftershocks assumed a more linear rate typical of long-term activity in the Kaoiki region. The pattern continued throughout 1985.

E. Earthquake Magnitude-Frequency

The pattern of earthquake distribution in magnitude that sometimes vary from volcanically-to tectonically-influenced environments were examined and graphically summarized in figure 9 (a-d). The magnitude-frequency parameter b from the logrithmic relationship of earthquake number (N) and earthquake magnitude (M), Log N = A - bM (Richter, 1958) provides an index for the size distribution of the earthquake data-set. High b-values characterize earthquake swarms concentrated in volcanic regions in a highly-fractured low-stress state; low b-values are associated with tectonic-aftershock sequences where wide magnitude-space-time intervals of earthquakes occur under high-stress conditions (Scholz, 1968; Klein, 1982). Earthquakes in Hawaii are generally constrained in b-values according to the regional and source parameters that would permit differentiation of volcanic and tectonic regimes, but of added interest is the temporal changes in the magnitude-frequency slope within an active sequence that describe the progressive changes in stress conditions as was reported for Kaoiki earthquakes preceding the 1983 event (Koyanagi, et. al., 1984). Similarly, temporal variations in b-values inferred the changing state of stress beneath Mauna Loa during the magmatic processes along the summit reservoir and plumbing system.

Mauna Loa earthquakes within map coordinates 19° 20'-35'N and 155° 25'-45'W at depths of 0-15 km that encompassed the dynamic summit reservoir and the connecting plumbing system in the lower crust were chosen at a lower-magnitude threshold of 1.5 for magnitude-frequency assessment. B-values were calculated with 200 or more events per data-set for critical inflation-deflation periods associated with the 1975 and 1984 eruptions.

During the period of accelerated seismicity and inflation preceding the 1975 eruption, b-values progressively increased for three consecutive semi-annual intervals (figure 9a). A b-value of 0.65 during the first half of 1974 increased to 0.85

in Jul-Dec 1974, and progressed to 1.28 during the last half year before the eruption. This progressive narrowing of the magnitude intervals reversed into a decreasing pattern during the post-eruption deflation and intrusion, and the period of general relaxation in strain-release rate (figure 9b).

The gradually developing seismicity and inflation before the 1984 eruption was accompanied by generally small earthquakes, and consequently high b-values that contrasted with the earlier activity in 1974-75. The pre-eruption temporal trend was similar, however, in that there was a progressive long-term increase in b-value prior to the outbreak (figure 9c). In contrast to the 1975 pattern, the post-eruption b-value increased (figure 9d). Contributing to this high b-value was the large number of small-shallow earthquakes that persisted after the major summit-deflation accommodating the voluminous 3-week eruption on the northeast-rift.

F. Classification of Seismic Waveform Signatures

The pre-eruption seismicity and the activity during and following the 1984 Mauna Loa eruption included a variety of signatures similar to those registered at Kilauea. The seismic events are generally classified into short-period earthquakes, long-period events and harmonic tremor according to waveforms as previously mentioned, and their relationship to volcanic structure and activity (Koyanagi, 1982; Koyanagi and others, in press) are detailed as follows:

(1) Short-period (SP) earthquakes are the most common type of earthquakes that occur widely in the southeastern part of the Hawaiian Islands, and particularly beneath the active volcanoes Mauna Loa and Kilauea. They constitute more than ninety percent of the earthquakes detected and processed in Hawaii, and are heavily concentrated in the crust from about 0 to 15 km in depth in tectonic regions subjected to volcanic stress. The shallowest earthquakes between 0 and 5 km generally coincide with magmatically-induced ground deformation events. Their occurrences define the locations and times of volcanic activity. The magnitude range of SP earthquakes is wide. Correspondingly, the magnitude-frequency parameter b (Richter, 1958, p. 359) is commonly low at about 0.5 to 1.5, with a tendency for shallow volcanic swarm-earthquakes to be relatively higher than aftershock sequences and isolated earthquakes in outlying tectonic regions. The seismic signature has a pronounced onset of high frequency waves that attenuate exponentially with time. The dominant frequency changes systematically from about 15 Hz at the onset to less than 1 Hz at the end of the coda. High-frequency body waves are strong on deeper SP earthquakes. Low-frequency and low-velocity surface waves, and signal envelopes that tend to elongate characterize shallow events recorded at increasing epicentral distances.

(2) Long-period (LP) earthquakes occur only in places of active volcanism and suspected magma movement such as beneath the summit region of Kilauea. They often accompany harmonic

tremor. Their seismic signature and mode of occurrence suggest that these events may be discrete episodes that, in some instances, increase in numerical rate to collectively form harmonic tremor. The frequencies of the seismic waves often range from 1 to 5 Hz, and do not substantially change from the start to the end of an individual event. The signal onset is emergent and elongated compared to typical SP earthquakes. Magnitude is low and narrow in range, and the poorly defined magnitude-frequency parameter b appears to be correspondingly high ranging from about 1.5 to 2.5.

(3) Harmonic tremor is the seismic indicator of magma movement and volcanic eruptions in Hawaii. It is classified into depth categories of shallow, intermediate and deep depending on amplitude differences recorded on the seismic network. In general, tremor signals are sustained in duration, and relatively constant in amplitude and frequency. In detail, amplitude and frequency constantly oscillate within a limited range at time intervals of a few to about 10 seconds. Shallow tremor (<5km) accompanies eruptions, and the recorded amplitude is highest in the active vent region and varies roughly in proportion to the lava output rate. The frequency of the seismic waves ranges mainly from about 1 to 10 Hz, and is sometimes superimposed on lower frequencies. Shallow tremor recorded within about 2 km of the eruptive vent has dominant frequencies of 2 to 5 Hz, and at more distant locations several tens of km away, 1 to 3 Hz signals are common. Bursts of tremor ranging from minutes to days in duration sometimes occur independent of eruptive activity. Shallow tremor may accompany intrusions recorded by ground deformation. The attenuation rate of amplitude across the seismic network distinguishes the intermediate depth tremor (mostly 6 to 12 km) in the lower crustal region beneath the summit from the deeper tremor (mostly 30 to 60 km) in the upper mantle that extends broadly southwest of Kilauea. The sources of tremor in Hawaii were further quantified by hypocenter distribution of associated long-period events (Koyanagi, et. al., 1987).

ERUPTION AND POST-ERUPTION SEISMICITY

A. Chronology

Swarm earthquakes and harmonic tremor accompanied the 1984 eruption of Mauna Loa. Signals telemetered to the Observatory from our summit stations MOK, WIL, and SWR that form a tripartite along the rim of Mokuaweoweo (figure 2) registered increase of shallow earthquakes at 22:55 HST, March 24. Tiny earthquakes less than 0.1 in magnitude recorded at a rate of 2 to 3 per minute. At 23:30 the increasing seismic background marking the onset of harmonic tremor, combined with the increased changes and pattern of ground-tilt, was attributed to accelerated movement of magma beneath the summit. The earthquake swarm and tremor strengthened rapidly before 01:00, March 25 (figure 10 and 11). Between 00:50 and 02:10 the earthquake swarm peaked with 7

moderate earthquakes registered at 3.0 to 4.2 in magnitude. An infrared detector from a military satellite recorded a positive signal from Mauna Loa at 01:25 March 25 to indicate the onset of the eruption (Lockwood, et.al., 1985).

The intrusion-related earthquake swarm and harmonic tremor at the summit decreased at about 02:15, marking the beginning of about 5 hours of comparatively low seismicity. Between 07:00 and 09:15 summit tremor continued to decrease, but small earthquakes increased at the summit and on the northeast rift zone midway between Mokuaweoweo and Pu'u Ulaula. The apparently shallow earthquakes were mostly too small for conventional hypocenter determination. A temporary increase of microearthquakes in the summit region was followed by a general decrease for nearly 3 days, followed by varying frequencies of relatively high counts associated with deflationary structural adjustments.

At 09:17 March 25 harmonic tremor increased in the northeast rift zone. The tremor intensity reached saturation level on the nearby Pu'u Ulaula seismometer, and the required reset in sensitivity was made later on April 4. The strong tremor was recorded on stations more than 30 km away. For the remainder of the vigorous eruption, tremor centered in the northeast rift zone with intensity generally attenuating as a function of distance from the active vents near Pu'u Ulaula. The dominant period of the tremor signals recorded on the seismographs varied from about 0.2- to 0.6-second and in part was controlled by recording distance from the eruption zone. The relatively shorter period of tremor dominated on stations within a few kilometers from the eruption. Short-period tremor was also prominent during the intrusion and early stage of eruption. Tremor remained constantly strong on nearby PLA station until April 12, and after several days of low activity, decreased to nearly background on April 15. The relatively distant stations MLO and HSS located about 8 km from the center of eruption showed highest tremor from March 25 to March 28, followed by a lower level until April 2, and a subsequent gradual decay until the end of the eruption on April 15. The tremor data is evaluated in further detail in the next section.

Shallow earthquakes associated with the summit deflation started to increase from March 28, peaked at 50 to 100 shocks per hour on April 5 to 8 and remained considerably high through mid-April (figures 12 and 13). The longer-termed daily frequency pattern indicates an increasing microearthquake rate at the summit in late March that double-peaked before mid-April, and rapidly decreased during the remainder of the month (figure 13a). These earthquakes related to subsidence of the summit were mostly smaller than magnitude 1, shallower that 5 kilometers, and centered in the caldera region. An exceptionally large one in April 9 measured magnitude 3.9 and located 2 kilometers beneath the caldera.

The decaying rate of daily earthquakes at the summit was compensated with corresponding increase in northeast rift events. Occurrences of numerous small short-period and long-period earthquakes near the vents on the northeast rift became obvious after the eruptive activity as the background of high tremor

subsided. As was indicated in figure 13, these events essentially less than 0.1 in magnitude increased from several hundreds to many hundreds per day from mid-April, peaking at nearly 2000 per day in early May, and subsiding to a gradually decaying pattern after June. The post-eruption events apparently caused by local stresses induced by gravitational and thermal gradients, and degassing activity at the vents decreased episodically with counts fluctuating between 50 to 100 per day until mid-1985. From about August 1985, micro-shock activity in the northeast-rift vent region decreased to nearly pre-eruption levels.

The 1984 eruption reportedly started at the summit-caldera Mokuaweoweo at about 01:25 March 25 and rapidly migrated along the northeast rift zone developing a 16-km spread of the linear vent-system (figure 14). After the initial day of spreading fissure eruption, the activity centered in the northeasternmost vent-system where the eruption continued with persistent high-rate of lava production for the remaining 20 days. The sustained eruption characterized by lava fountains tens of meters in height produced lava flows extending 25 km northeast from Pu'u Ulaula and approaching the principal cultural center of Hilo by about 6 km. The 1984 lavas enveloped an area of 48 km^2, with an estimated 220 million cubic meters of output.

Kilauea's continuation of episodic eruption at Puu Oo since 1983 was unaffected by the Mauna Loa eruption. Correspondingly, a Puu Oo eruptive episode near the end of March 1984 showed no anomalous affect on the ongoing eruption at Mauna Loa. The independent response of shallow seismicity and ground deformation maintained during the simultaneous eruptions provided evidence of separate summit-reservoir and rift systems within the crustal depths of the adjacent Mauna Loa and Kilauea volcanoes.

B. Eruption Tremor

Seismograms from the summit and near-vent stations were under constant manifestation of harmonic tremor during the pre-eruption intrusion and throughout the eruptive activity. The early intrusive and eruptive period was marked by relatively erratic seismicity with numerous shallow earthquakes and high-frequency tremor typically of 5 to 10 Hz signals at stations within a few kilometers of the source of activity. As intrusions and intermittent fissure outbreaks progressively diminished into more stable continuous lava-fountaining from a confined vent system on the northeast rift, the seismic activity accordingly followed with relatively constant-amplitude harmonic tremor with frequencies that dominated at about 1 to 5 Hz at distances of a few kilometers from the active vent. The amplitude and frequency were generally highest near the vent. Amplitude varied according to the eruptive vigor and accompanying rate of magma flow. Tremor intensity responded positively to apparent barriers which restrict magma flow within the conduit system and degassing activity. Characteristically, the amplitude and frequency of harmonic tremor constrained within a limited range varied repeatedly at short intervals of time.

The initially high tremor and earthquake rate at the summit

station MOK followed the intrusion and eruption pattern and migrated along the northeast rift to the local station PLA (also in figure 10). The eruption stabilized with sustained output of lava from a single-vent-system that resided 1.7 km northeast of PLA station for the remainder of the eruption sustained until April 15. During this prolonged stage of eruption the amplitude of tremor remained consistently highest at PLA station. In the outlying stations (MLO, HSS, MOK) there is a progressive decrease in tremor amplitude during the latter weeks of eruption. Part of this decrease coincided with gradual decrease in eruptive rate. But the consistent overall pattern of tremor decrease does not satisfactorily correlate with the pattern of decreased lava output. This is attributed to increasing efficiency in the conduit system caused by the gradual breakdown of barriers with continuous flow of magma during the course of the eruption (Aki and Koyanagi, 1981; Koyanagi, et. al., 1986).

The continuous harmonic tremor during the sustained eruption in early April recorded by the HVO network of permanent seismograph stations was additionally monitored intermittently with a portable seismograph at 17 temporary stations to provide a 20-km long profile along the Mauna Loa trail extending from the eruptive area southeastward towards Kilauea (figure 15). Samples of seismograms for alternate stations along the profile in figure 15 indicate the generally attenuating pattern of tremor intensity with increasing distance from the eruptive vent. Dominant frequencies of the recorded tremor varied from about 1 to 5 Hz.

The dominance of strong high-frequency tremor generated by near-vent oscillations and fountaining during the outbreaks of both Kilauea and Mauna Loa on March 30, 1984, is illustrated in figure 16. At normal sensitivities stations PLA and KMM located about a km from the eruptive vents, respectively at Mauna Loa and Kilauea, were simultaneously saturated with high frequency tremor. Amplitude of tremor at the temporary stations recorded on strip-chart paper using the portable seismographs were reduced according to system response and magnification, and normalized with a continuously-recording permanent station MLO. Amplitudes from the temporary stations were divided by amplitudes from MLO station for the respective time-interval to compensate for any changes in tremor amplitude caused by variations in the eruptive intensity. Allowing for background noise and site variations in ground amplification, the reduced amplitudes of the eruption tremor attenuated logrithmically as a function of distance from the active vent. The decay pattern and slope for the tremor samples taken from April 4 - 12 may be formulated from a line fitted to the data points in a log-log relation, $\log A = 1.94 - 1.08 \log D$, where A refers to relative amplitude of tremor and D indicates station-to-vent distance (figure 17). The constant derived at 1.08 describes the slope of the tremor decay pattern.

Permanent stations on the HVO network that continuously recorded the seismic activity were independently selected for limited time-intervals and additionally monitored on a 6-channel recorder. Samples of tremor signals filtered with center frequencies set at 0.625, 1.25, 2.5, 5.0 and 10.0 Hz in figure 18 describe the short-term variation in the tremor. The signal

constahtly fluctuates in dominant frequency at intervals of a few to many seconds apart. This characteristic oscillation in the tremor signal correlates with the common pattern of intense lava fountaining which appears to be sustained by successive pulsations of fountain-bursts that repeatedly occur seconds apart overlapped by longer separations of episodes in minutes. This signature pattern of tremor is also seen in deep tremor unrelated to eruptive activity, and may be related to a fundamental process of alternating increase and decrease in pressure and conduit configuration that drives magma through the conduit system and finally reflected in the observed lava-fountaining.

Amplitudes from the filtered signals of these four stations were normalized and reduced according to the system response and magnification. Allowances were made for station variations in background noise and ground amplifications and leakage in the filtered system. The adjusted amplitudes were plotted for the 5 filtered signals (figure 19). Dominant frequencies were generally higher at stations located near the source vent. At PLA located 1.7 km from the eruptive vent the 2.5 Hz signal was strongest. At MLO and HSS stations at distances of 7.5 and 8.7 km, respectively, 1.25 and 2.5 Hz tremor dominated. MOK station located 17 km from the active vent was dominated by signals that decreased to lower dominant frequencies, ranging from 0.625 to 2.5 Hz. MOK, located on the north rim of the caldera was also influenced by a less-intense secondary source of seismicity associated with deflation and the withdrawal of magma from the summit reservoir.

The normalized amplitudes of tremor from the filtered signals of the four stations follow the logrithmic distance-attenuation pattern as in figure 17 (figure 20). Expectedly the higher frequencies with center frequencies at 10 and 5 Hz attenuate with distance more rapidly than the lower frequencies. Accordingly, decreasing slope angles are reflected by the decreasing slope constants on the 5.0 to 0.625 Hz plots in the log-log amplitude-distance relationship. The slope constants as shown are 2.92 for 10 Hz, 2.30 for 5 Hz, 1.96 for 2.5 Hz, 1.60 for 1.25 Hz and 0.65 for 0.625 Hz.

SUMMARY

The concepts of volcanic structure and process developed from analyses of comprehensive data-sets accumulated on Kilauea during its past three decades of accelerated seismo-volcanic activity provide the base to construct a model for Mauna Loa. Fundamental similarities in geologic structure, and seismicity and ground-deformation pertaining to volcanic behavior exist between these neighboring volcanoes. The regional stress system generated by the progressive southeasterly growth of the Hawaiian ridge, in turn, dictates structural configuration and process of new volcanic systems that form on the advancing front.

The rate and pattern of growth of the Hawaiian islands are

controlled by the amount of magma generated in the mantle that feed volcanic intrusions onto the dynamic Pacific plate. The plate moves northwestward and constantly away from the Hawaiian "hot spot" at a rate of few centimeters per year. The rate of lava output is episodically influenced by the variations in stress caused by major tectonic earthquakes and volcanic events. Near-surface stress drops in the delicately balanced pressure system are effectively translated through the fluid column to increase buoyant forces and accelerate the upward fluid-flow.

The spatial-distribution of inflation-related swarm earthquakes at less than 5 km beneath the eruptive volcanic-centers and complementary tectonic earthquakes along the volcano's flanks constrain the volumetric configuration of summit reservoir and rift conduit. A reservoir within a 8-km wide zone and centered about 3 to 9 km beneath the summit-caldera is connected to a 5-km wide subvertical conduit zone extending below 50 km in depth. The conduit links laterally to a 30 km-wide central magma-complex to the south at 30 to 60 km in depth. Hypocenters of long-period events associated with volcanic tremor further outline a feeding system from this deep mantle system that radiate to the 3 dynamic volcanic systems of Kilauea, Mauna Loa and Loihi. The pattern reflects progressive southeasterly growth of the island chain as the Pacific plate drifts northwesterly over the relatively fixed location of the Hawaiian "hot spot".

Earthquake frequency is increasingly influenced by swarms of small events that accommodate localized stress-drops and ultimately reflects regional buildup of strain. Seismic moment rate, on the other hand, is dictated by scattered high-magnitude earthquakes that relate to a regional relief of stress and would expectedly accelerate episodically to accommodate the gradual development of regional strain. Accordingly, the cumulative number of earthquakes follows the temporal pattern of regionally-elastic ground deformation indicated by horizontal and vertical micro-strain measurements. Seismic-moment rate accommodates regional rupture patterns and inelastic tectonic displacement emphasized by high-magnitude earthquakes from regional buildup of strain.

Magnitude-frequency distribution of earthquakes describes the stress conditions in the dynamic volcanic regime. B-values vary inversely to the effective state of stress. The temporal decrease in stress caused by continuing seismic activity during the inflationary period are sometimes reflected in a trend of increasing b-values. B-values are generally higher in shallow highly-fractured volcanic-regimes influenced by concentrated changes in stress, and contrastingly lower in outlying high-stress tectonic regions characterized by earthquakes distributed at wide space-time-magnitude intervals. The magnitude-frequency slope increase temporally as the range of earthquake-magnitude narrows during swelling of the summit and persistent influx of magma in the volcanic environment. The progressive increase in microearthquake rate and microfracturing relieve the stresses in the retaining wallrocks.

Inflation-related shallow earthquakes increase episodically

at intervals of 3 to 6 months and temporarily decrease within a few days before the eruption describing the sequence of shallow magma influx that ultimately result in fissure-opening, and subsequent eruption. The increasing rate of migration of deep to shallow crustal-earthquakes attests to the increasing efficiency of stress interaction within the pressure regime as the inflationary process advances toward eruption. Earthquakes are generated from lateral stresses induced by the magma ascent as the flanks are incrementally displaced away from the intruded summit-rift axis along a weakened zone of separation between the oceanic floor and volcanic rocks that lie above. Shallow earthquakes swarm in the caprocks above at 3 to 5 km depth along the summit-rift axis with the force of the rising magma.

Short-period earthquakes reflect the tectonic response to magma pressure and regional strain. These separate into "volcanic earthquakes" that occur episodically in swarms localized in time and place of magma-intrusion, and "tectonic earthquakes" that accompany volcanic events over a wide range of time, space and magnitude. Harmonic tremor and related long-period events uniquely occur in places and times of vigorous magma movement and volcanic eruption.

These seismic parameters placed in temporal and spatial context with corroborating first-motion data outline the magmatically-induced stress orientation and volcanic process at Mauna Loa. Figure 21 portray the dynamic magma transport system and sequence constrained by the hypocentral distribution of inflation-related earthquakes. Magma from the central source region in the mantle beneath south Hawaii is transmitted laterally into the Mauna Loa plumbing system. The magma rises subvertically along a sinuous plumbing system. The clustered pattern of hypocenter distribution along the steep transport path indicates localizations in lateral stresses and magma volumes. Pressure buildup at the top of the column forming the reservoir system about 3-9 km below the summit lead to eruptions. Over-pressurization may be accommodated by eruptions at the summit or along one of two laterally-extensive rift zones. The rift zones maintain intrusive susceptibility by over-pressurization in the summit-reservoir complex and tectonic displacement of the flanks that lowers stresses along the rift zones. Rift growth is accommodated by the lateral displacement of the flanks along the subhorizontal zone separating the local volcanic rocks that rest onto the regional oceanic floor.

ACKNOWLEDGEMENT

This compilation of data is dedicated primarily to the seismic staff of the Hawaiian Volcano Observatory who contributed many years of constant effort maintaining an islandwide network of seismographs and daily processing of the collected data. George Kojima assisted by Gary Honzaki kept the extensive seismic instrumentation in constant operation throughout the past two decades. Jennifer Nakata, Wilfred Tanigawa, and Alvin Tomori responsibly conducted day-to-day processing of the seismic data.

The technical preparation of this report benefited from the effective support of student employees. Sandra Zane assisted in the preparation of figures, and Pauline Tamura prepared typed drafts of the manuscript. The author is grateful to Tom Wright and Reggie Okamura for their helpful suggestions and reviews of the paper.

REFERENCES

Aki, K., and Koyanagi, R.Y., 1981, Deep volcanic tremor and magma ascent mechanism under Kilauea, Hawaii: Journal of Geophysical Research, v. 86, n. B8, p. 7095-7109.

Ando, M., 1979, The Hawaii earthquake of November 29, 1975: Low dip angle faulting due to forceful injection of magma: Journal of Geophysical Research, v. 84, p. 7616-7626

Crosson, R.S., and Endo, E.T., 1981, Focal mechanisms of earthquakes related to the 29 November 1975 Kalapana, Hawaii earthquake: The effect of structure models. Bulletin of the Seismological Society of America, v. 71, p. 713-729.

Decker, R.W., Koyanagi, R.Y., Dvorak, J.J., Lockwood, J.P., Okamura, A.T., Yamashita, K.M., and Tanigawa, W.R., 1983, Seismicity and surface deformation of Mauna Loa Volcano, Hawaii: American Geophysical Union Transactions, Eos, v. 64, no. 37 p. 545-547.

Dzurisin, D., Koyanagi, R.Y., and English, T.T., 1984, Magma supply and storage at Kilauea Volcano, Hawaii, 1956-1983: Journal of Volcanology and Geothermal Research, v. 21, p. 177-206.

Eaton, J.P., 1962, Crustal structure and volcanism in Hawaii, in Crust of the Pacific Basin: American Geophysical Union Monograph, no. 6, p. 13-29.

Eaton, J.P., 1969, HYPOLAYR, a computer program for determining hypocenters of local earthquakes in an earth consisting of uniform flat layers over a half space: U.S. Geological Survey Open-File Report, 155 p.

Ellsworth, W.L., and Koyanagi, R.Y., 1977, Three-dimensional crust and mantle structure of Kilauea Volcano, Hawaii: Journal of Geophysical Research, v. 82, p. 5379-5394.

Endo, E.T., 1985, Seismotectonic framework for the southeast flank of Mauna Loa Volcano, Hawaii: Seattle, University of Washington, PhD dissertation, 350 p.

Endo, E.T., Koyanagi, R.Y., Nakata, J.S., and Tanigawa, W.R., in preparation, Strike-slip faulting associated with the inflation of the summit magma-reservoir of Mauna Loa Volcano, Hawaii.

Endo, E.T., Koyanagi, R.Y., and Okamura, A.T., 1972, Hawaiian Volcano Observatory Summary 57: Preliminary Report of the U.S. Geological Survey, 54 p.

Fiske, R.S., and Jackson, E.D., 1972, Orientation and growth of Hawaiian volcanic rifts: the effect of regional structure and gravitational stresses: Proceedings from

the Royal Society of London, series A, v. 329, p. 299-326.

Hill, D.P., 1969, Crustal structure of the island of Hawaii from seismic-refraction measurements: Bulletin of the Seismological Society of America, v. 59, p. 101-130.

Johnston, A.C., 1978, Localized compressional velocity decrease precursory to the Kalapana, Hawaii earthquake: Science, v. 199, p. 882-885.

Johnston, A.C., Wyss, M., Koyanagi, R.Y., and Habermann, R.E., 1982, P-wave travel times: stability and change within the source volume of a M=7.2 earthquake: Journal of Geophysical Research, v. 87, p. 6889-6905.

Klein, F.W., 1978, Hypocenter location program HYPOINVERSE: U.S. Geological Survey Open-File Report 78-694, 113 p.

Klein, F.W., 1982a, Earthquakes at Loihi submarine volcano and the Hawaiian hot spot: Journal of Geophysical Research, v. 87, p. 7719-7726.

Klein, F.W., and Koyanagi, R.Y., 1980, Hawaiian Volcano Observatory seismic network history 1950-79: U.S. Geological Survey Open-File Report 80-302, 84 p.

Koyanagi, R.Y., 1982, Procedure for routine analyses and classification of seismic events at the Hawaiian Volcano Observatory, part 1. U.S. Geological Survey Open-File Report 82-1036, 77 p.

Koyanagi, R.Y., Chouet, B., Aki, K., 1987, Volcanic tremor in Hawaii part I: Compilation of seismic data from the Hawaiian Volcano Observatory, 1969 to 1985: U.S. Geologic Survey Professional Paper 1350, v. 2, ch. 45, p. 1221-1257.

Koyanagi, R.Y., Endo, E.T., and Ebisu, J.S., 1975, Reawakening of Mauna Loa Volcano, Hawaii: A preliminary evaluation of seismic evidence: Geophysical Research Letters, v. 2, no. 9, p. 405-408.

Koyanagi, R.Y., Endo, E.T, Tanigawa, W.R., Nakata, J.S., Tomori, A.H., and Tamura, P.N., 1984, Kaoiki, Hawaii earthquake of November 16, 1983: A preliminary compilation of seismographic data at the Hawaiian Volcano Observatory: U.S. Geological Survey Open-File Report 84-798.

Koyanagi, R.Y., Krivoy, H.L., and Okamura, A.T., 1966, The 1962 Kaoiki, Hawaii, earthquake and its aftershocks: Bulletin of the Seimological Society of America, v. 56, p. 1317-1335.

Koyanagi, R.Y., Meagher, K., Klein, F.W., and Okamura, A.T., 1978b, Hawaiian Volcano Observatory Summary 75 January

to December 1975: Preliminary Report of the U.S. Geological Survey, 117 p.

Koyanagi, R.Y., Nakata, J.S., and Tanigawa, W.R., 1981, Seismicity of the lower east rift zone of Kilauea Volcano, Hawaii, 1960 to 1980: U.S. Geological Survey Open-File Report 81-984, 26 p.

Koyanagi, R.Y., Stevenson, P., Endo, E.T., and Okamura, A.T., 1978a, Hawaiian Volcano Observatory Summary 74 January to December 1974: U.S. Geological Survey Preliminary Report, 164 p.

Koyanagi, R.Y., Swanson, D.A., and Endo, E.T., 1972, Distribution of earthquakes related to mobility of the south flank of Kilauea Volcano, Hawaii: U.S. Geological Survey Professional Paper, 800-D, p. D89-D97.

Koyanagi, R.Y., Tanigawa, W.R, and Nakata, J.S., Seismicity associated with the eruption of Kilauea Volcano from January 1983 to July 1984: U.S. Geological Survey Professional Paper 1463, ch. 7 (in press).

Koyanagi, R.Y., Unger, J.D., Endo, E.T., and Okamura, A.T., 1976a, Shallow earthquakes associated with inflation episodes at the summit of Kilauea Volcano, Hawaii: Bulletin Volcanologique, v. 39, p. 621-631.

Lipman, P.W., 1980, Rates of volcanic activity along the southwest rift zone of Mauna Loa Volcano, Hawaii: Bulletin Volcanologique, v. 43-4, p. 703-725.

Lockwood, J.P., Banks, N.G., English, T.T., Greenland, L.P., Jackson, D.B., Johnson, D.J., Koyanagi, R.Y., McGee, K.A., Okamura, A.T., and Rhodes, J.M., 1985, The 1984 eruption of Mauna Loa Volcano, Hawaii: American Geophysical Union Transactions, Eos, v. 66, no. 16, p. 169-171.

Macdonald, G.A., and Abbott, A.T., 1970, Volcanoes in the Sea: University of Hawaii Press, Honolulu, Hawaii, 441 p.

Nakata, J.S., Koyanagi, R.Y., Tomori, A.H., Tanigawa, W.R., 1986, Hawaiian Volcano Observatory Summary 84: Prelimiary Report of the U.S. Geological Survey, 86 p.

Richter, C.F., 1958, Elementary Seismology: W.H. Freeman and Co, Inc.; eds. James Gilluly and A.O. Woodford, 768 p.

Ryall, A., and Bennett, D.L., 1968, Crustal structure of southern Hawaii related to volcanic processes in the upper mantle: Journal of Geophysical Research, v. 73, p. 4561-4582.

Scholz, C.H., 1968, The frequency-magnitude relation of

microfracturing in rock and its relation to earthquakes: Bulletin of the Seismological Society of America, v. 58, p. 399-415.

Swanson, D.A., Duffield, W.A., and Fiske, R.S., 1976, Displacement of the south flank of Kilauea volcano: the result of forceful intrusion of magma into the rift zones: U.S. Geological Survey Professional Paper 963, 39 p.

Tilling, R.I., Koyanagi, R.Y., Lipman, P.W., Lockwood, J.P., Moore, J.G., and Swanson, D.L., 1976, Earthquakes and related catastrophic events, island of Hawaii, November 29, 1975: U.S. Geological Survey Circular 740, 33 p.

Wyss, M., 1986, Seismic quiescence precursor to the 1983 Kaoiki (Ms=6.6), Hawaii, earthquake: Bulletin of the Seismological Society of America, v. 76, p. 785-800.

Zucca, J.J., and Hill, D.P., 1980b, Crustal Structure of the southeast flank of Kilauea Volcano, Hawaii from seismic refraction measurements: Bulletin of the Seimological Society of America, v. 70, p.1149-1159.

Zucca, J.J., Hill, D.P., and Kovach, R.L., 1982, Crustal structure of Mauna Loa Volcano, Hawaii, from seismic refraction and gravity data: Bulletin of the Seismological Society of America, v. 72, p. 1535-1550.

TABLE

Table 1. Amount and rate of earthquake number and moment of Mauna Loa earthquakes for various intervals of time with changes in earthquake rates as graphically inferred in figure 8 (a-d).

FIGURES

Figure 1. Map of the island of Hawaii, showing the five major

volcanoes that make up the island, and the historic lava flows (after Macdonald and Abbott, 1970).

Figure 2. Seismograph network operated on the island of Hawaii by the U.S. Geological Survey's Hawaiian Volcano Observatory. Seismometer locations are dotted and stations MOK, WIL, SWR, HSS, PLA, MLO, and AHU are emphasized with larger dots.

Figure 3. System response curves for short-period seismographs operated in Hawaii during the 1983-84 eruption of Kilauea are shown in the upper plot. The Type 1 curve applies to the standard HVO high-gain vertical components on a Develocorder based FM system, and the Wood-Anderson response applies to the lower sensitivity horizontal seismometers on 3-component stations. A filter system with center frequencies at 0.625 Hz, 1.25 Hz, 2.5 Hz, 5.0 Hz, and 10.0 Hz as shown in the lower plot was designed for a 6-channel chart recorder for spectral analysis of specific seismic events. The filtered signals from a designated station were assigned to 5 of the channels, and the normal unfiltered signal was recorded on the sixth channel.

Figure 4a. Daily number of microearthquakes in the summit region of Mauna Loa preceding and following the July 1975 eruption.

Figure 4b. Daily number of microearthquakes in the summit region of Mauna Loa preceding and following the March-April 1984 eruption.

Figure 5a. Earthquake locations in the Mauna Loa region from January 1, 1974-July 31, 1975. Included are earthquakes of magnitude 1.5 and greater, with vertical and horizontal standard error of less than 5 km, and within the geographic coordinates 19° 18'-40'N latitude and 155° 20'-50'W longitude.

Figure 5b. Earthquake locations in the Mauna Loa region from August 1, 1975-December 31, 1979. Included are earthquakes of magnitude 1.5 and greater, with vertical and horizontal standard error of less than 5 km, and within the geographic coordinates 19° 18'-40'N latitude and 155° 20'-50'W longitude. Earthquake symbols for depth in km and symbol sizes for magnitude are shown on the left.

Figure 5c. Earthquake locations in the Mauna Loa region from January 1, 1980-April 30, 1984. Included are earthquakes of magnitude 1.5 and greater, with vertical and horizontal standard error of less than 5 km, and within the geographic coordinates 19° 18'-40'N latitude and 155° 20'-50'W longitude.

Figure 6a. Earthquake locations in the Mauna Loa region from January 1, 1974 to April 30, 1984. Included are earthquakes of magnitude 1.5 and greater, with vertical and horizontal standard error of less than 5 km, and within the geographic coordinates 19° 18'-40'N latitude and 155° 20'-50'W longitude. A-B and C-D are reference lines for depth section plots in Figures 6b and 6c.

Figure 6b. Depth section along a 10-km wide zone centered on line A-B, perpendicular to the summit-rift axis, as shown in Figure 6a.

Scale and earthquake symbols are as in Figure 6a.

Figure 6c. Depth section along a 10-km wide zone centered on line C-D parallel to the summit-rift axis, as shown in Figure 6a. Scale and earthquake symbols are as in Figure 6a.

Figure 7. Time sequence of Mauna Loa earthquakes with respect to depth (upper plot) and magnitude (lower plot). Earthquakes sampled were those of magnitude 1.5 or greater from January 1, 1974 to April 30, 1984 located within the map coordinates 19° 18'-40'N latitude and 155° 20'-50'W longitude. To maintain suitable scaling, the major 6.6-magnitude Kaoiki earthquake on November 16, 1983, was omitted. The increase in the number of earthquakes from late 1983 is influenced by the aftershock activity in the southeast flank.

Figure 8a-d. Number and seismic moment of earthquakes at 4 regions beneath Mauna Loa plotted cumulatively as a function of time from 1962 to 1985. The selected earthquakes included those with magnitude of 2.0 or greater and horizontal and vertical standard errors in location of less than 5.0 km. Seismic moment was derived from the earthquake magnitude relation, Seismic moment=$10^{(A + B \times \text{magnitude})}$, where the constants A and B are designated at -6 and 1.4, respectively. Onset times of significant earthquakes and volcanic events are indicated numerically in chronological order: (1) 6.1-magnitude Kaoiki earthquake June 27, 1962; (2) 4.8-magnitude Kaoiki earthquake September 21, 1963; (3) 5.3-magnitude Kaoiki earthquake October 23, 1963; (4) several 3.0 to 3.5 magnitude earthquakes at various depths beneath the summit region in late 1970 and early 1971 (5) 4.8-magnitude Kaoiki earthquake June 19, 1974; (6) 5.5-magnitude Kaoiki earthquake November 30, 1974; (7) 4.7-magnitude shallow Mauna Loa summit earthquake December 15, 1974; (8) 4.8-magnitude Kaoiki earthquake December 15, 1974; (9) 5.5-magnitude Kilauea southwest rift earthquake December 31, 1974, accompanied by intrusion-swarm and eruption; (10) earthquake swarm and eruption Mauna Loa summit region July 5-6, 1975; (11) 7.2-magnitude Kilauea south flank earthquake November 29, 1975; (12) 6.6-magnitude Kaoiki earthquake November 16, 1983; (13) earthquake swarm and Mauna Loa summit to northeast rift eruption March 25-April 15, 1984. The earthquakes were separated and plotted according to 4 structural regions subjected to magmatically induced stresses beneath Mauna Loa; (a) shallow-summit region at 0-5 km depth within map coordinates 19° 20'-35'N and 155° 31'-45'W; (b) intermediate-depth summit region at 5-13 km depth within map coordinates 19° 20'-35'N and 155° 31'-45'W; (c) deep-summit region at 13-60 km depth within map coordinates 19° 20'-35'N and 155° 31'-45'W; (d) Kaoiki region on the southeast flank of Mauna Loa at 5-15 km depth within map coordinates 19° 19'-29'N and 155° 22'-32'W.

Figure 9a-d. Magnitude-frequency relation for Mauna Loa summit earthquakes at sequential time increments separated generally according to variations in seismic rates of shallow to intermediate depth summit earthquakes before and after the 1975 and 1984 eruptions as indicated in figure 8 (a-b). The data-set includes Mauna Loa summit earthquakes located within 19° 20'-35'N

latitude and 155° 31'-45'W longitude, and at depths of 0 to 15 km below the summit. The magnitude-frequency parameter b was calculated according to the logrithmic relationship of earthquake number (N) and earthquake magnitude (M), Log N = A - bM (Richter, 1958).

Figure 10. Number of earthquakes (upper 3 plots) and amplitude of tremor (lower 4 plots) plotted hourly during the Mauna Loa eruption, March 25-April 15, 1984. Earthquakes as small as 0.1 in magnitude detected on the summit and NE rift stations during times when the pertinent stations were not obscured by intense tremor were separated and tabulated according to their signature characteristics and source locality. Harmonic tremor read hourly from 4 seismograph stations were reduced to microns of ground motion; signals from PLA station only a km from the major eruptive activity on the NE-rift was saturated from March 25 - April 4 before sensitivity at the sensor was lowered.

Figure 11. Seismogram from Ahua (AHU) revolving smoke drum seismograph with sensor located 30 km southeast of the summit of Mauna Loa. Earthquake swarm starting at 22:50 HST and harmonic tremor related to the eruption are recorded in the lower portion.

Figure 12. Seismogram from Mokuaweoweo (MOK) revolving drum seismograph with sensor located on the NW-rim of Mokuaweoweo. Numerous small earthquakes generaly less than magnitude 0.5 followed the eruption-related collapse of the summit.

Figure 13a-d. Daily number of short- and long- period earthquakes detected locally on the summit stations (MOK, WIL, SWR) and short-period events detected near the northeast rift station Puu Ulaula (PLA). Detection threshold for these local events between January 1984 to December 1985 is about 0.1-magnitude.

Figure 14. Map showing distribution of eruptive vents and lava flows formed by the 1984 Mauna Loa eruption (after Lockwood, et. al., 1985).

Figure 15. Map of stations occupied by portable seismograph and the active vent during the continuing Mauna Loa eruption on April 11-12, 1984 (black dots) and 30-second samples of harmonic tremor recorded at alternating stations along the profile. Magnification is 16x higher on seismograms for stations 5 to 8 than that of stations 1 to 4.

Figure 16. Strip-chart recordings of harmonic tremor from simultaneous eruptions at Kilauea and Mauna Loa volcanoes at 12:50 H.S.T., March 30, 1984. Recording sensitivities are essentially the same for all six stations; stations located nearest the active vents, PLA for Mauna Loa and KMM for Kilauea, were saturated at clipping levels.

Figure 17. Tremor amplitude plotted as a function of distance from the eruptive vent during relatively constant and localized eruptive fountaining. Amplitudes were reduced from signals recorded on a portable seismograph and normalized with signals from a continuously recording permanent station MLO located 7.5

km from the active vent. The log-log relation is calculated from the line fitted to the data points indicated by circles.

Figure 18a-d. Fifty-second sections of tremor recorded intermittently at stations (a) PLA located 1.7 km southwest of the eruptive vent, (b) MLO located 7.5 km southeast of the eruptive vent, (c) HSS located 8.7 km north of the eruptive vent, and (d) MOK located on the north rim of the summit caldera Mokuaweoweo at 17 km west of the active vent. On each of the strip-chart seismograms, the lowermost signal on channel 6 is unfiltered HVO Type 1 system, and the signals above on channels 1 to 5 are filtered. The peak responses and relative magnifications for the filtered channels are, respectively, 0.625 Hz at x2, 1.25 Hz at x10, 2.5 Hz at x26, 5.0 Hz at x60, and 10.0 Hz at x100. The overall relative magnifications of the filtered signals between stations are x1 for PLA, x2 for MLO and HSS, and x4 for MOK.

Figure 19. Amplitudes averaged and normalized from 50-second samples of filtered signals with center frequencies at 0.625, 1.25, 2.5, 5.0, and 10.0 Hz. The tremor was recorded on April 11, 1984, at 4 stations ranging from 1.7 to 17 km in epicentral distances to the eruptive vent. For clarity, the amplitudes plotted for station MOK is magnified 10x that of the other stations HSS, MLO, and PLA that were located closer to the eruptive vent.

Figure 20. Amplitude attenuation of filtered tremor signal plotted as a function of distance from the eruptive vent on the northeast rift zone. Filtered signals of tremor were recorded at various stations and times on April 11, 1984, as indicated in figures 18 and 19. The log-log relation for each frequency category is calculated from a line fitted to the circled data points.

Figure 21. Characterization of the magma transport system beneath Mauna Loa constrained by earthquake hypocenters as profiled normal to the summit-rift axis in figure 6b. The dynamic transport zone is outlined by a matrix of dots of increasing density to infer relative sensitivity to pressure changes within the conduit system; the highly responsive summit-reservoir system is defined within a 8-km-wide zone 3 to 9 km beneath Mokuaweoweo. Arrows infer the sinuous path of magma ascent from the mantle source region to the summit reservoir.

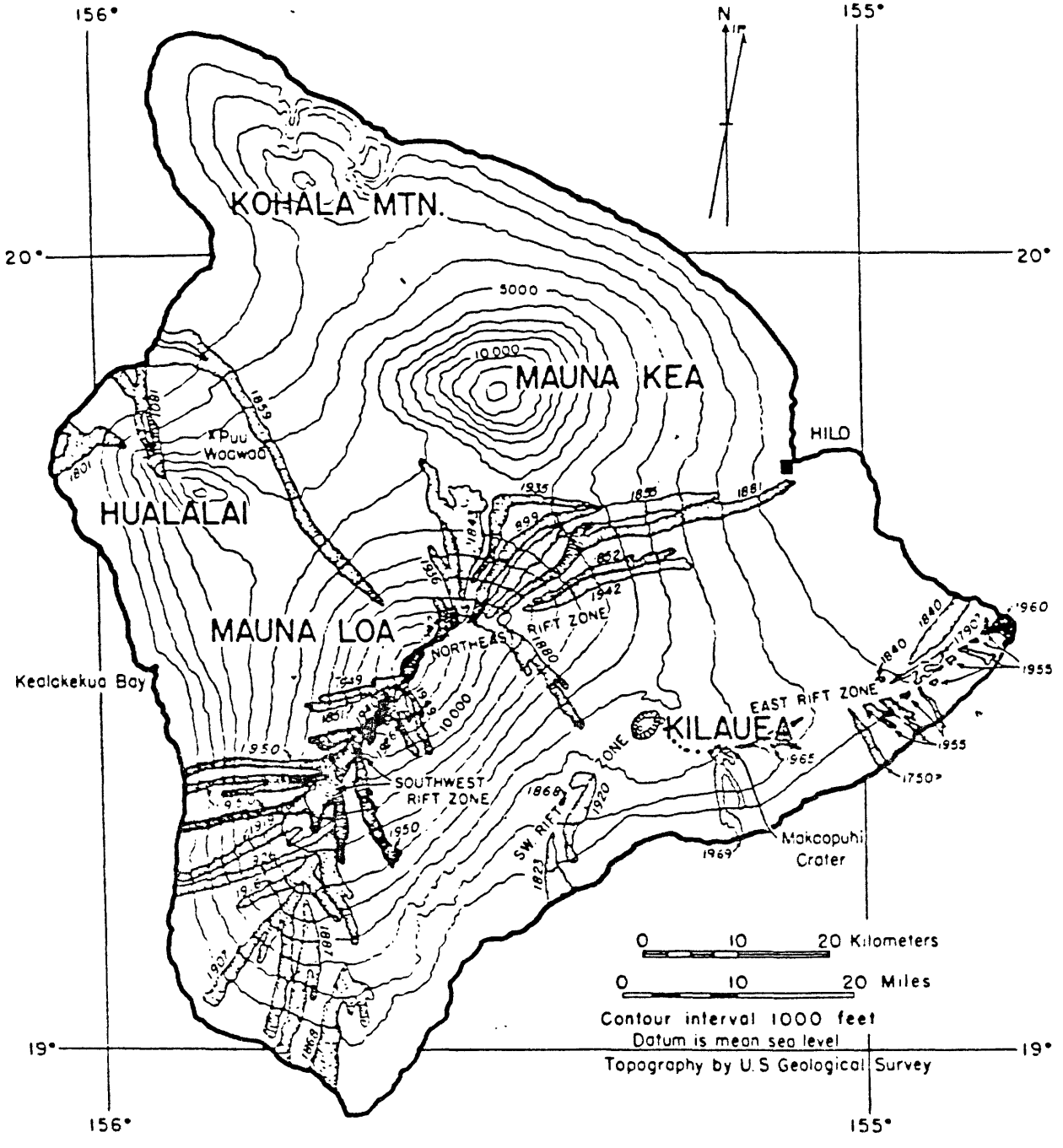
156°
155°
N
20°
19°
KOHALA MTN.
MAUNA KEA
HILO
Puu Waawaa
HUALALAI
MAUNA LOA
NORTHEAST RIFT ZONE
EAST RIFT ZONE
KILAUEA
SOUTHWEST RIFT ZONE
SW. RIFT ZONE
Makaopuhi Crater
Kealakekua Bay
5000
10000
0 10 20 Kilometers
0 10 20 Miles
Contour interval 1000 feet
Datum is mean sea level
Topography by U.S Geological Survey

Figure 1

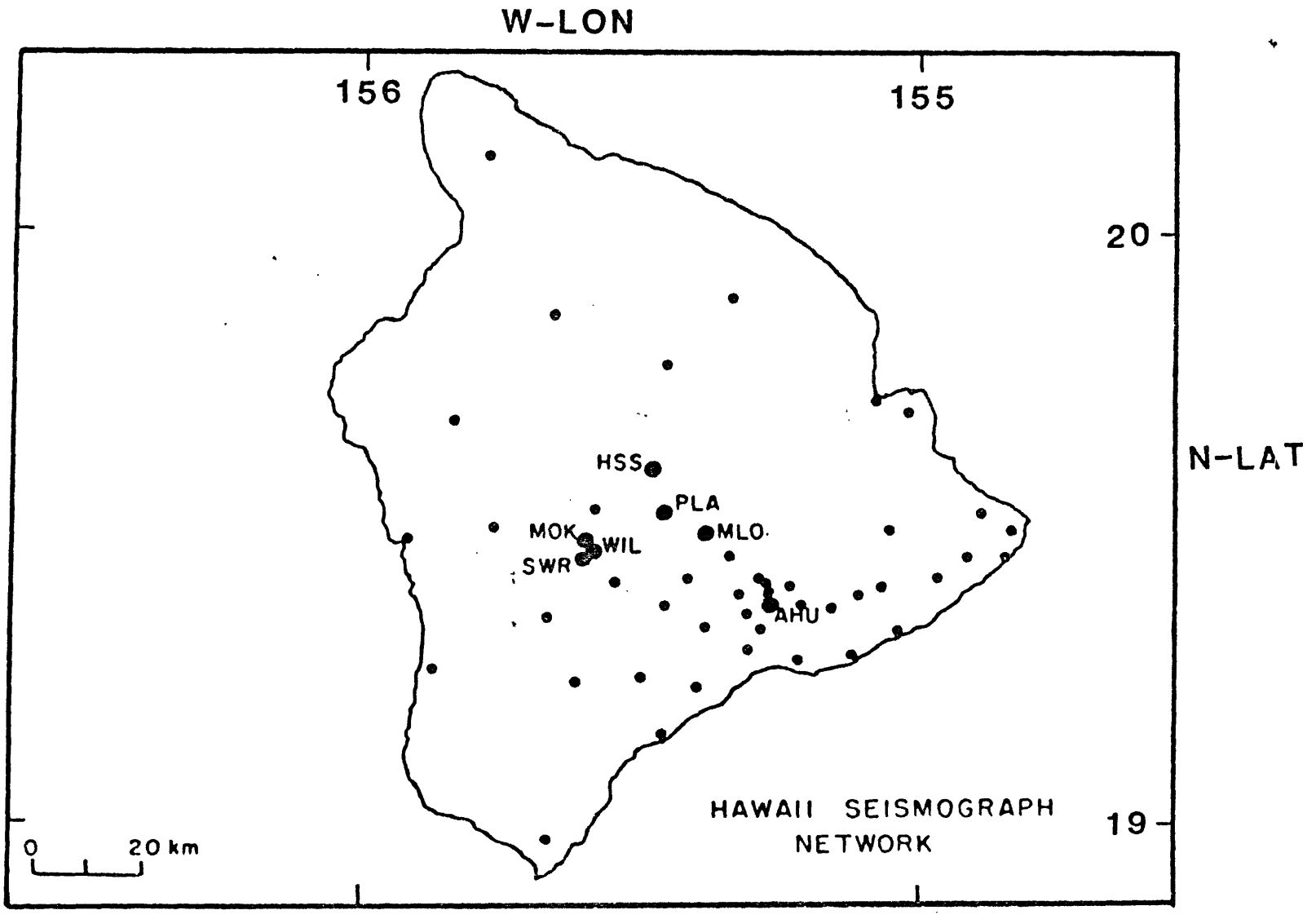
W-LON
156
155
20
19
N-LAT
HSS
PLA
MLO
MOK
WIL
SWR
AHU
0
20 km
HAWAII SEISMOGRAPH
NETWORK

Figure 2

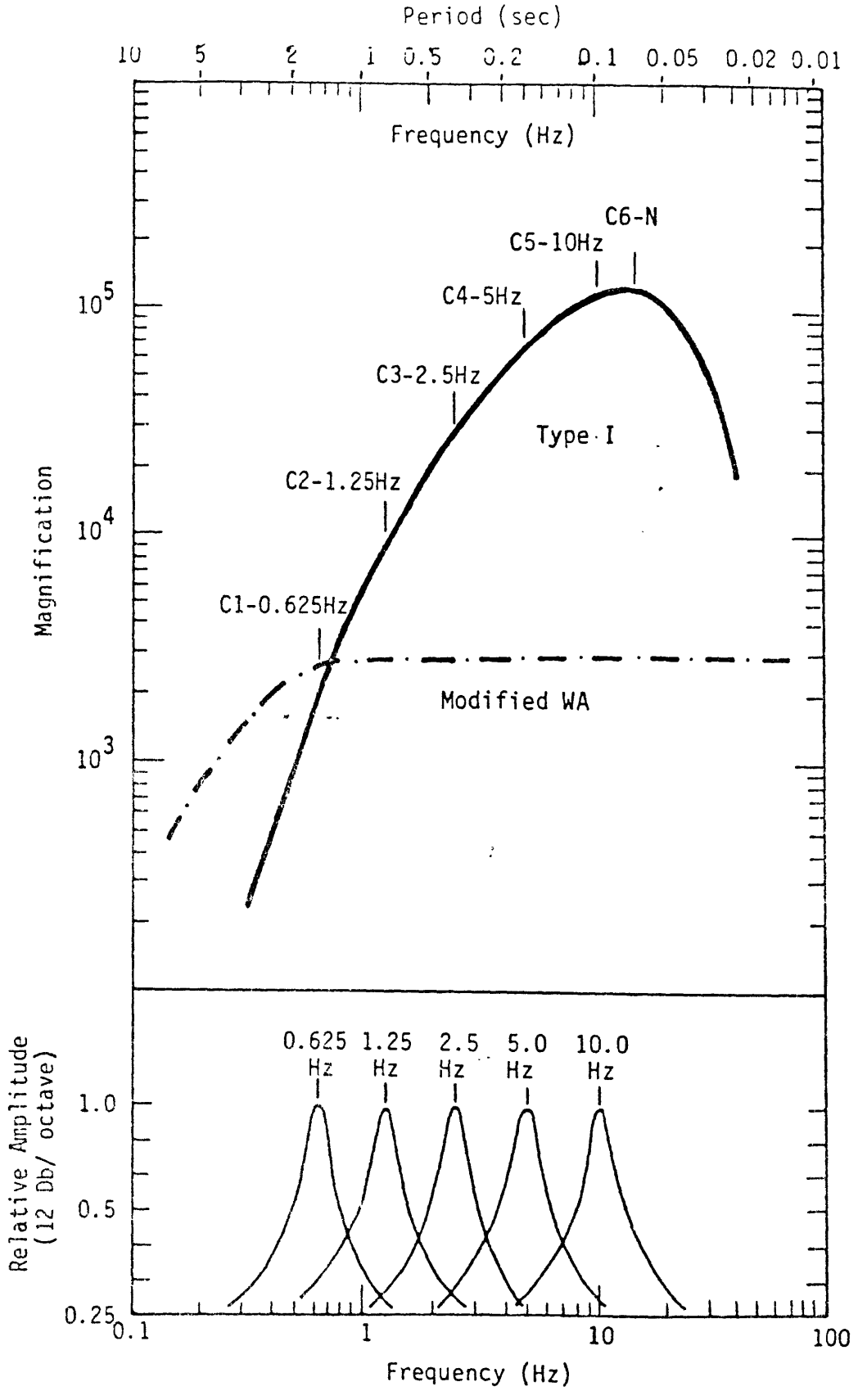
Period (sec)
10
5
2
1
0.5
0.2
0.1
0.05
0.02
0.01
Frequency (Hz)
C6-N
C5-10Hz
C4-5Hz
C3-2.5Hz
Type I
C2-1.25Hz
C1-0.625Hz
Modified WA
Magnification
10^5
10^4
10^3
0.625 Hz
1.25 Hz
2.5 Hz
5.0 Hz
10.0 Hz
Relative Amplitude (12 Db/ octave)
1.0
0.5
0.25
0.1
1
10
100
Frequency (Hz)

Figure 3

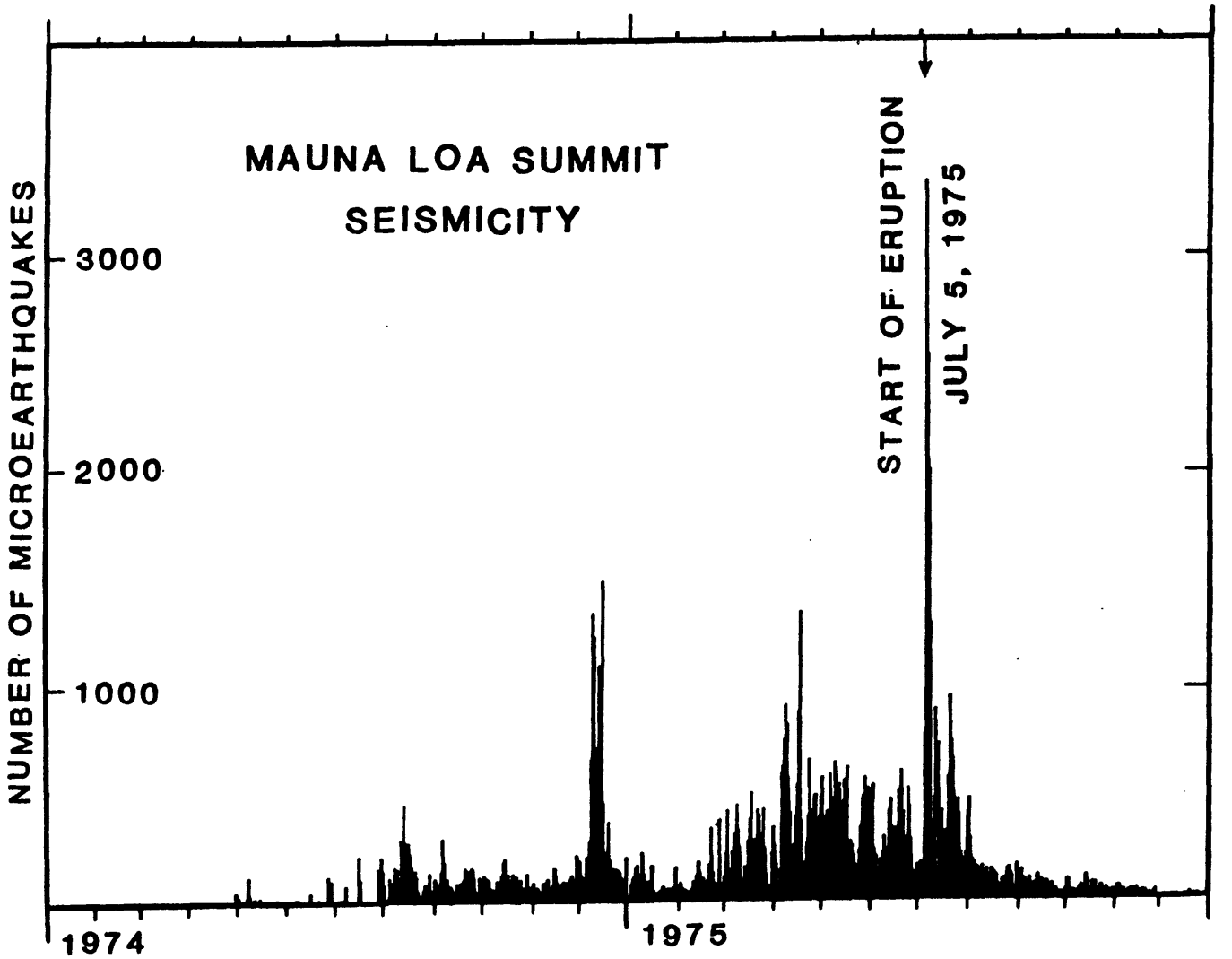
MAUNA LOA SUMMIT
SEISMICITY
NUMBER OF MICROEARTHQUAKES
3000
2000
1000
START OF ERUPTION
JULY 5, 1975
1974
1975

Figure 4a

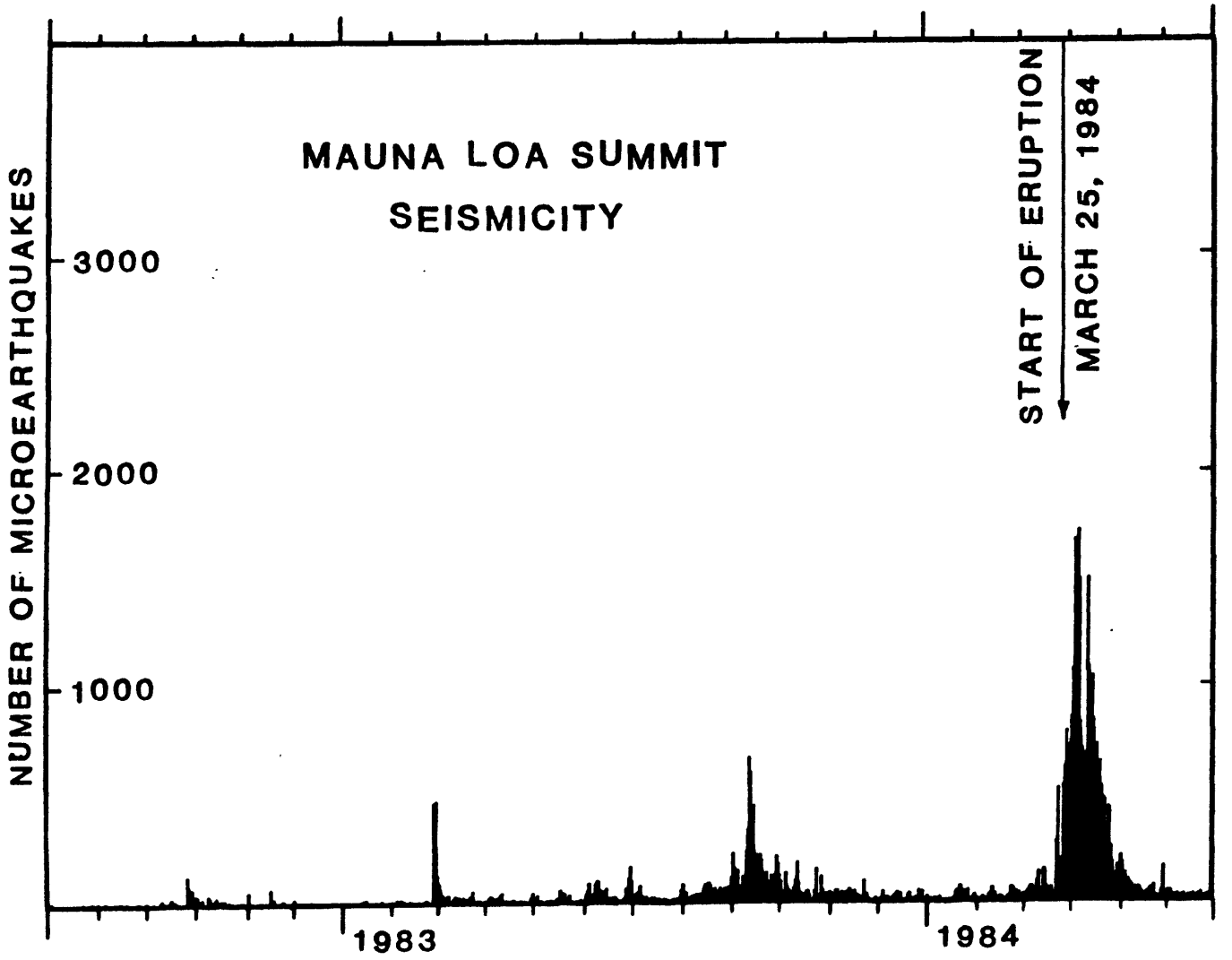
MAUNA LOA SUMMIT
SEISMICITY
NUMBER OF MICROEARTHQUAKES
3000
2000
1000
START OF ERUPTION
MARCH 25, 1984
1983
1984

Figure 4b

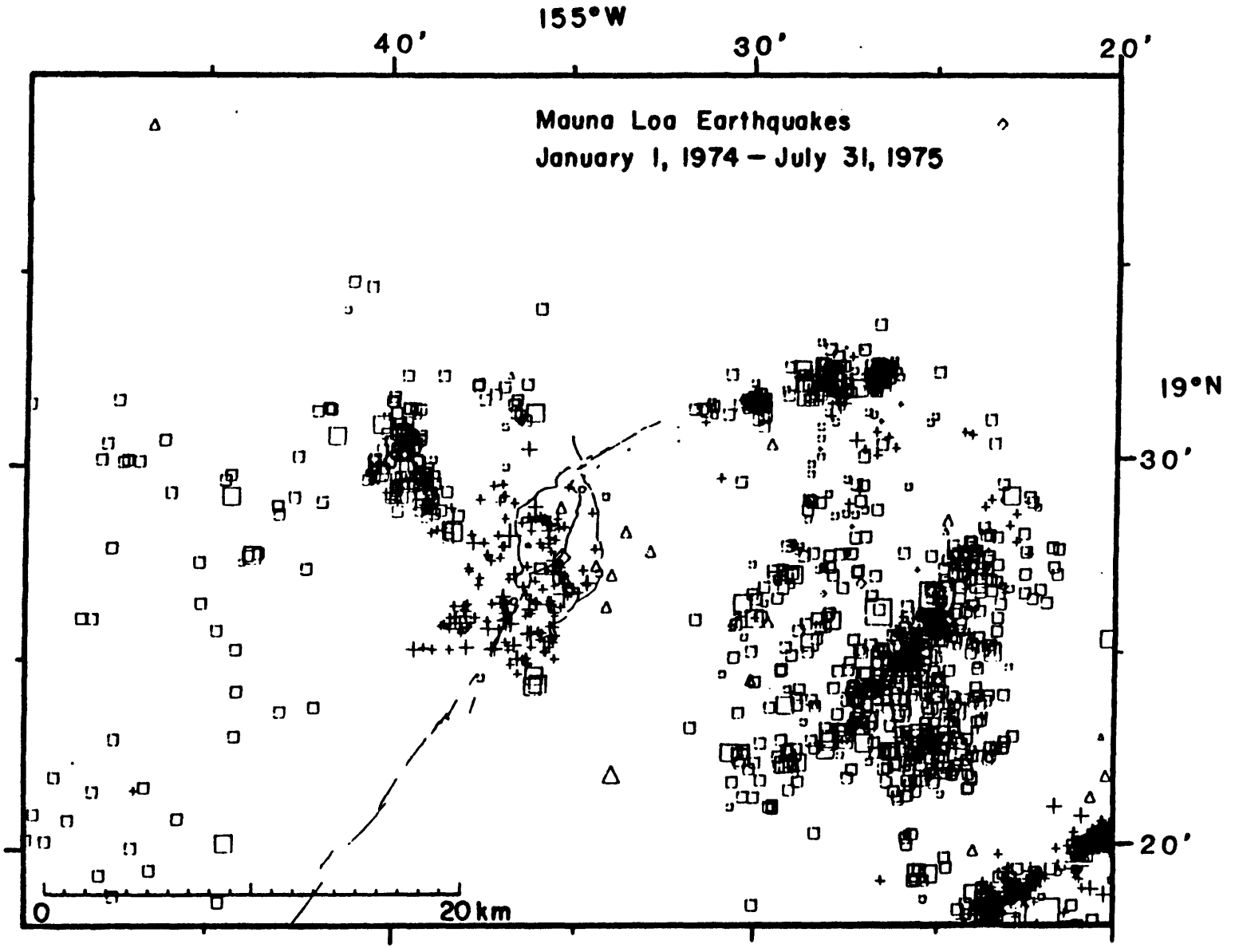
155°W
40'
30'
20'
Mauna Loa Earthquakes
January 1, 1974 – July 31, 1975
19°N
30'
20'
0
20 km

Figure 5a

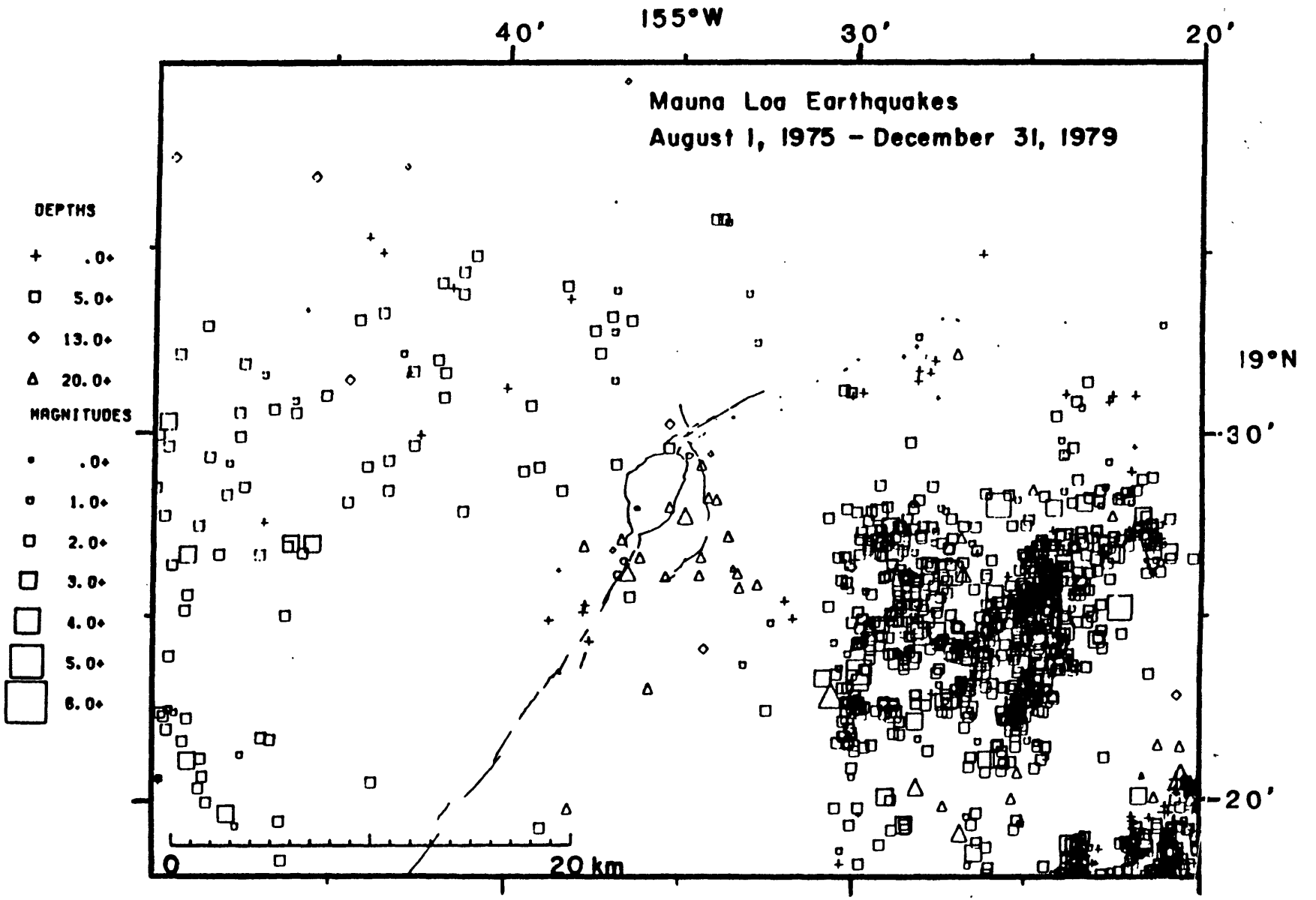
Mauna Loa Earthquakes
August 1, 1975 – December 31, 1979
155°W
40'
30'
20'
19°N
30'
20'
DEPTHS
.0♦
5.0♦
13.0♦
20.0♦
MAGNITUDES
.0♦
1.0♦
2.0♦
3.0♦
4.0♦
5.0♦
6.0♦
0
20 km

Figure 5b

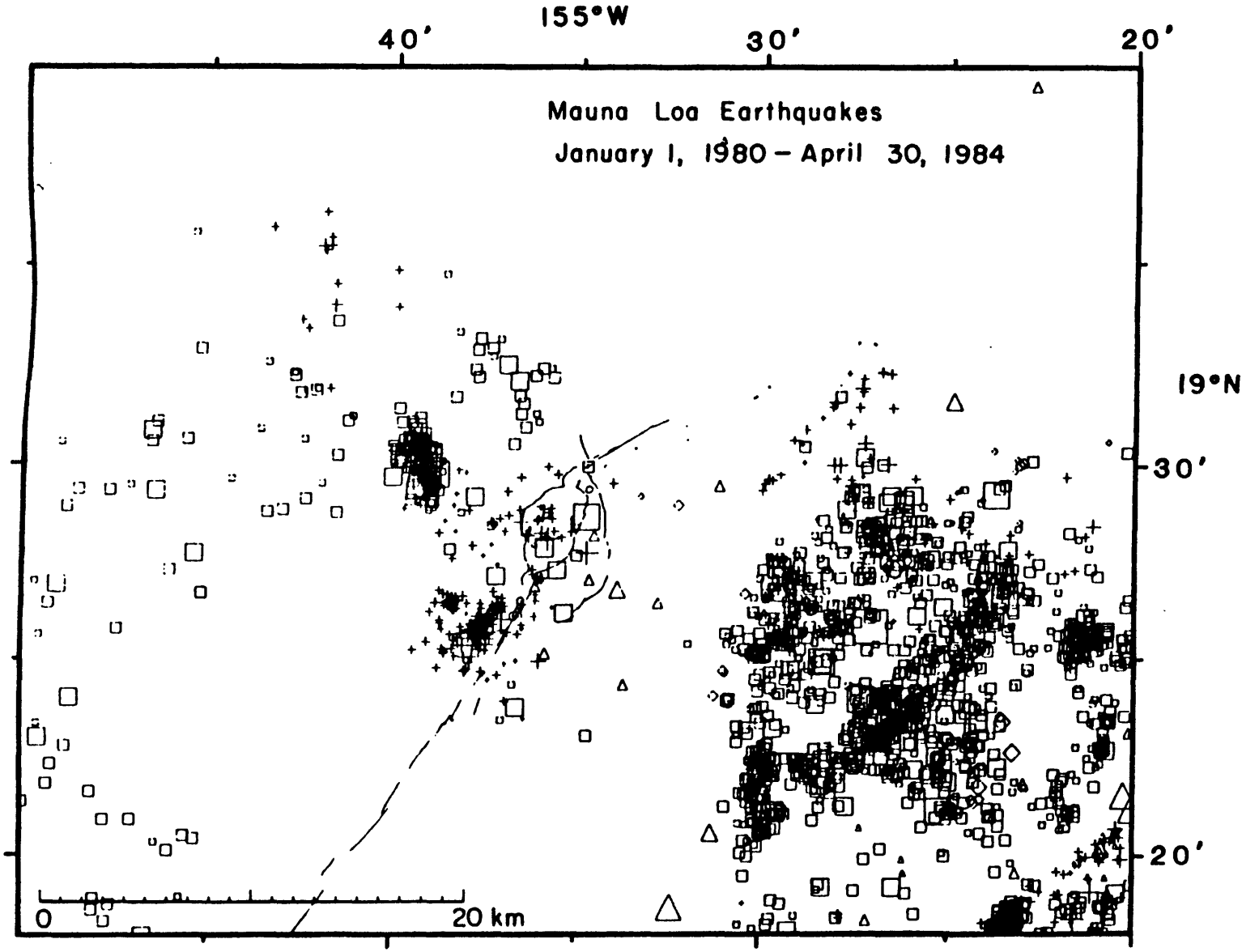
155°W
40'
30'
20'
Mauna Loa Earthquakes
January 1, 1980 – April 30, 1984
19°N
30'
20'
0
20 km

Figure 5c

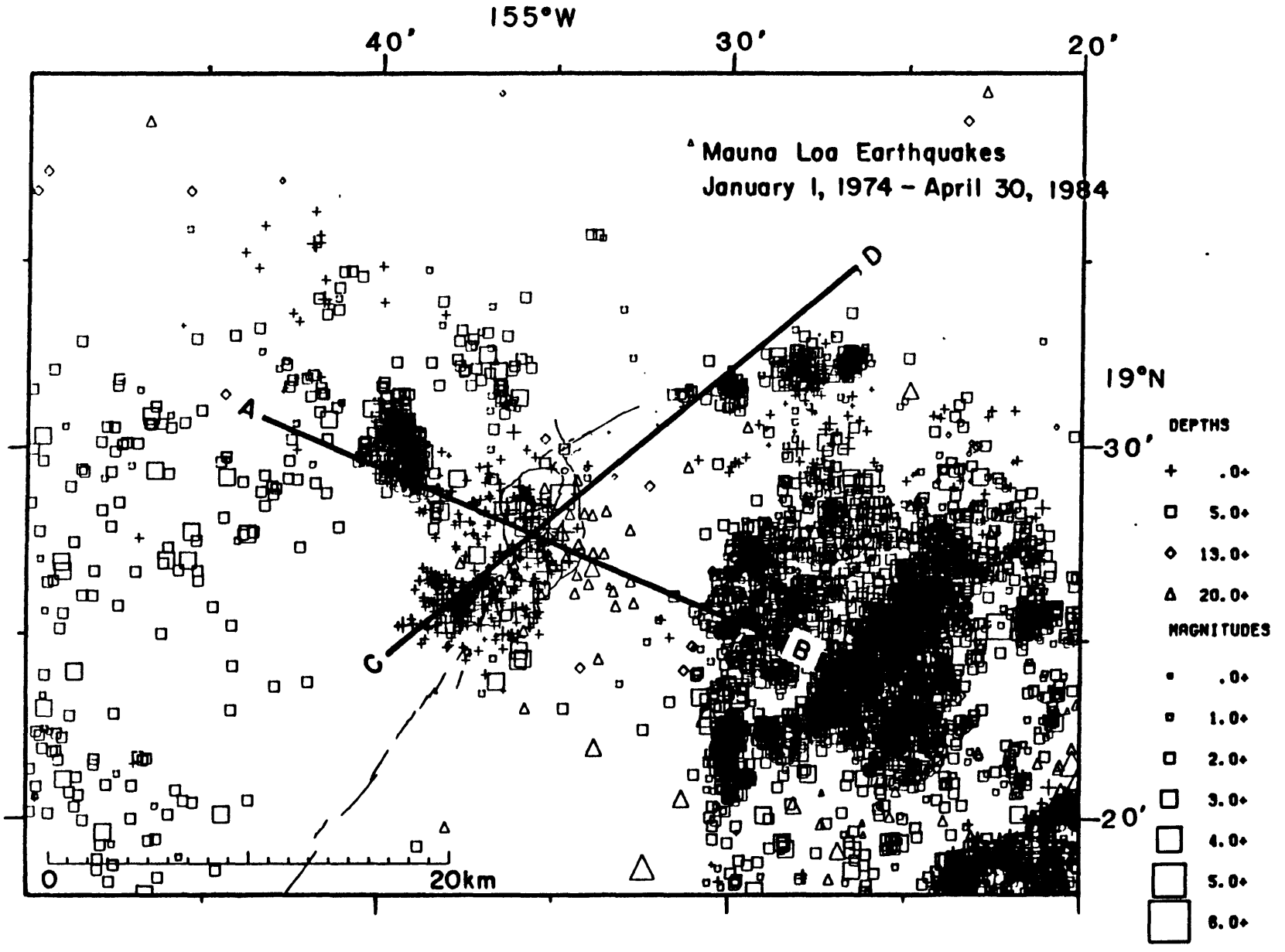
155°W
40'
30'
20'
Mauna Loa Earthquakes
January 1, 1974 - April 30, 1984
19°N
30'
20'
A
B
C
D
0
20km
DEPTHS
.0+
5.0+
10.0+
20.0+
MAGNITUDES
.0+
1.0+
2.0+
3.0+
4.0+
5.0+
6.0+

Figure 6a

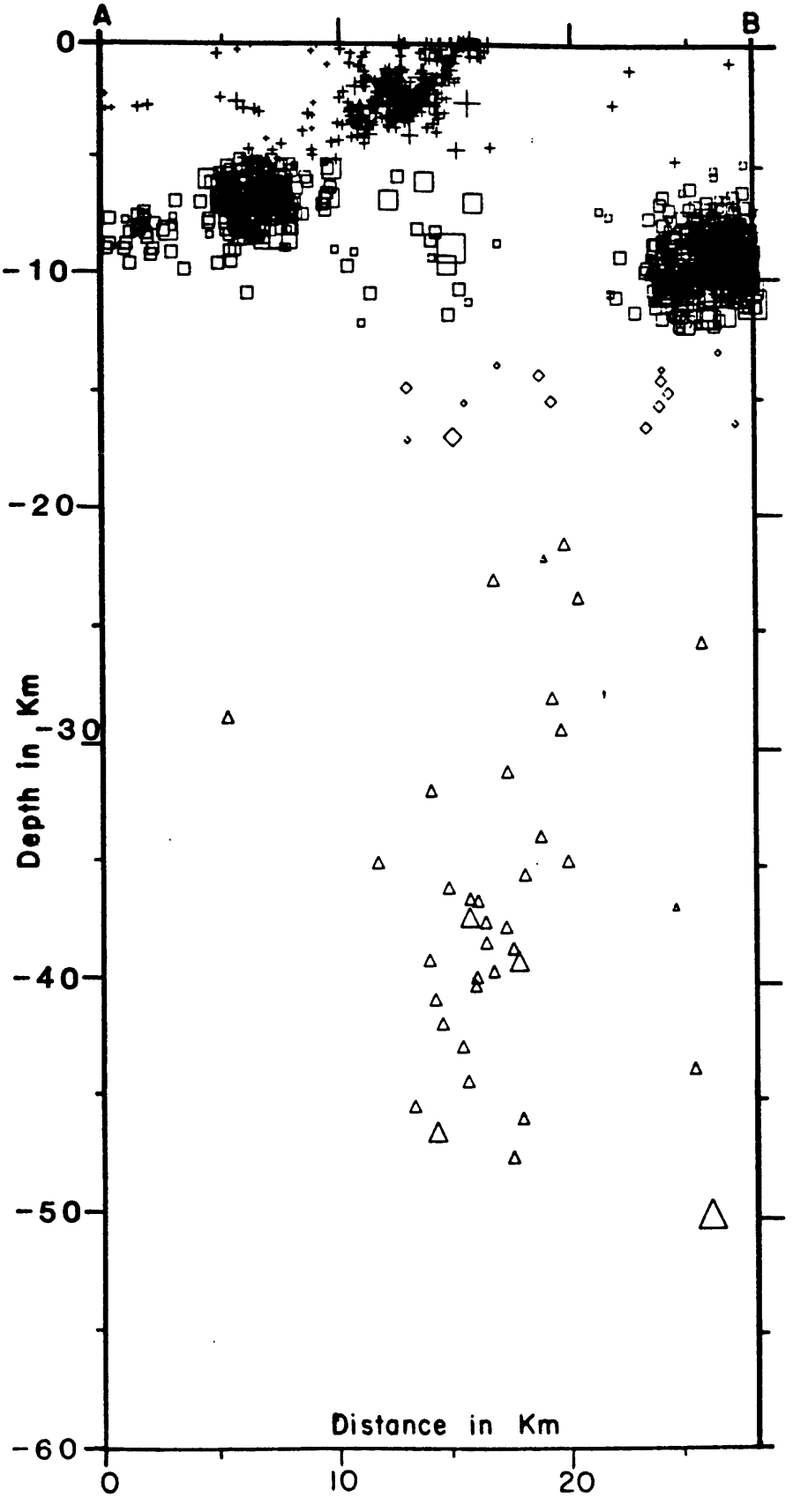

Figure 6b

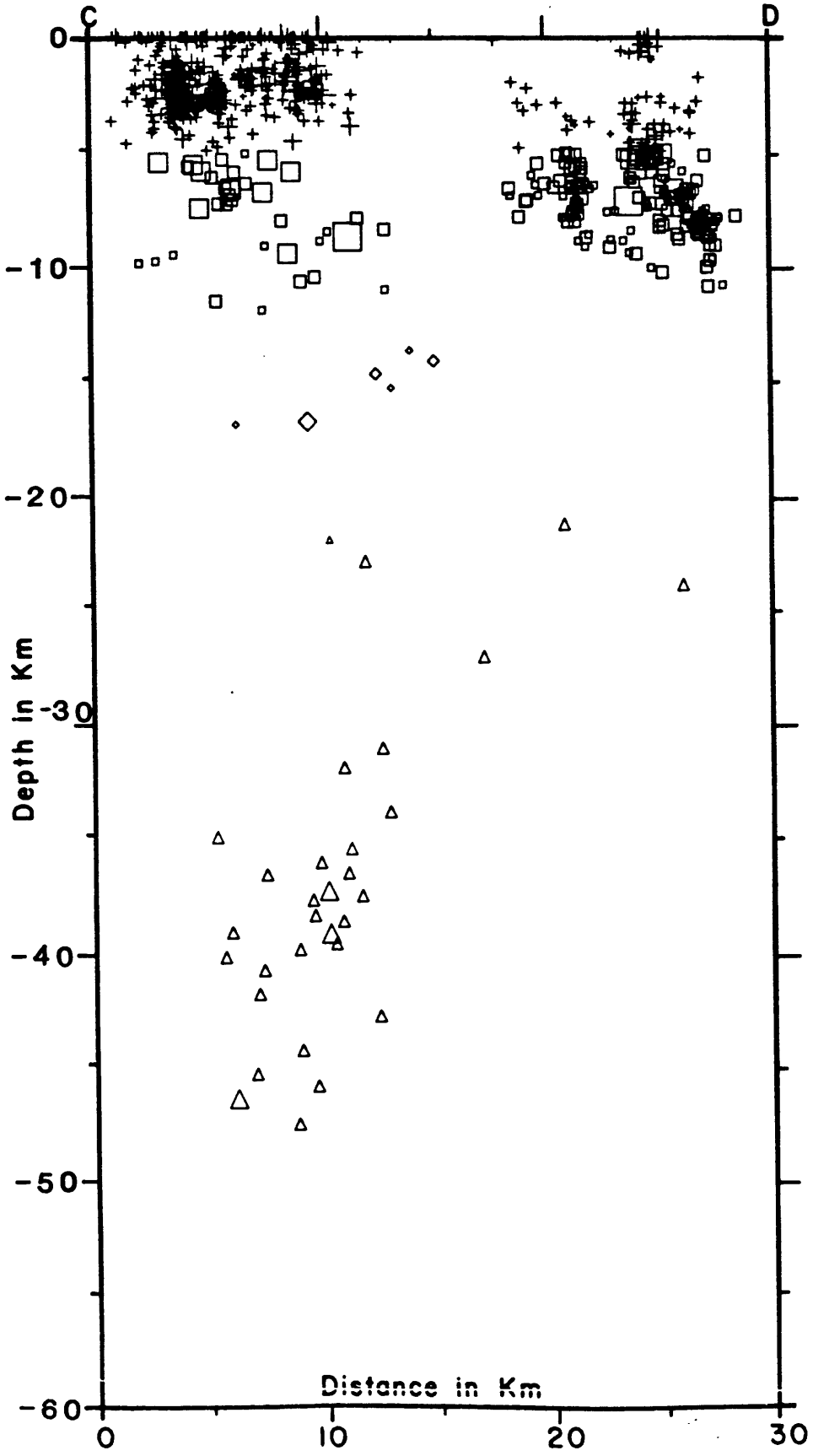

Figure 6c

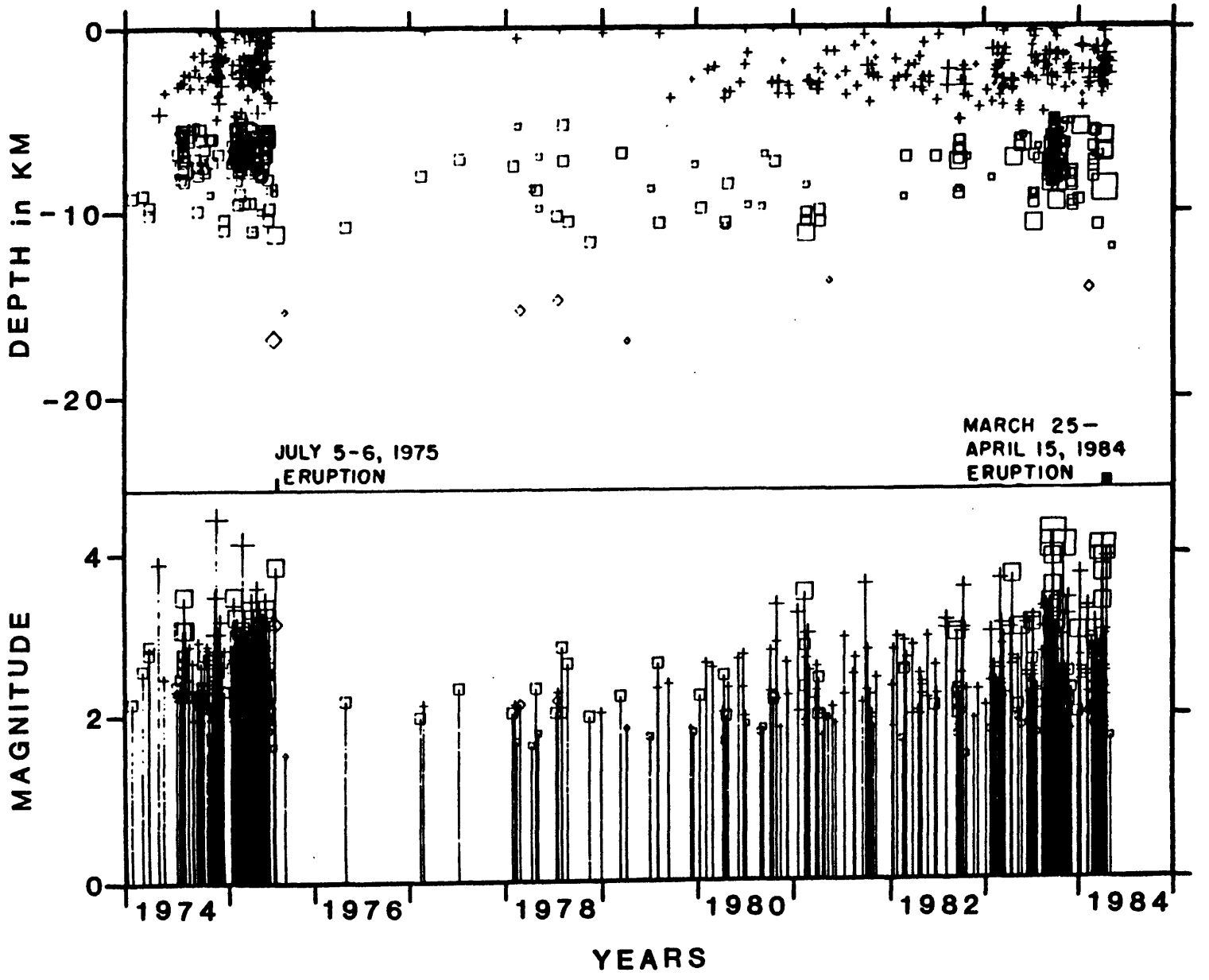
0
-10
-20
DEPTH in KM
JULY 5-6, 1975
ERUPTION
MARCH 25-
APRIL 15, 1984
ERUPTION
4
2
0
MAGNITUDE
1974
1976
1978
1980
1982
1984
YEARS

Figure 7

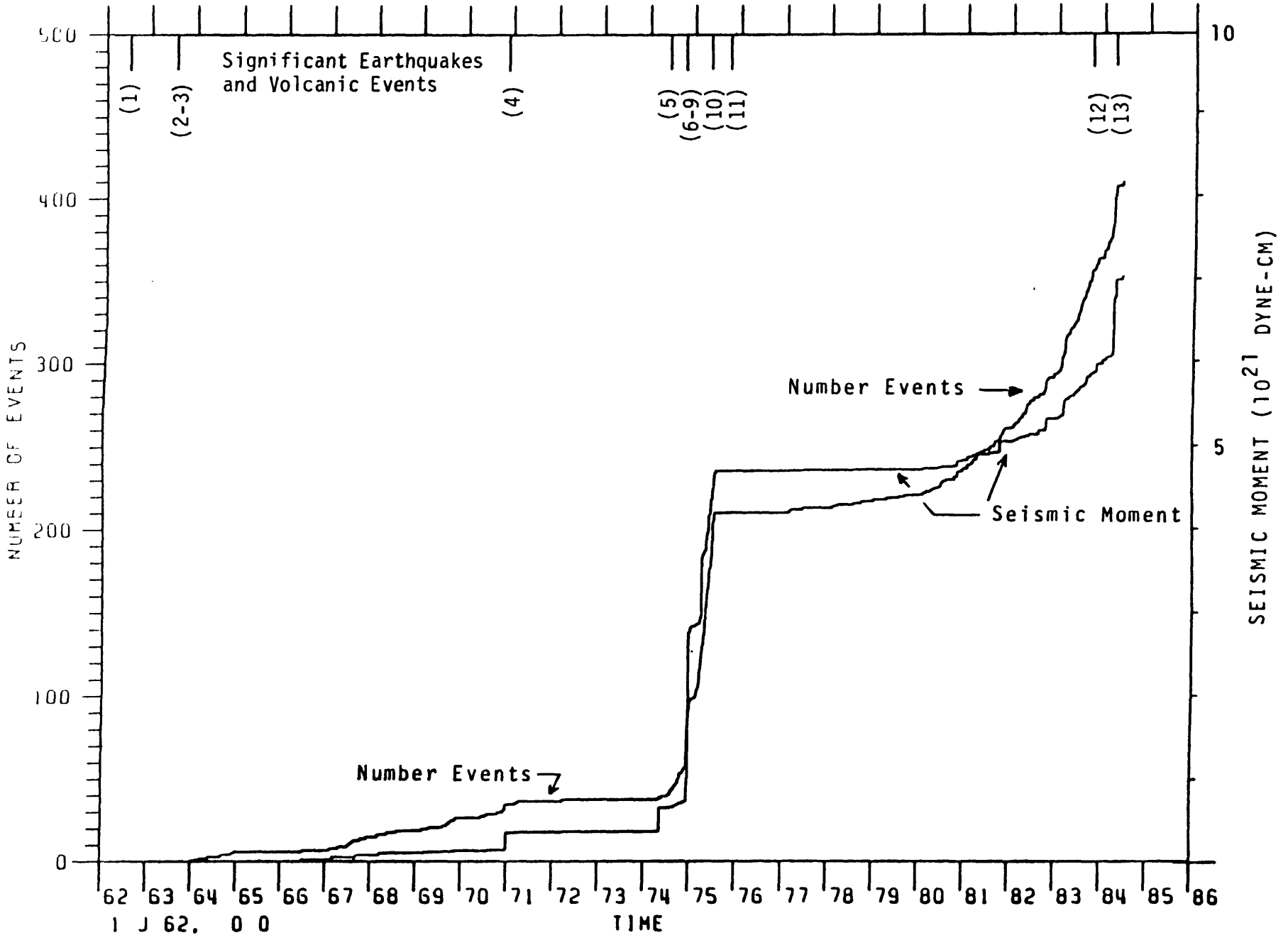
Significant Earthquakes
and Volcanic Events
(1)
(2-3)
(4)
(5)
(6-9)
(10)
(11)
(12)
(13)
Number Events
Seismic Moment
Number Events
NUMBER OF EVENTS
SEISMIC MOMENT (10^{21} DYNE-CM)
TIME
0
100
200
300
400
500
5
10
62 63 64 65 66 67 68 69 70 71 72 73 74 75 76 77 78 79 80 81 82 83 84 85 86
1 J 62, 0 0

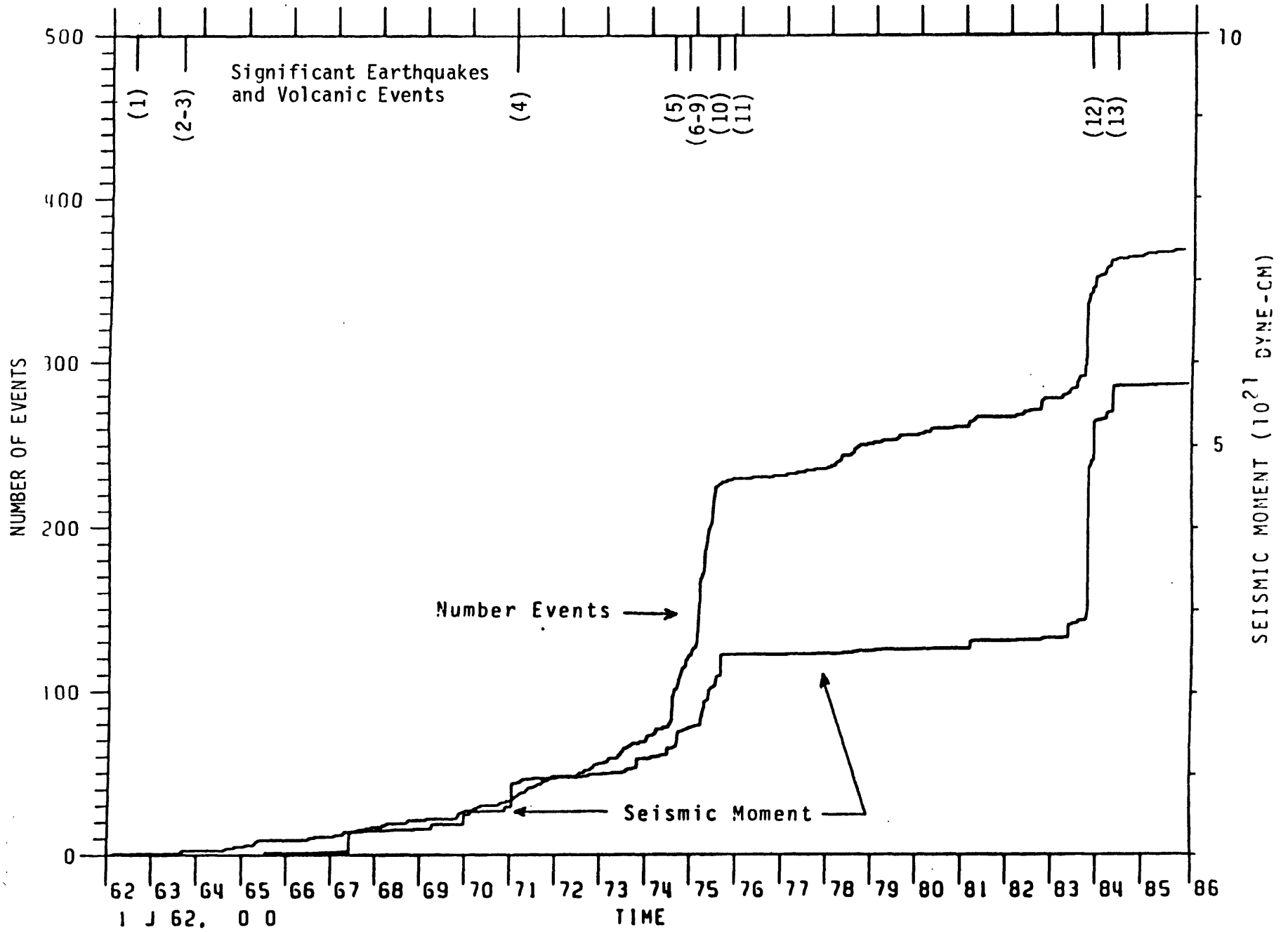
Significant Earthquakes
and Volcanic Events
(1)
(2-3)
(4)
(5)
(6-9)
(10)
(11)
(12)
(13)
Number Events
Seismic Moment
NUMBER OF EVENTS
SEISMIC MOMENT (10^{21} DYNE-CM)
TIME
0
100
200
300
400
500
5
10
62 63 64 65 66 67 68 69 70 71 72 73 74 75 76 77 78 79 80 81 82 83 84 85 86
1 J 62. 0 0

Figure 8b

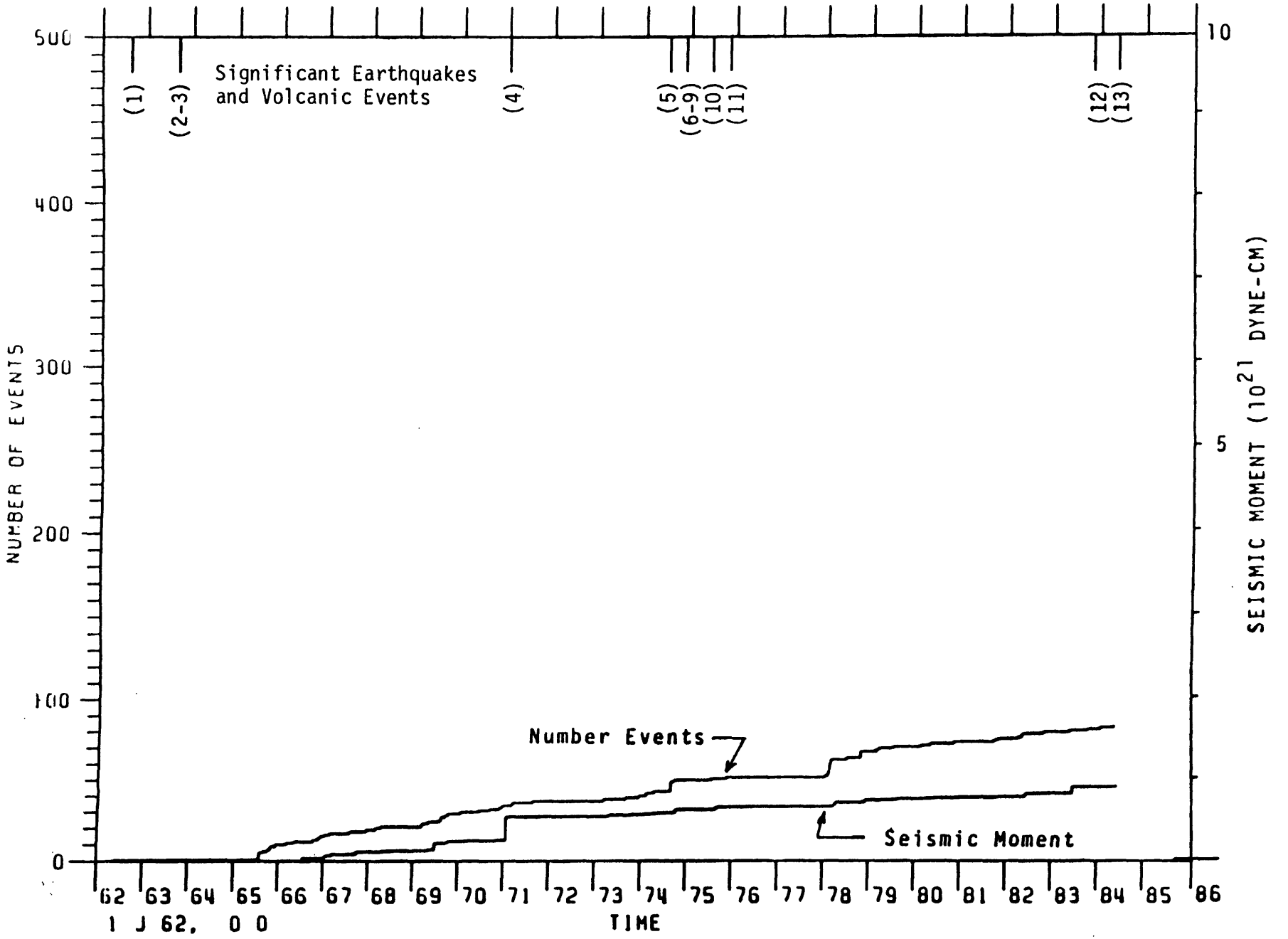
Significant Earthquakes and Volcanic Events
(1)
(2-3)
(4)
(5)
(6-9)
(10)
(11)
(12)
(13)
Number Events
Seismic Moment
NUMBER OF EVENTS
SEISMIC MOMENT (10^{21} DYNE-CM)
TIME
500
400
300
200
100
0
10
5
62 63 64 65 66 67 68 69 70 71 72 73 74 75 76 77 78 79 80 81 82 83 84 85 86
1 J 62, 0 0

Figure 8c

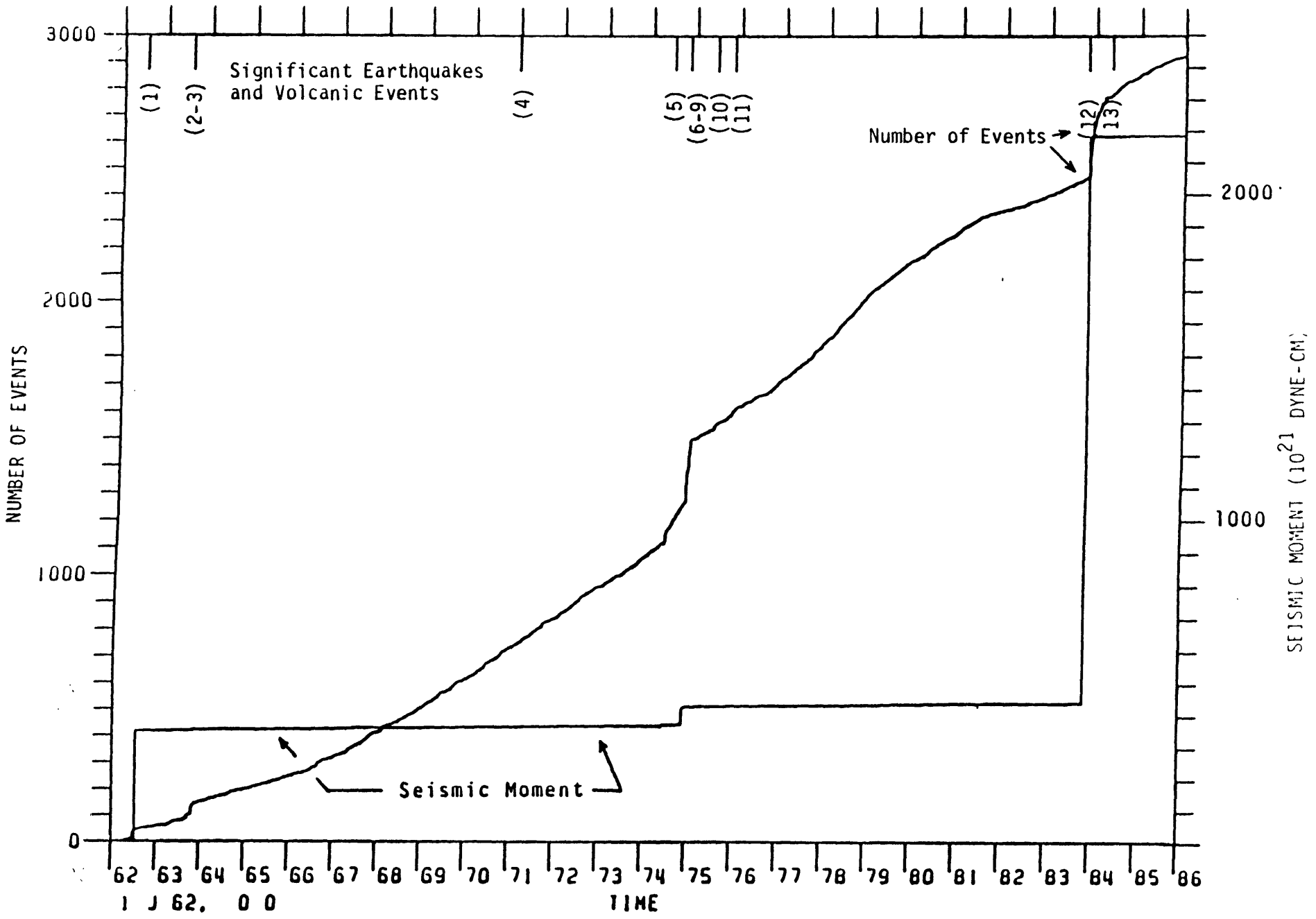
3000
2000
1000
0
NUMBER OF EVENTS
Significant Earthquakes
and Volcanic Events
(1)
(2-3)
(4)
(5)
(6-9)
(10)
(11)
(12)
(13)
Number of Events
Seismic Moment
2000
1000
SEISMIC MOMENT (10^{21} DYNE-CM)
62 63 64 65 66 67 68 69 70 71 72 73 74 75 76 77 78 79 80 81 82 83 84 85 86
1 J 62, 0 0
TIME

Figure 8d

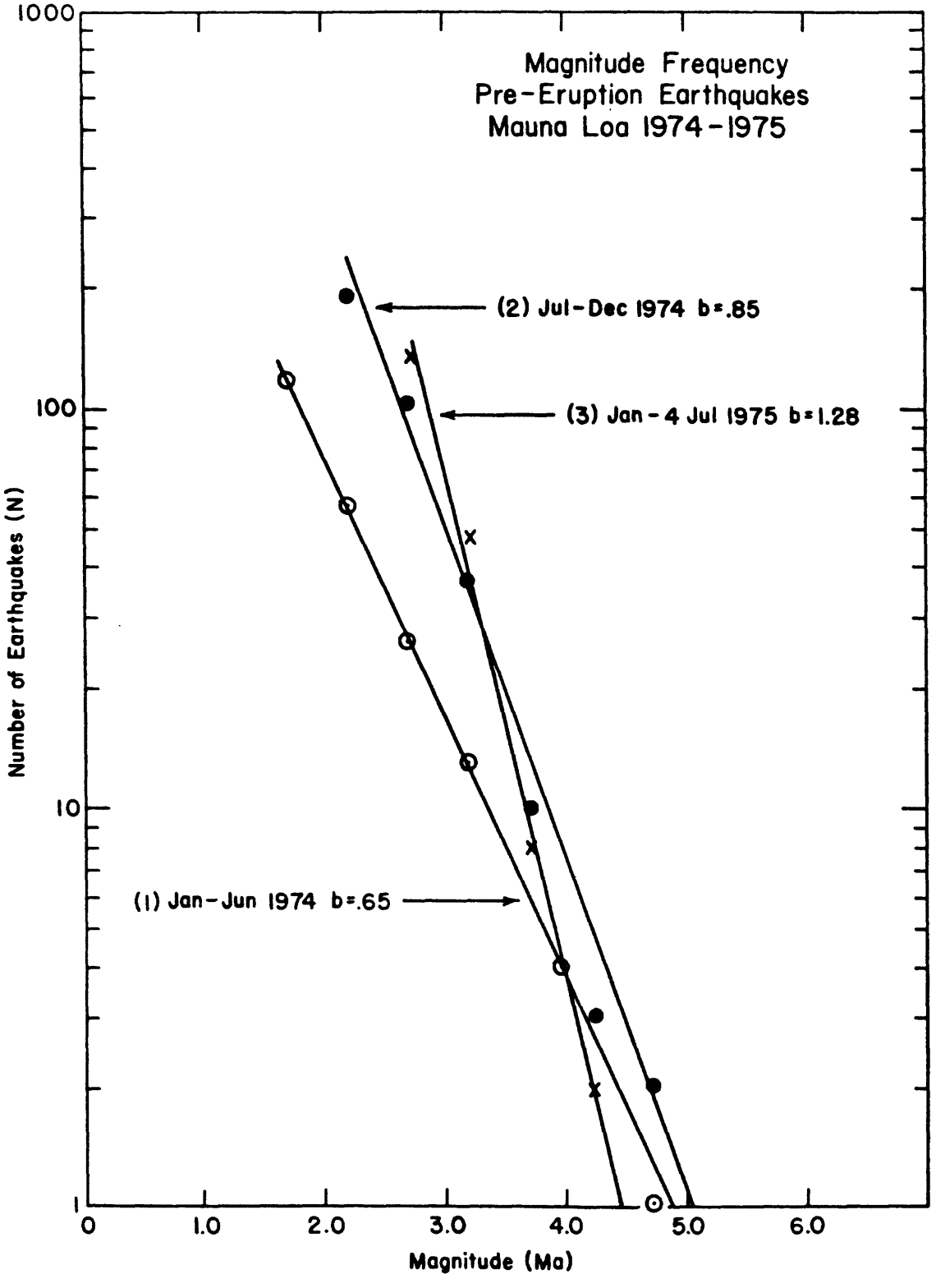
Magnitude Frequency
Pre-Eruption Earthquakes
Mauna Loa 1974-1975
(2) Jul-Dec 1974 b=.85
(3) Jan-4 Jul 1975 b=1.28
(1) Jan-Jun 1974 b=.65
Number of Earthquakes (N)
Magnitude (Ma)
1000
100
10
1
0
1.0
2.0
3.0
4.0
5.0
6.0

Figure 9a

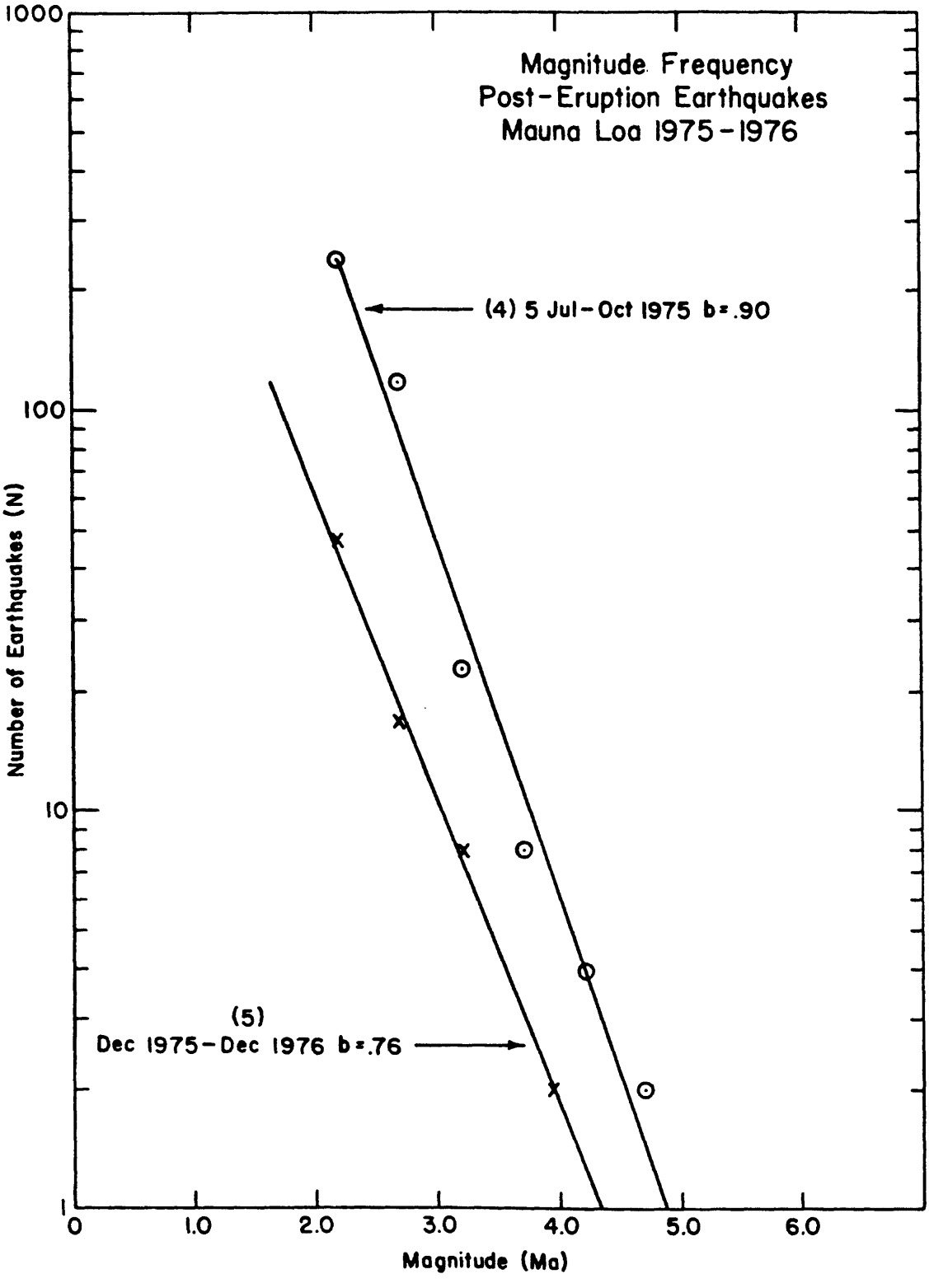
Magnitude Frequency
Post-Eruption Earthquakes
Mauna Loa 1975-1976
(4) 5 Jul-Oct 1975 b=.90
(5)
Dec 1975-Dec 1976 b=.76
Number of Earthquakes (N)
Magnitude (Ma)
1000
100
10
1
0
1.0
2.0
3.0
4.0
5.0
6.0

Figure 9b

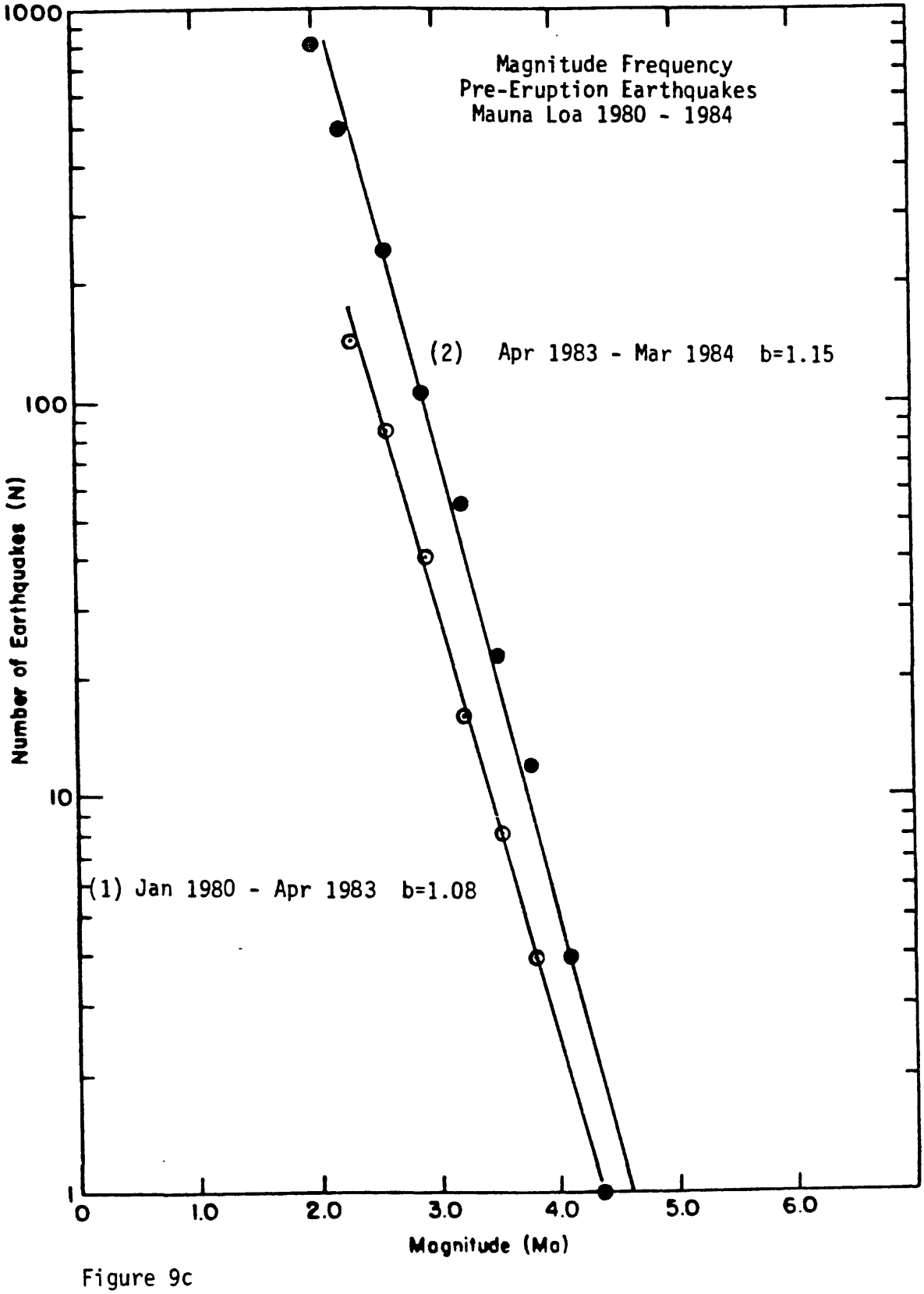
Magnitude Frequency
Pre-Eruption Earthquakes
Mauna Loa 1980 - 1984
(2) Apr 1983 - Mar 1984 b=1.15
(1) Jan 1980 - Apr 1983 b=1.08
Number of Earthquakes (N)
1000
100
10
1
0
1.0
2.0
3.0
4.0
5.0
6.0
Magnitude (Mo)

Figure 9c

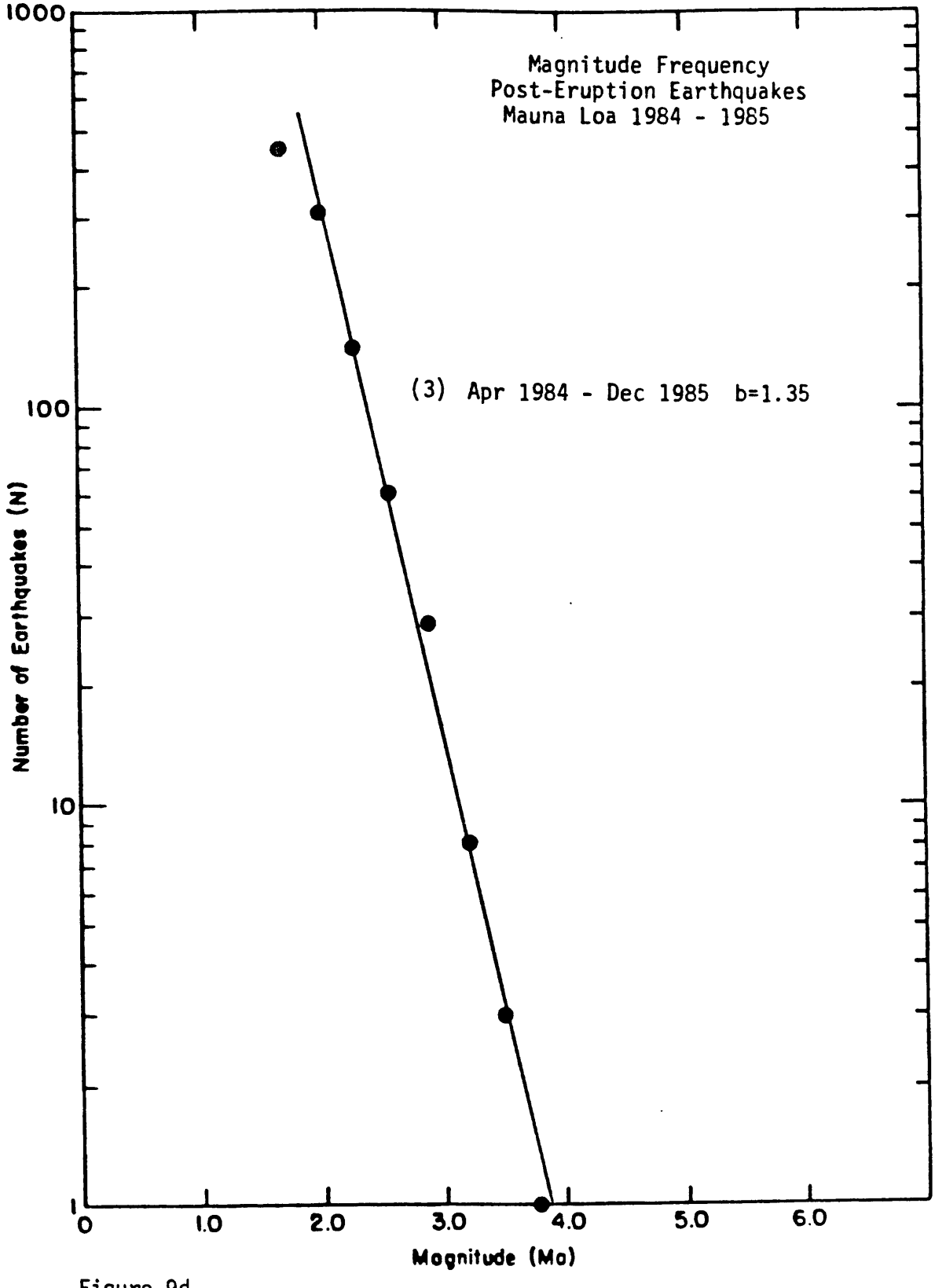
Magnitude Frequency
Post-Eruption Earthquakes
Mauna Loa 1984 - 1985
(3) Apr 1984 - Dec 1985 b=1.35
Number of Earthquakes (N)
1000
100
10
1
0
1.0
2.0
3.0
4.0
5.0
6.0
Magnitude (Mo)

Figure 9d

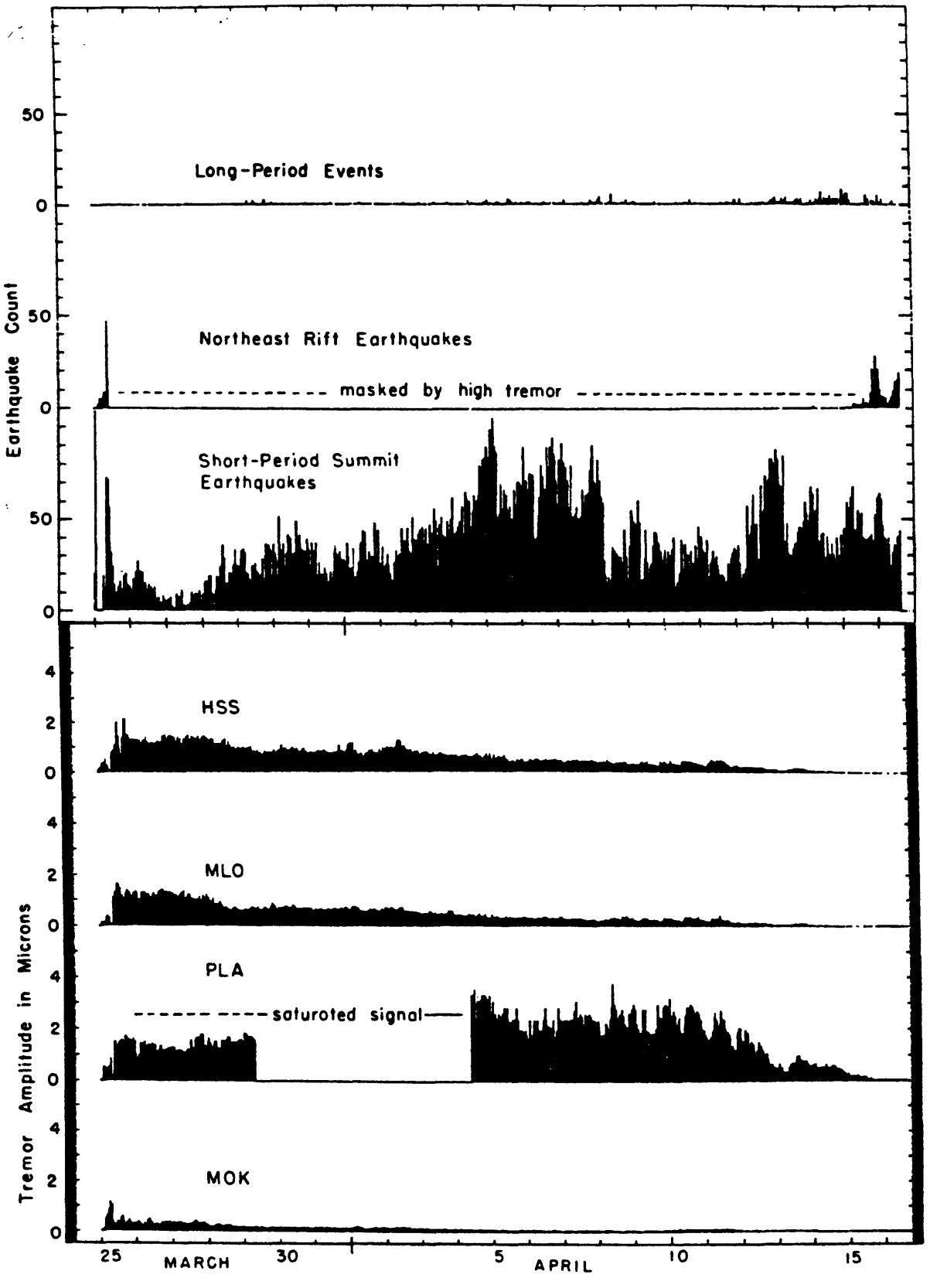
Long-Period Events
Northeast Rift Earthquakes
masked by high tremor
Short-Period Summit Earthquakes
Earthquake Count
50
0
HSS
MLO
PLA
saturoted signal
MOK
Tremor Amplitude in Microns
4
2
0
25
MARCH
30
5
APRIL
10
15

Figure 10

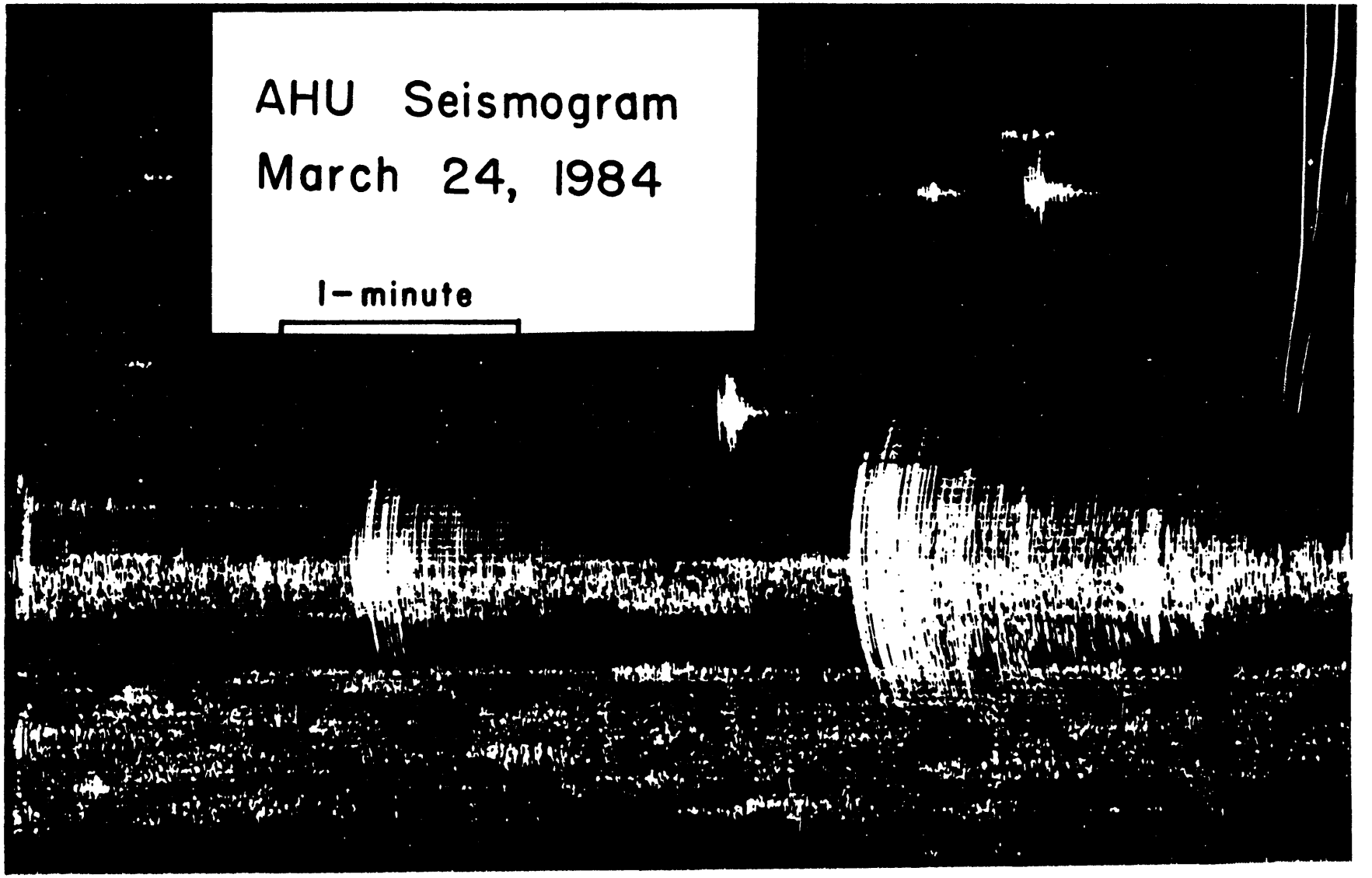

Figure 11

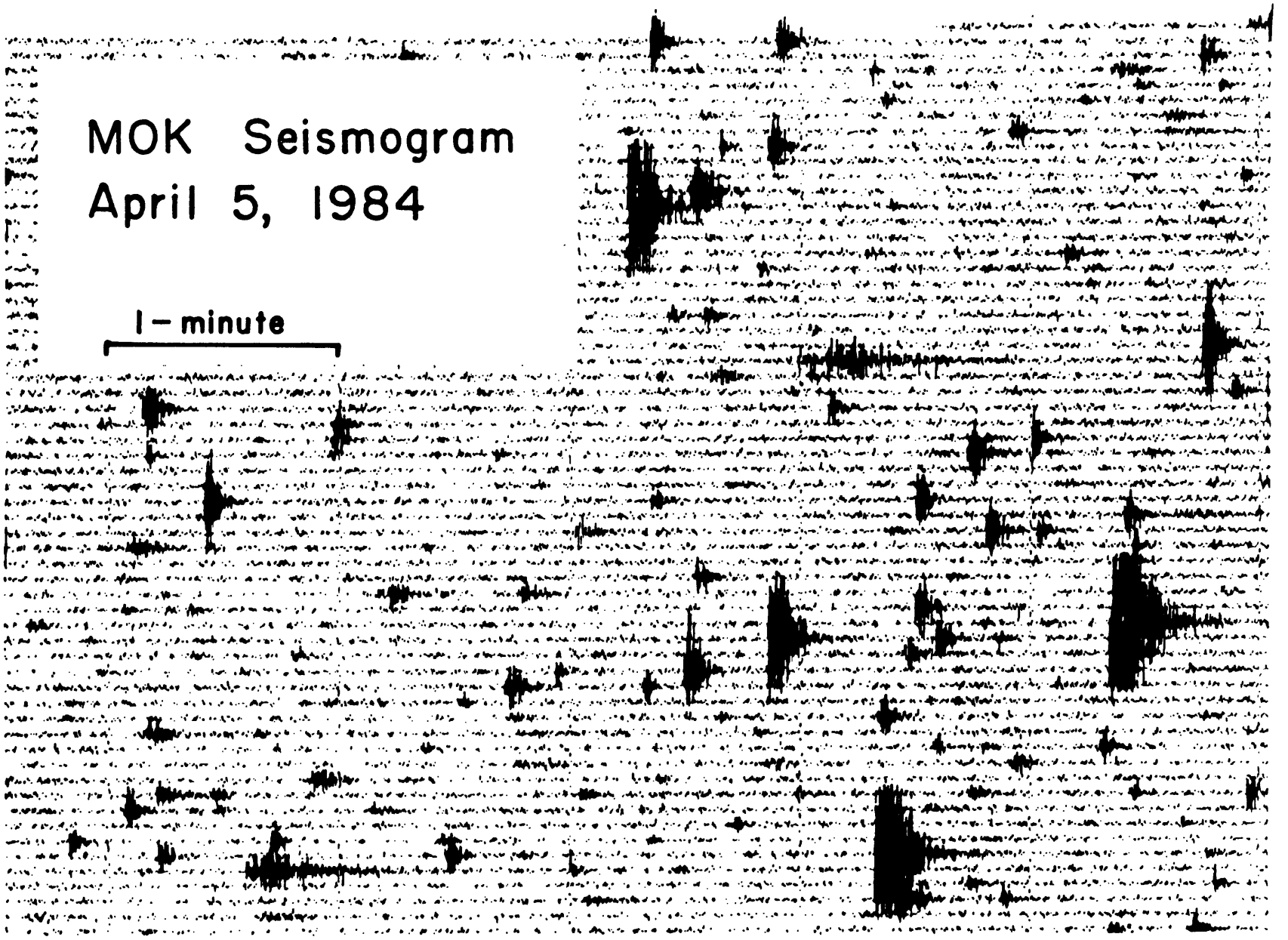

Figure 12

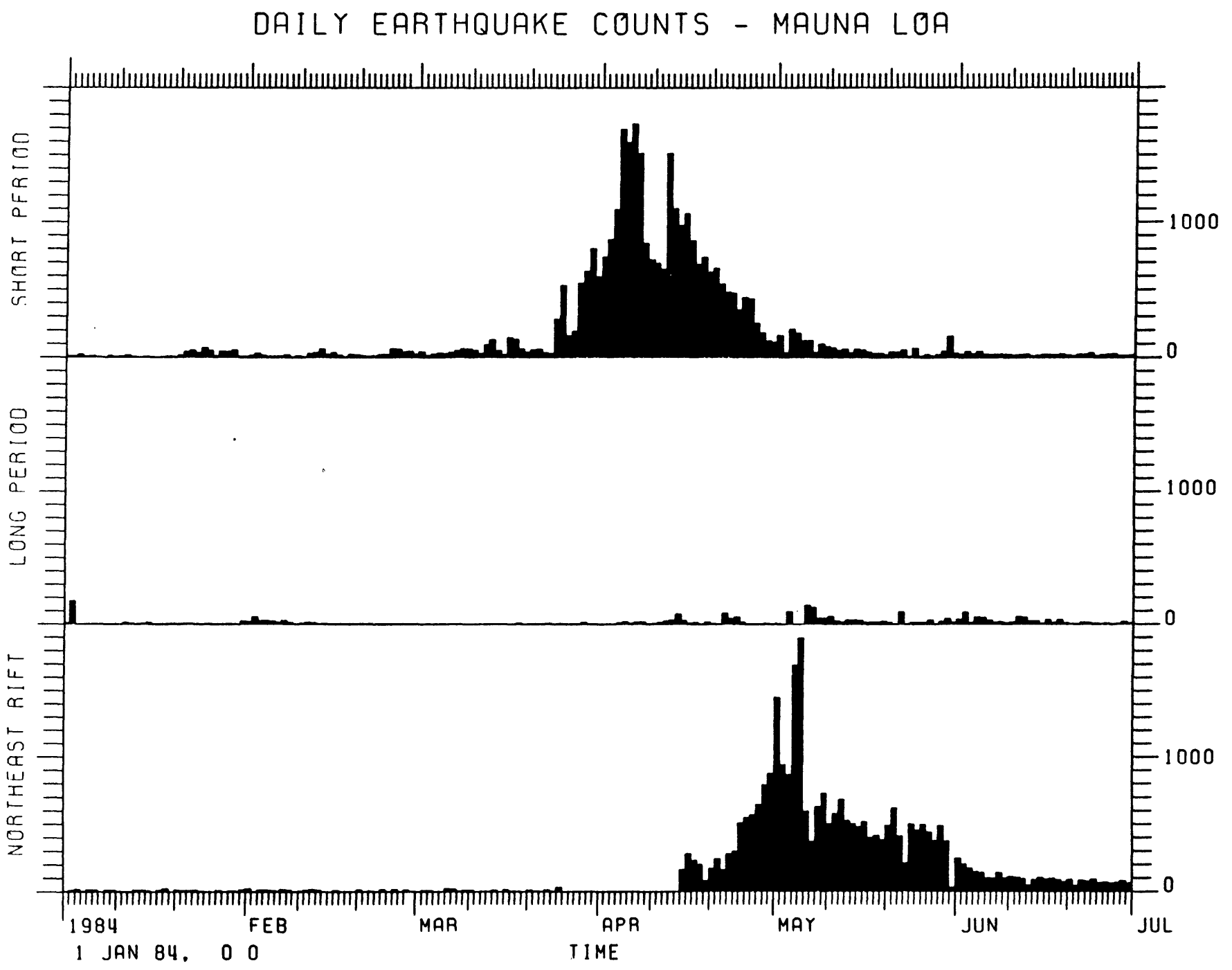
DAILY EARTHQUAKE COUNTS - MAUNA LOA
SHORT PERIOD
LONG PERIOD
NORTHEAST RIFT
1000
0
1000
0
1000
0
1984
FEB
MAR
APR
MAY
JUN
JUL
1 JAN 84, 0 0
TIME

Figure 13a

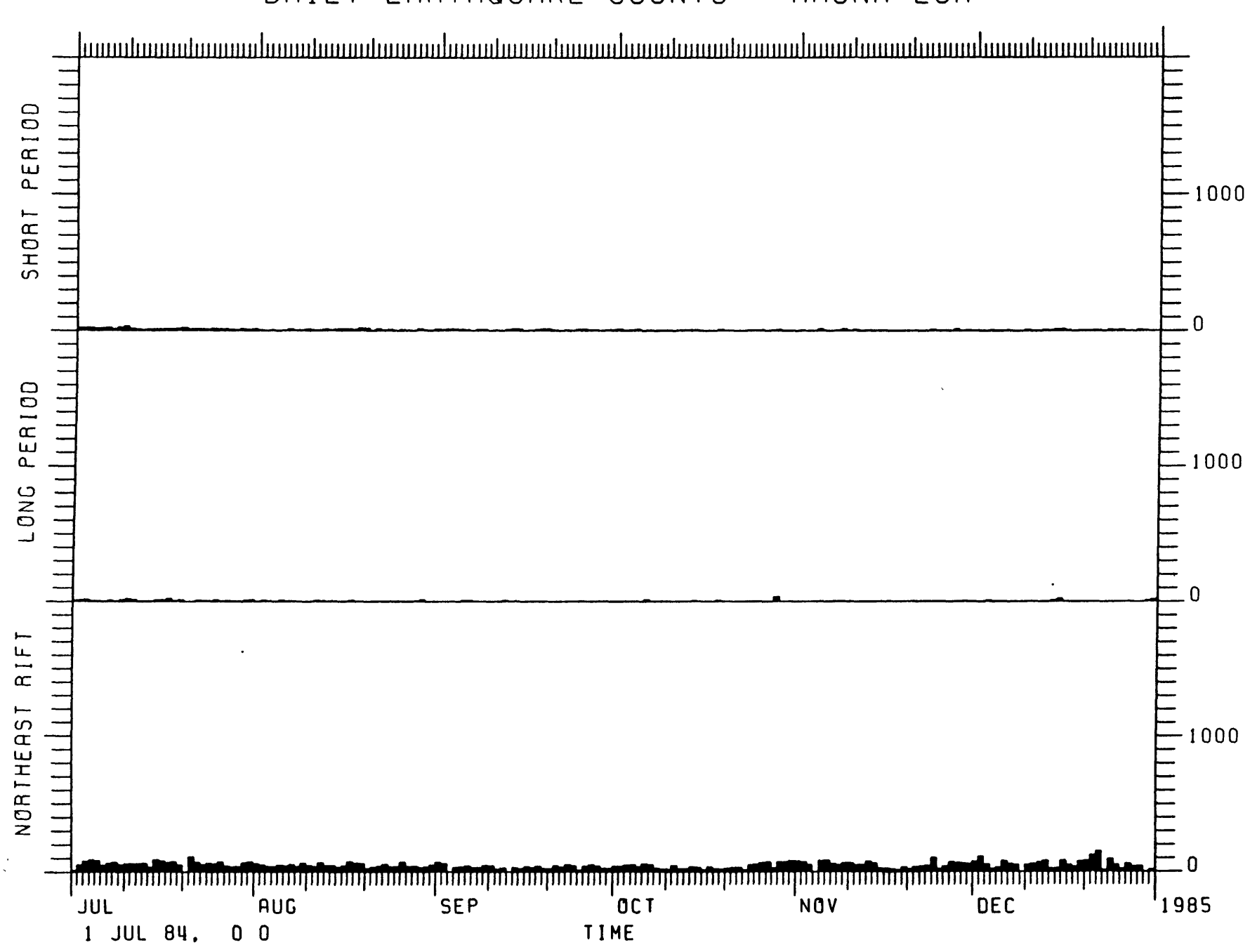
DAILY EARTHQUAKE COUNTS - MAUNA LOA
SHORT PERIOD
LONG PERIOD
NORTHEAST RIFT
1000
0
1000
0
1000
0
JUL
AUG
SEP
OCT
NOV
DEC
1985
1 JUL 84, 0 0
TIME

Figure 13b

DAILY EARTHQUAKE COUNTS - MAUNA LOA

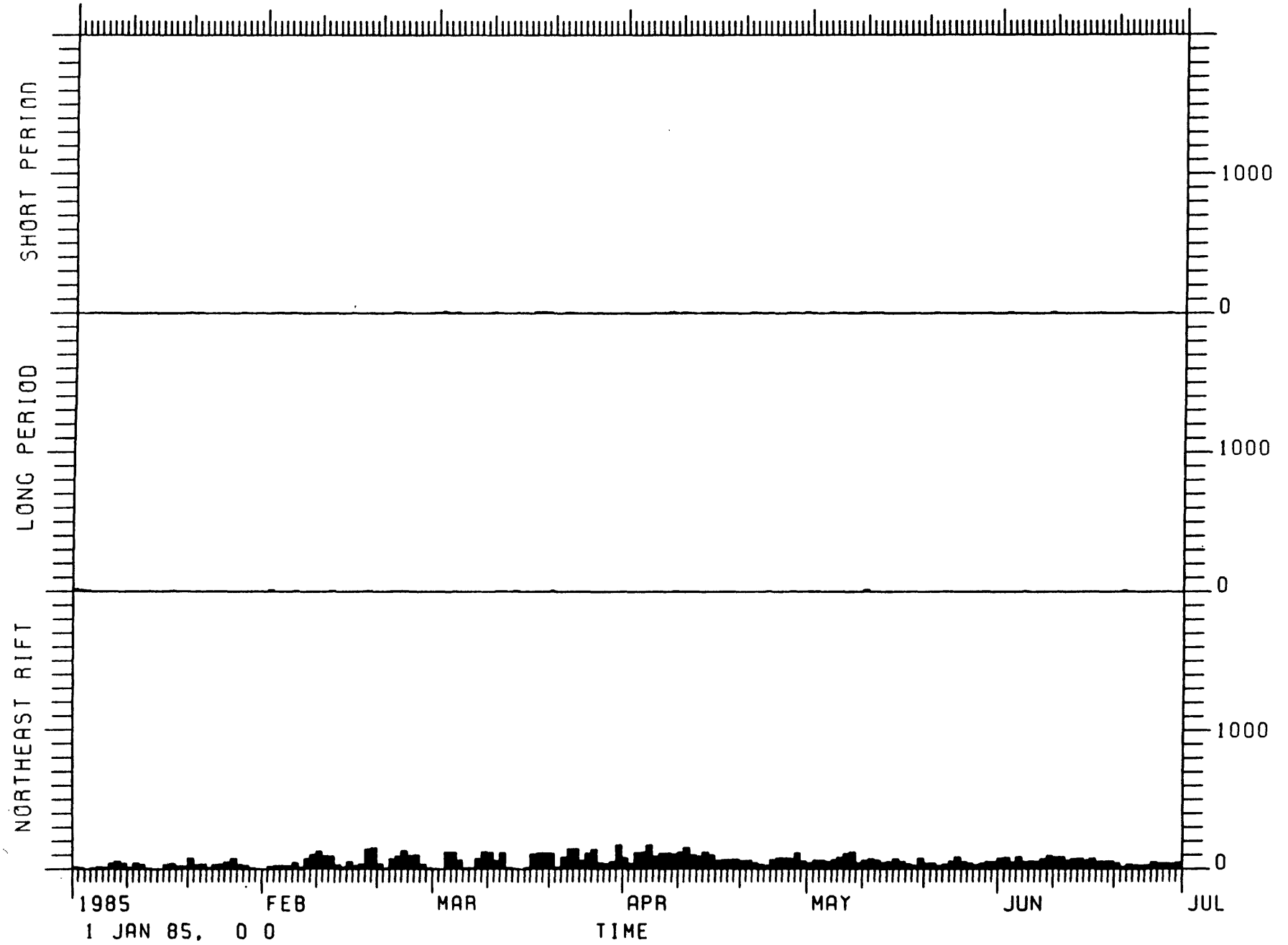

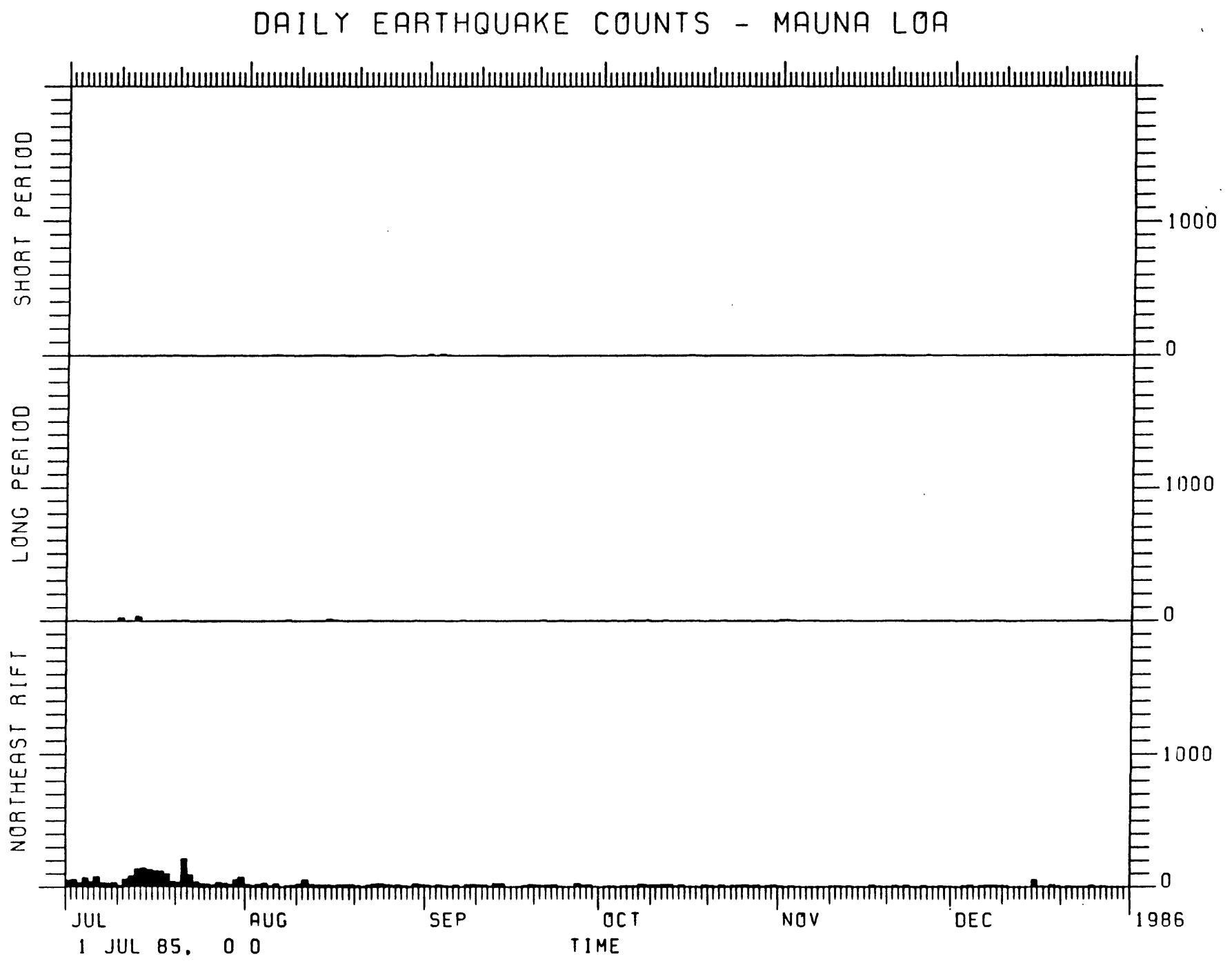
DAILY EARTHQUAKE COUNTS - MAUNA LOA
SHORT PERIOD
LONG PERIOD
NORTHEAST RIFT
1000
0
1000
0
1000
0
JUL
AUG
SEP
OCT
NOV
DEC
1986
1 JUL 85, 0 0
TIME

Figure 13d

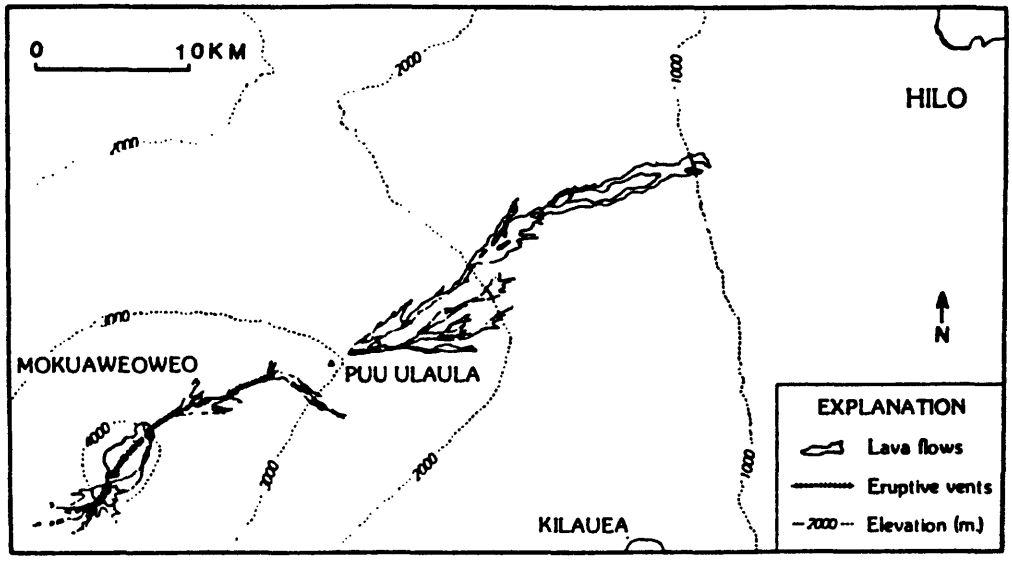
0
10KM
HILO
N
MOKUAWEOWEO
PUU ULAULA
KILAUEA
EXPLANATION
Lava flows
Eruptive vents
Elevation (m)

Figure 14

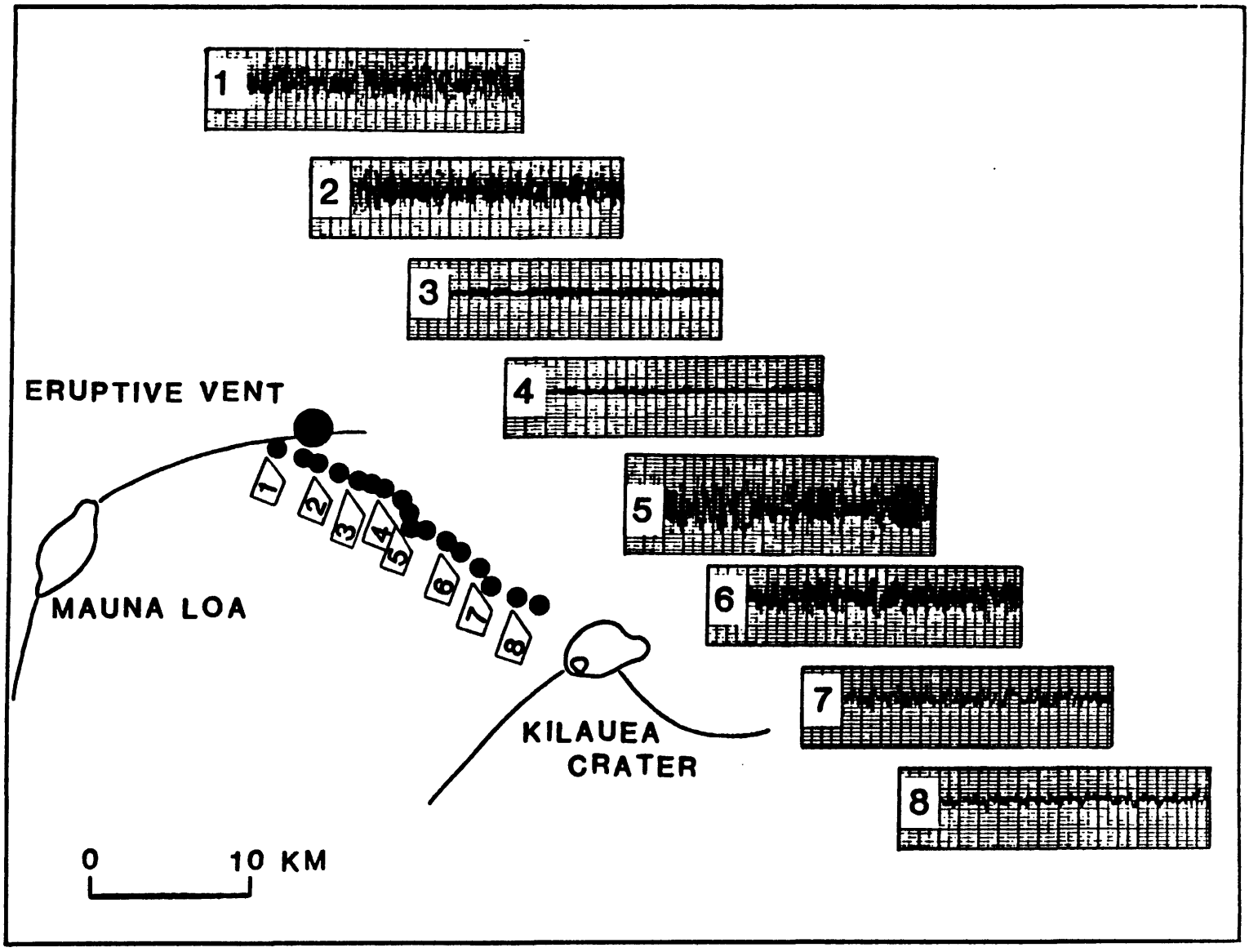

Figure 15

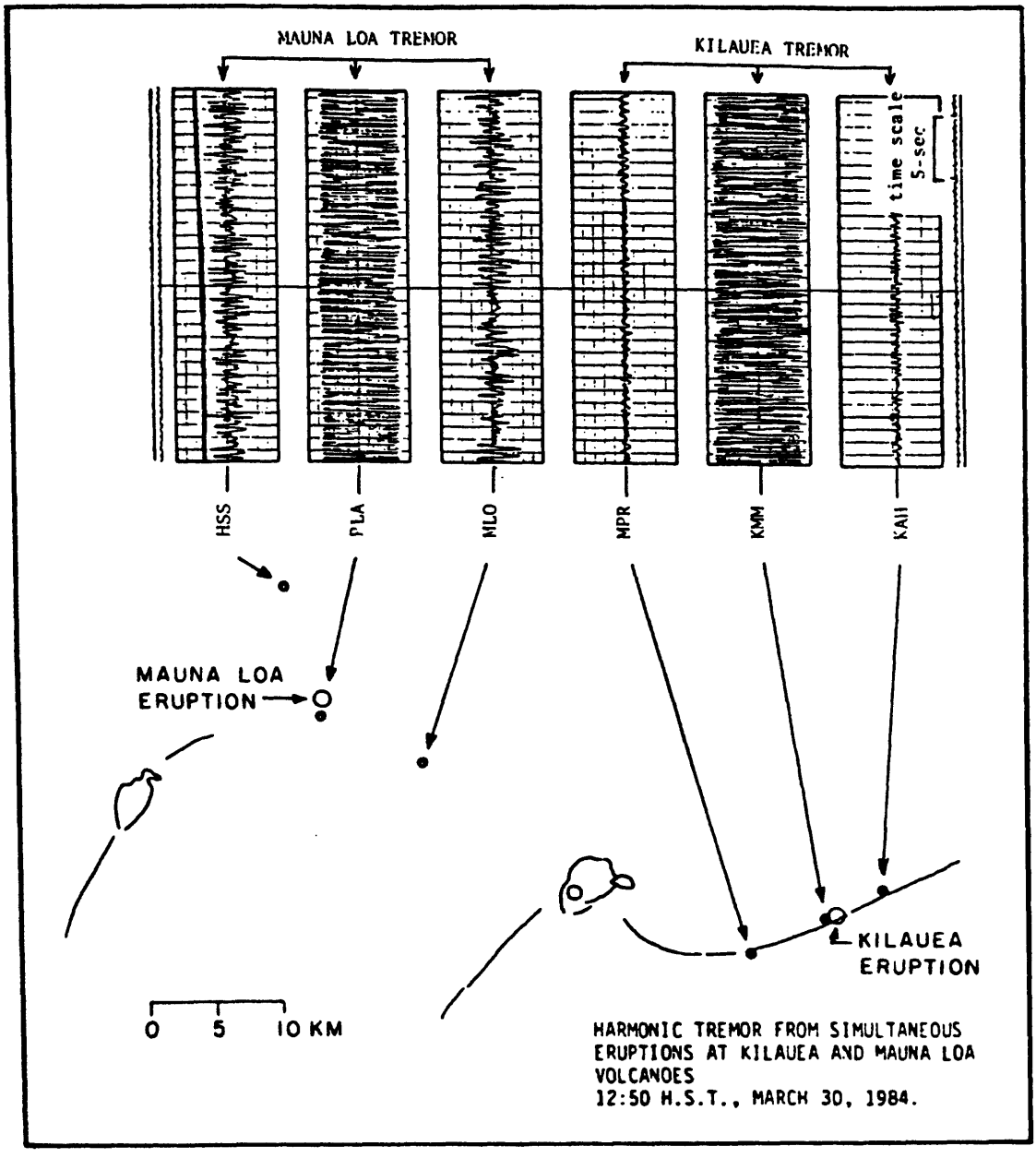
MAUNA LOA TREMOR
KILAUEA TREMOR
time scale
5-sec
HSS
PLA
NLO
MPR
KMM
KAU
MAUNA LOA
ERUPTION
KILAUEA
ERUPTION
0 5 10 KM
HARMONIC TREMOR FROM SIMULTANEOUS
ERUPTIONS AT KILAUEA AND MAUNA LOA
VOLCANOES
12:50 H.S.T., MARCH 30, 1984.

Figure 16

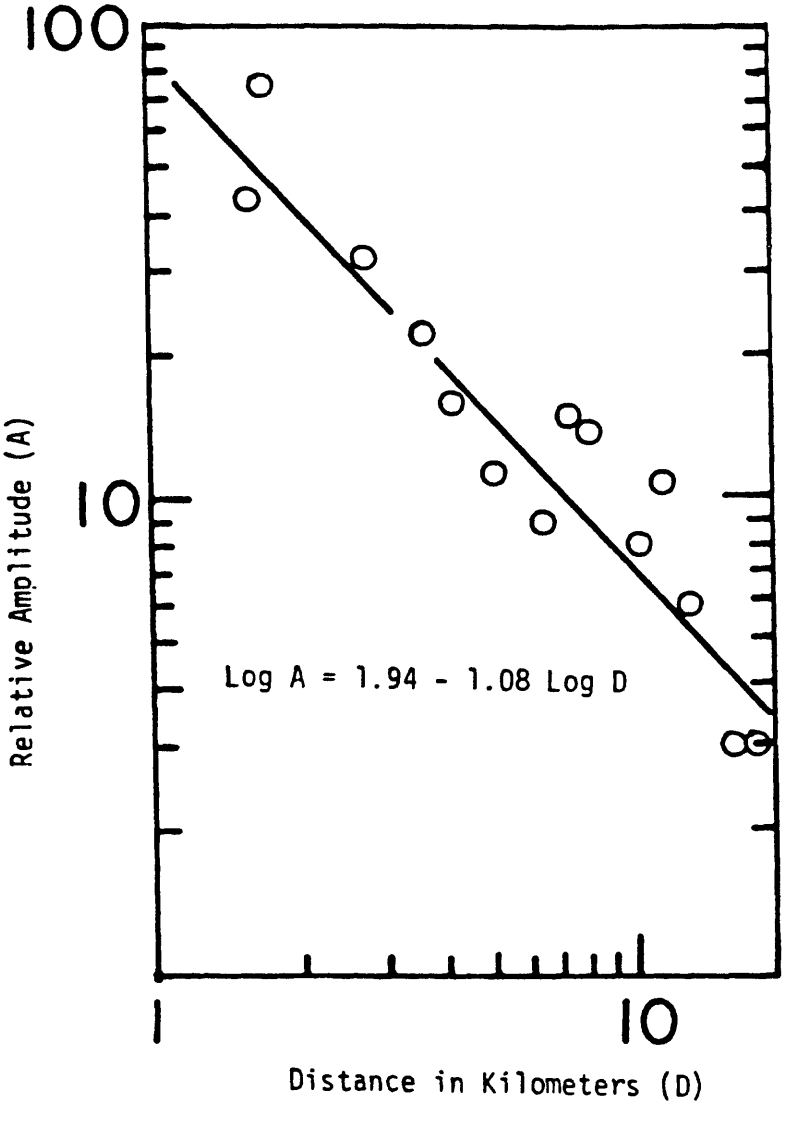
100
10
Relative Amplitude (A)
Log A = 1.94 - 1.08 Log D
1
10
Distance in Kilometers (D)

Figure 17

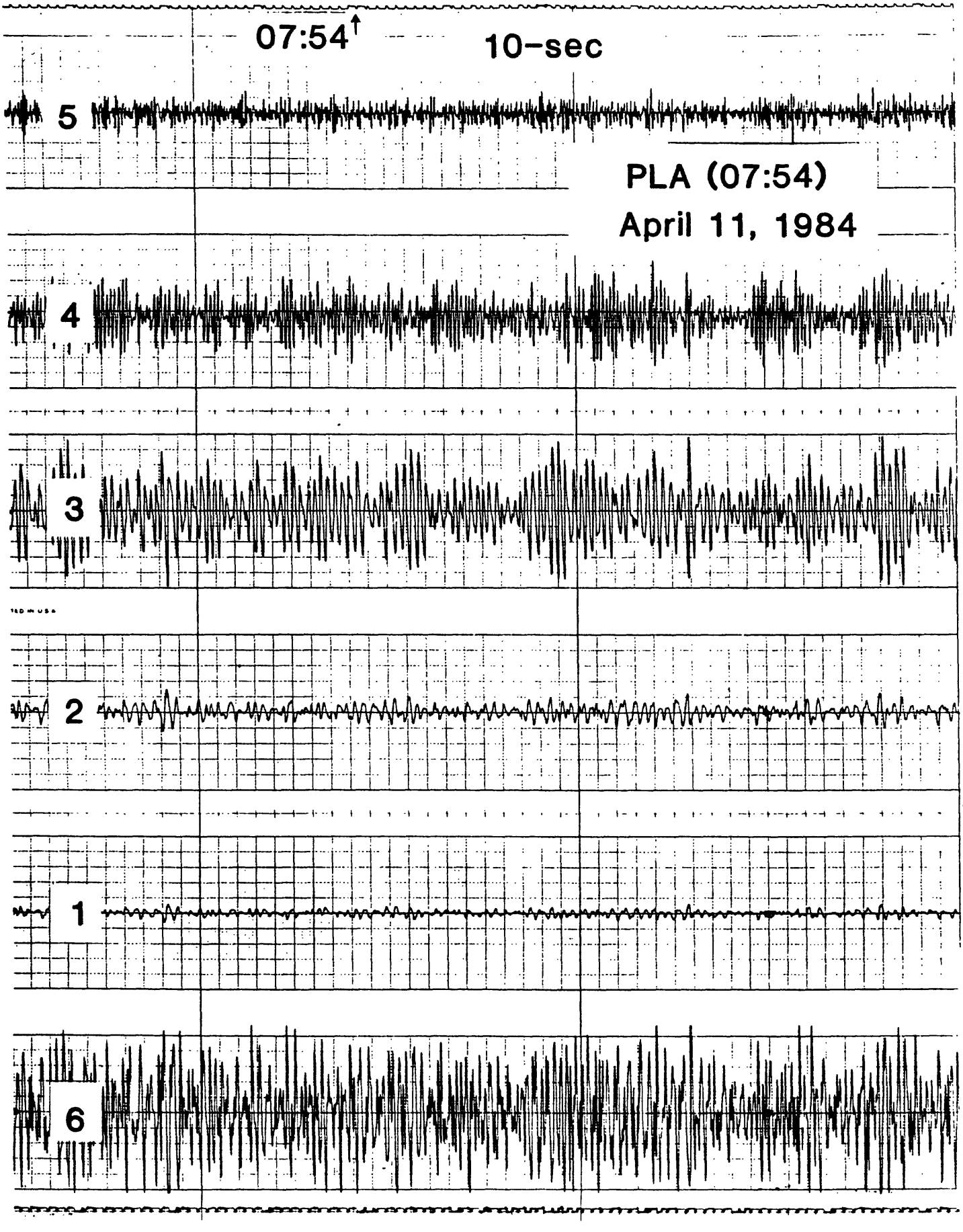

Figure 18a

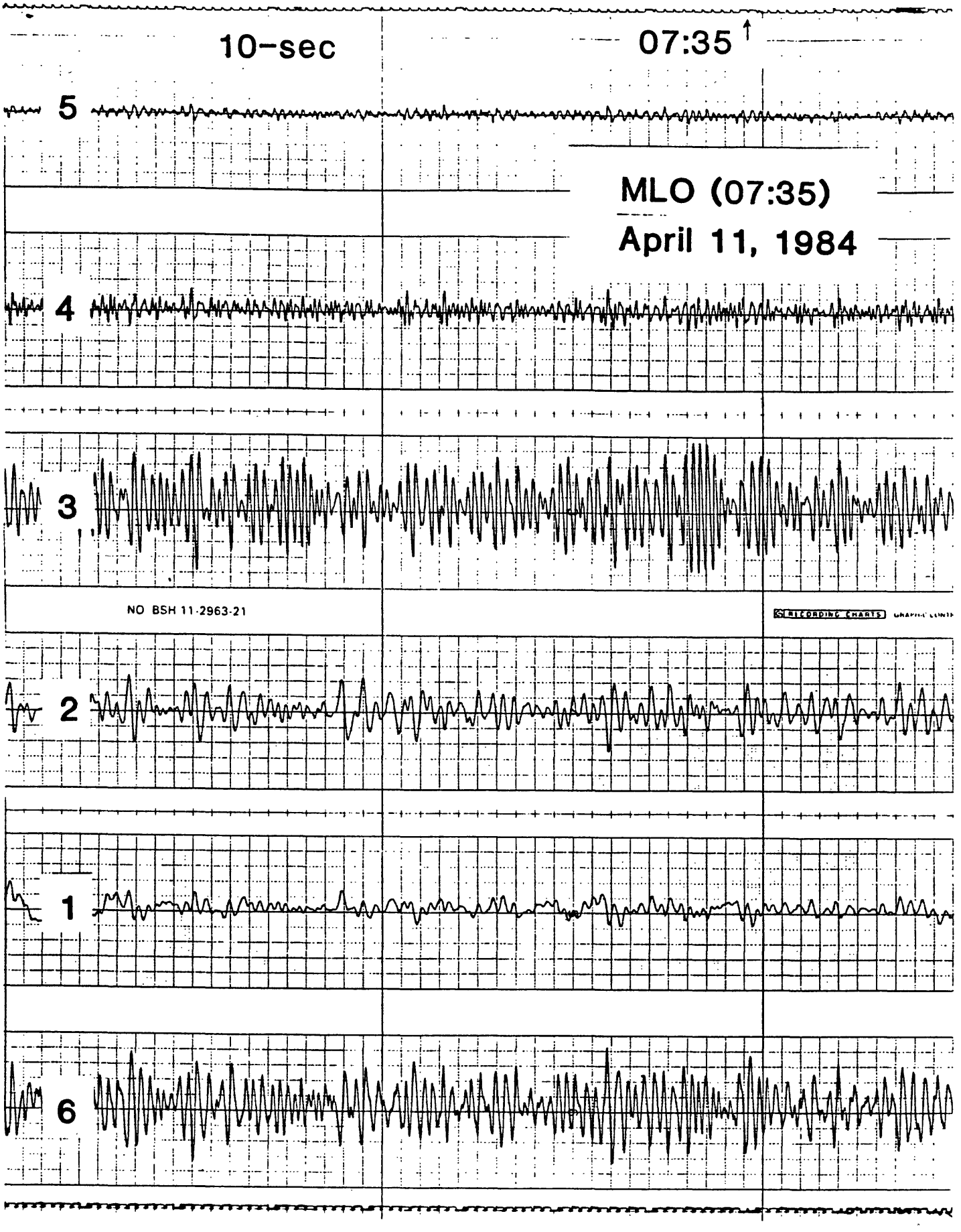
10-sec
07:35
5
MLO (07:35)
April 11, 1984
4
3
NO BSH 11-2963-21
RECORDING CHARTS
2
1
6

Figure 18b

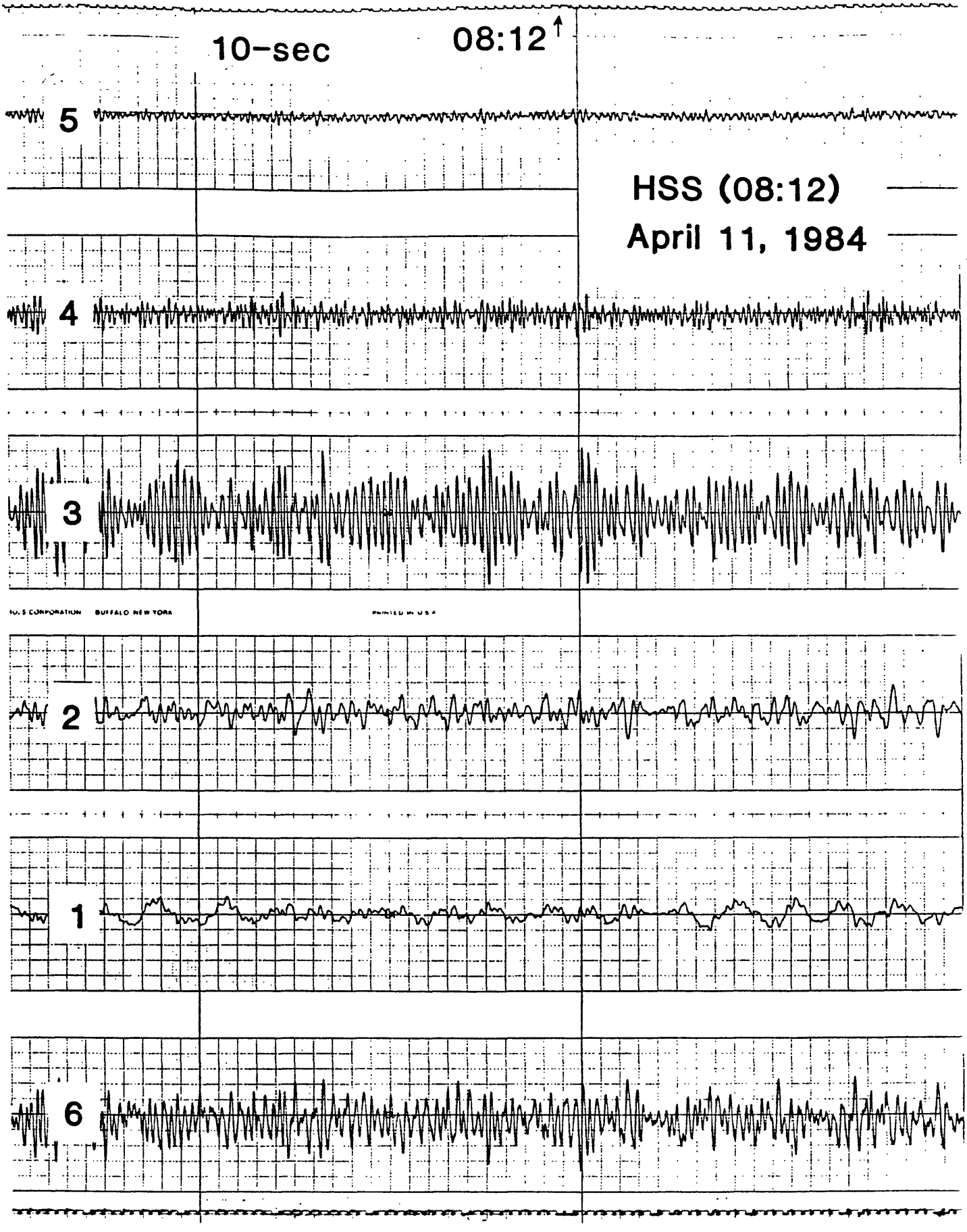

Figure 18c

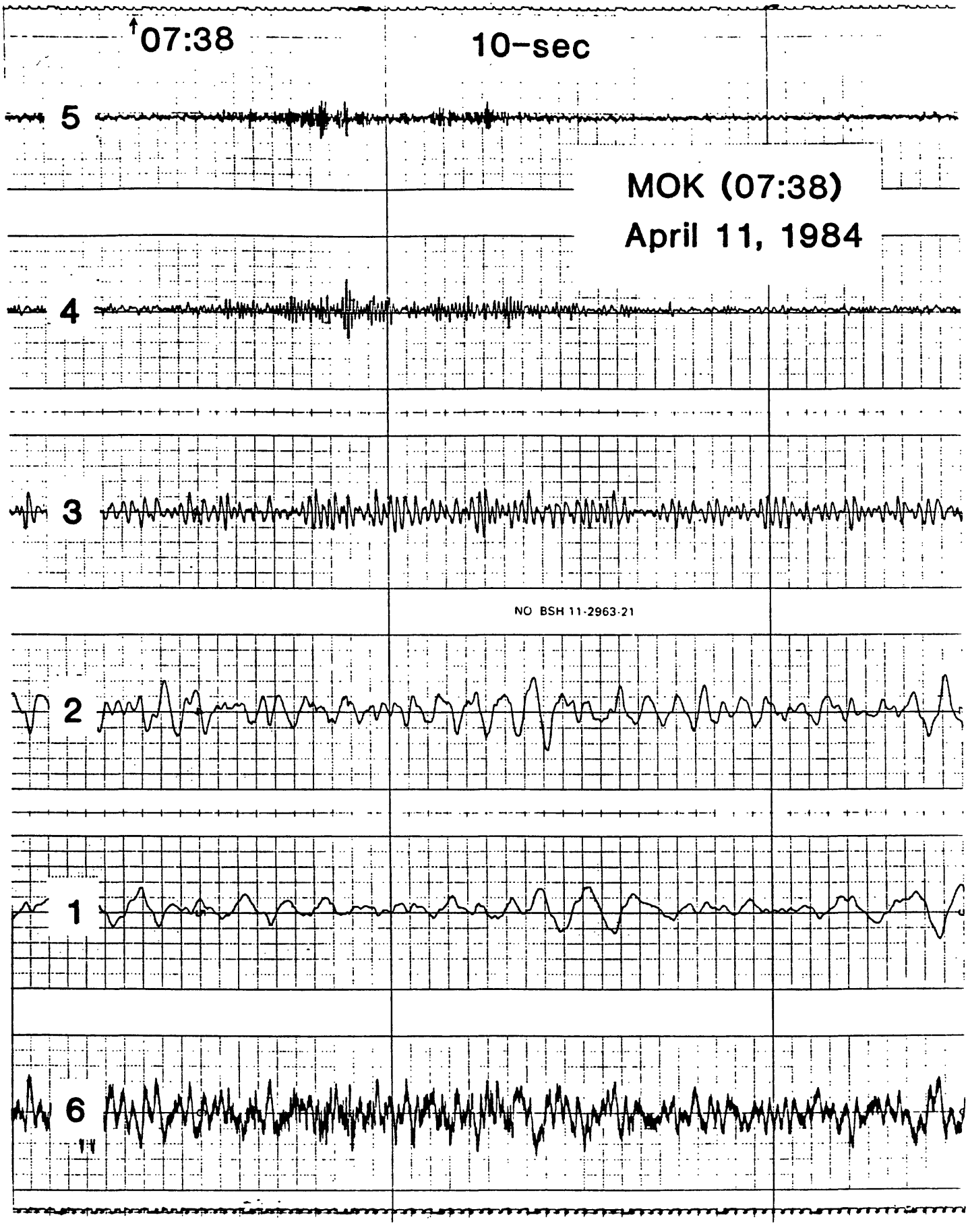

Figure 18d

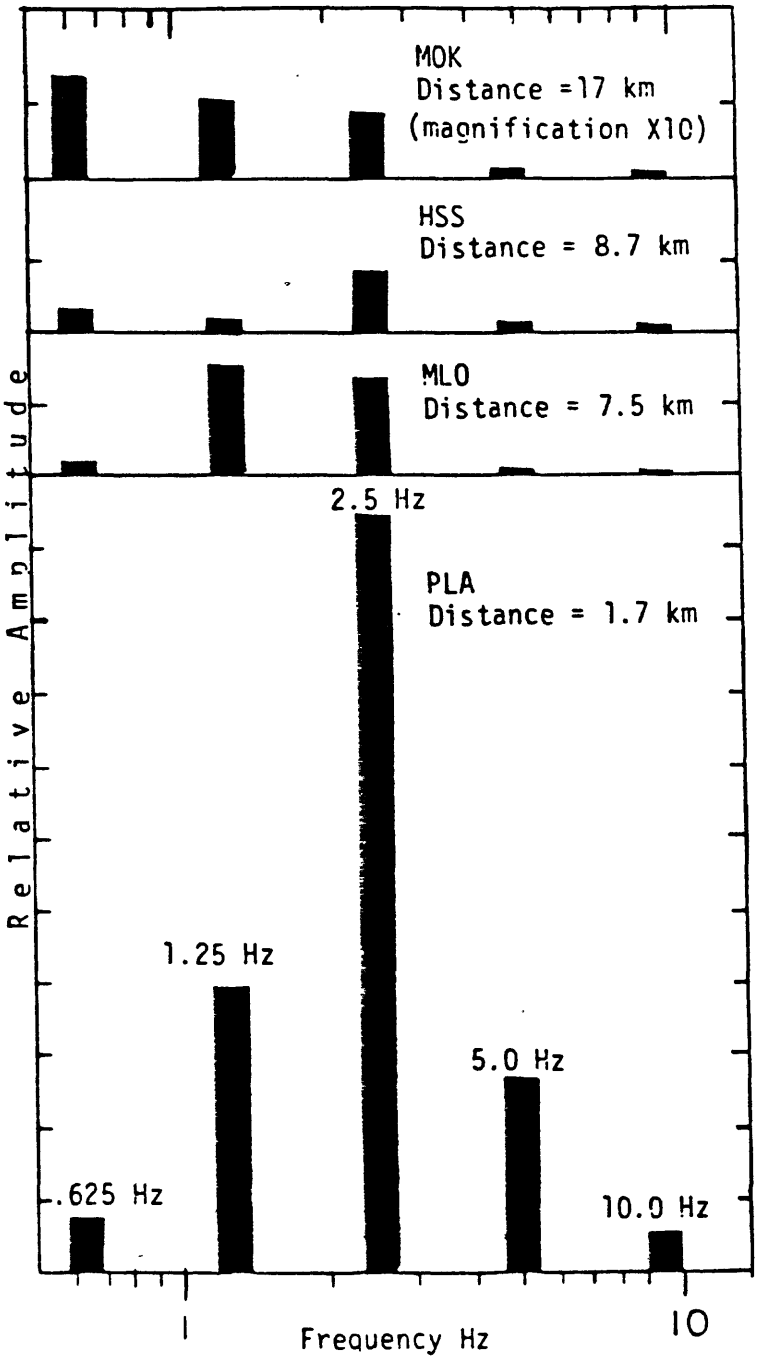
MOK
Distance =17 km
(magnification X10)
HSS
Distance = 8.7 km
MLO
Distance = 7.5 km
2.5 Hz
PLA
Distance = 1.7 km
1.25 Hz
5.0 Hz
.625 Hz
10.0 Hz
Relative Amplitude
1
Frequency Hz
10

Figure 19

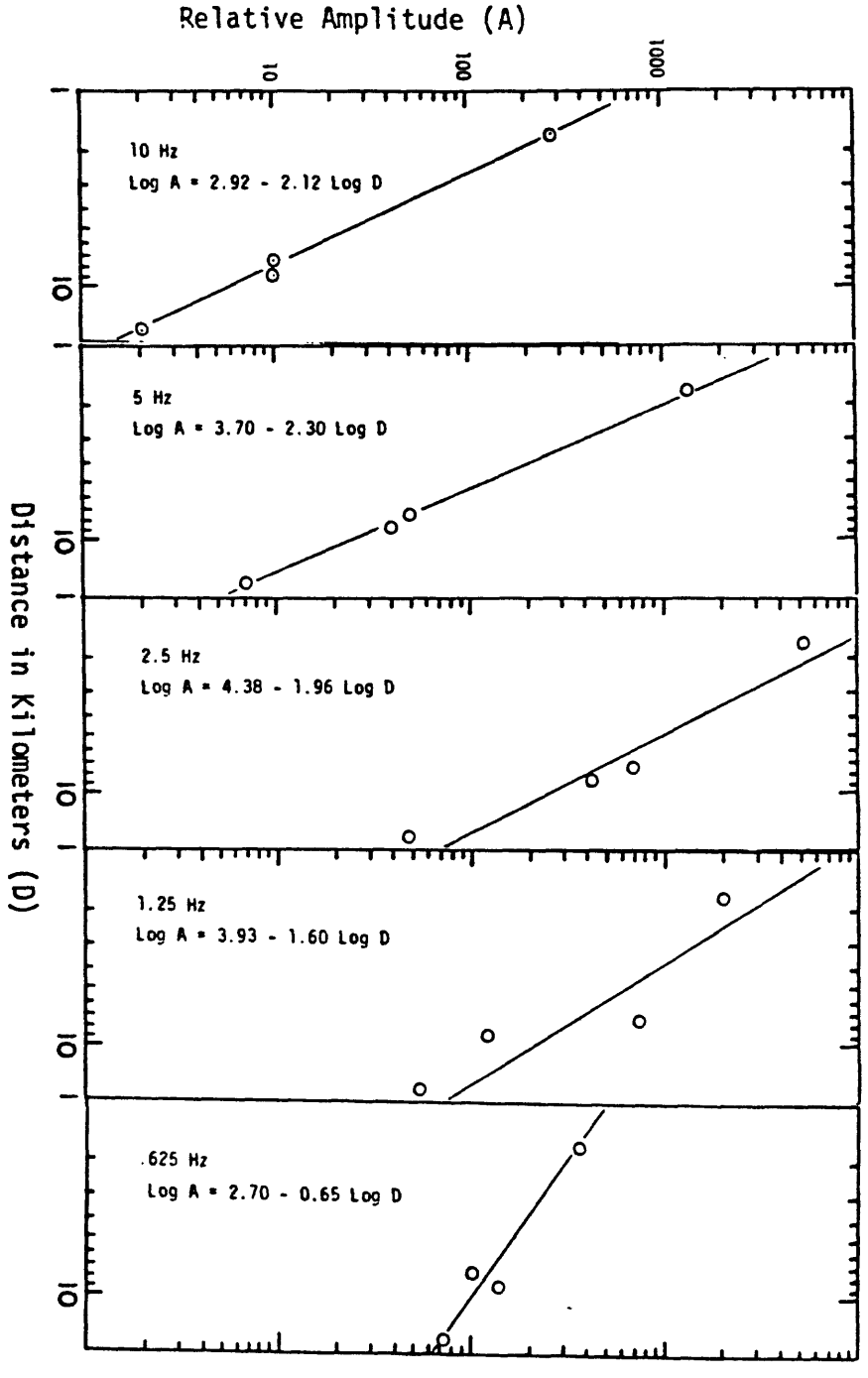
Relative Amplitude (A)
10
100
1000
Distance in Kilometers (D)
10 Hz
Log A = 2.92 - 2.12 Log D
5 Hz
Log A = 3.70 - 2.30 Log D
2.5 Hz
Log A = 4.38 - 1.96 Log D
1.25 Hz
Log A = 3.93 - 1.60 Log D
.625 Hz
Log A = 2.70 - 0.65 Log D
10
1
10
1
10
1
10

Figure 20

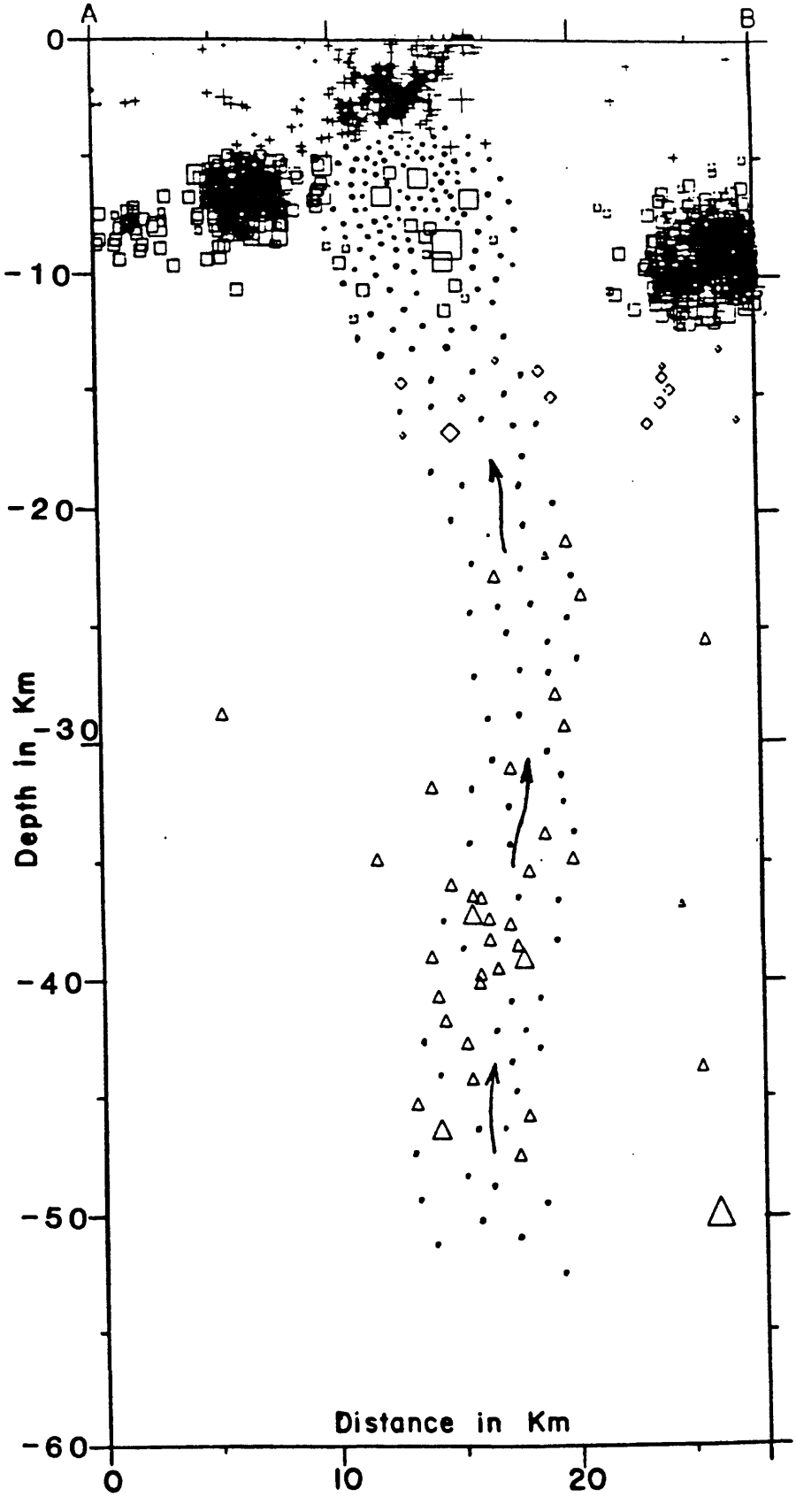

Figure 21

TABLE 1

SEISMIC REGION	TIME INTERVAL	NUMBER MONTHS	NUMBER EARTHQUAKES number	NUMBER EARTHQUAKES rate/ month	SEISMIC MOMENT x 10^{21} dyne-cm moment	SEISMIC MOMENT rate/ month	RATIO MOMENT/ NUMBER
Shallow summit (0-5 km) 19°20'-35'N 155°31'-45'W	Apr 64-Dec 66	33	5	0.15	0.10	.003	.020
	Jan 67-Dec 70	48	28	0.58	0.20	.004	.007
	Jan 71-Mar 74	39	2	0.05	0.30	.008	.150
	Apr 74-Dec 74	9	20	2.22	0.10	.011	.005
	Jan 75-Jun 75	6	150	25.00	3.50	.583	.023
	Jul 75-Dec 79	54	12	0.22	0.10	.002	.008
	Jan 80-Jan 83	37	53	1.43	0.50	.014	.009
	Feb 83-Feb 84	13	110	7.33	0.60	.046	.005
	Mar 84-Apr 84	2	34	17.00	0.95	.475	.028
	May 84-Dec 85	20	2	0.10	0.05	.003	.025
Intermediate-Depth Summit (5-13 km) 19°20'-35'N 155°31'-45'W	Jul 63-Feb 70	80	25	0.31	0.50	.006	.020
	Mar 70-Jul 74	52	50	0.96	0.80	.015	.016
	Aug 74-Mar 75	8	57	7.13	0.25	.031	.004
	Apr 75-Jun 75	3	100	33.33	0.70	.233	.007
	Jul 75-Feb 78	32	3	0.09	0.25	.008	.083
	Mar 78-Jun 78	4	10	2.50	0.05	.013	.005
	Jul 78-Aug 82	50	20	0.40	0.20	.004	.010
	Sep 82-Aug 83	12	20	1.67	0.25	.021	.013
	Sep 83-	1	45	45.00	2.50	2.50	.056
	Oct 83-Apr 84	6	26	4.33	0.35	.058	.013
	May 84-Dec 85	20	4	0.20	0.07	.004	.018
Deep Summit (13-60 km) 19°20'-35'N 155°31'-45'W	Jul 65-Feb 71	68	37	0.44	0.50	.007	.016
	Mar 71-Feb 73	24	2	0.08	0.02	.001	.013
	Mar 73-Nov 74	21	10	0.48	0.10	.005	.010
	Dec 74-Jun 75	7	2	0.29	0.10	.014	.050
	Jul 75-Jan 78	31	2	0.07	0.10	.003	.050

SEISMIC REGION	TIME INTERVAL	NUMBER MONTHS	NUMBER EARTHQUAKES number	NUMBER EARTHQUAKES rate/ month	SEISMIC MOMENT x 10^{21} dyne-cm moment	SEISMIC MOMENT x 10^{21} dyne-cm rate/ month	RATIO MOMENT/ NUMBER
Deep Summit (con't)	Feb 78-Feb 84	73	30	0.41	0.20	.003	.007
	Apr 84-Dec 85	21	1	0.05	0.05	.002	.002
Kaoiki (5-15 km) 19°19'-29'N 155°22'-32'W	Nov 63-Jul 66	32	130	4.060	7.0	.219	.054
	Aug 66-Feb 67	7	60	8.570	4.0	.571	.067
	Mar 67-Jun 74	87	80	9.310	10.0	.115	.012
	Jul 74-Oct 74	4	150	37.500	10.0	2.500	.067
	Nov 74-Feb 75	4	230	57.500	55.0	13.75	.239
	Mar 75-Jun 75	4	50	12.50	3.0	.750	.060
	Jul 75-Jun 77	24	250	10.420	8.0	.333	.032
	Jul 77-Jan 79	19	280	14.740	4.0	.211	.014
	Feb 79-Apr 81	27	250	9.260	5.0	.185	.020
	May 81-Oct 83	30	150	5.000	5.0	.167	.033
	Mar 84-Dec 85	22	155	7.050	8.0	.364	.052